UNIVERSITA' DELLA CALABRIA

Facoltà di Farmacia e Scienze della Nutrizione e della Salute

Università della Calabria

Facoltà di Farmacia e Scienze della Nutrizione e della Salute

Dipartimento Farmaco Biologico

(MED/04 PATOLOGIA GENERALE)

Dottorato di Ricerca in "Biochimica Cellulare ed Attività dei Farmaci in Oncologia" (XX° ciclo)

Evidences that leptin upregulates E-cadherin expression in breast cancer: effects on tumor growth and progression

Coordinatore

Ch.mo Prof. Sebastiano Andò

Dottorando

Dott. Michele Pellegrino

Docente Tutor

Dott.ssa Loredana Mauro

Anno Accademico 2006-2007

SUMMARY

Leptin, a cytokine mainly produced by adipocytes, appears to play a crucial role in mammary carcinogenesis. In the present study, we explored the mechanism of leptin-mediated promotion of breast tumor growth using xenograft MCF-7, in 45 days old female nude mice, and an *in vitro* model represented by MCF-7 three-dimensional cultures. Xenograft tumors, obtained only in animals with estradiol (E_2) pellet implants, doubled control value after 13 weeks of leptin exposure.

In three-dimensional cultures leptin and/or E_2 enhanced cell-cell adhesion. This increased aggregation appears to be dependent on E-cadherin, since it was completely abrogated in the presence of function-blocking E-cadherin antibody or EGTA, a calcium-chelating agent. In three-dimensional cultures leptin and/or E_2 treatment significantly increased cell growth, which was abrogated when E-cadherin function was blocked. These findings well correlated with an increase of mRNA and protein content of E-cadherin in 3D cultures as well as in xenografts. In MCF-7 cells both hormones were able to activate E-cadherin promoter.

Mutagenesis studies, EMSA and ChIP assays revealed that CREB and Sp1 motifs, present on E-cadherin promoter, were important for the upregulatory effects induced by both hormones on E-cadherin expression in breast cancer MCF-7 cells. In conclusion, the present study demonstrates how leptin is able to promote tumor cell proliferation and homotypic tumor cell adhesion via an increase of E-cadherin expression. This combined effect may give reasonable emphasis to the important role of this cytokine in stimulating primary breast tumor cell growth and progression particularly in obese women.

INDEX

Scientific Publications 55

- *Evidences that leptin upregulates E-cadherin expression in breast cancer: effects on tumor growth and progression*

- *Fas Ligand expression in TM4 Sertoli cells is enhanced by estradiol "in situ" production*

- *Evidence that low doses of Taxol enhance the functional transactivatory properties of p53 on p21 waf promoter in MCF-7 breast cancer cells*

- *Peroxisome Proliferator-Activated Receptor (PPAR)γ is expressed by human spermatozoa: its potential role on the sperm physiology*

INTRODUCTION

Leptin is an adipocyte-derived hormone (1) which, in addition to the control weight homeostasis by regulating food intake and energy expenditure (Fig.1) (2,3), is implicated in the modulation of many other processes such as reproduction, lactation, haematopoiesis, immune responses, cell differentiation and proliferation (4,5).

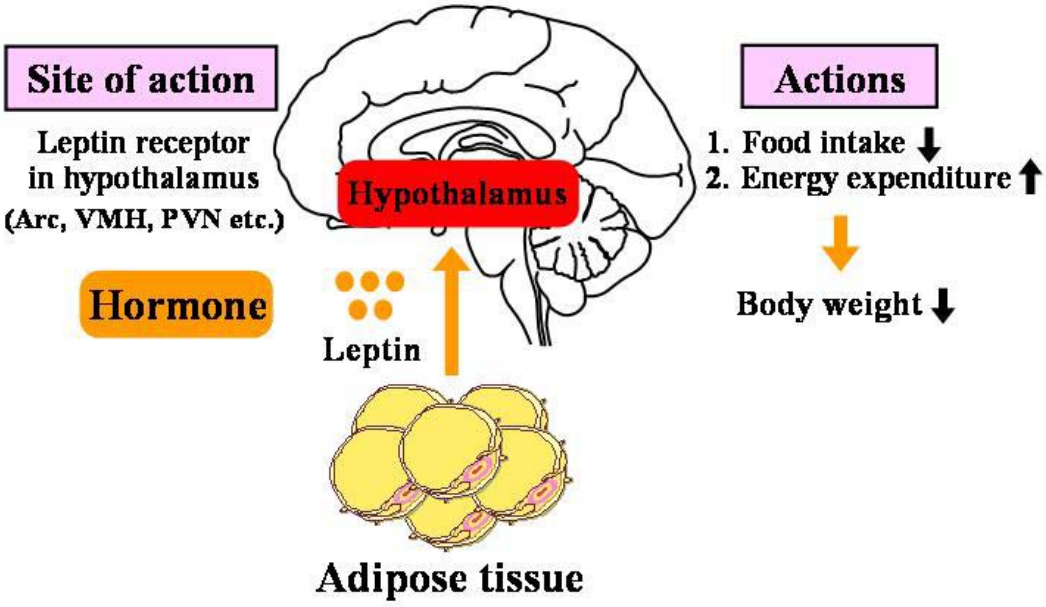

Figure 1. Site of action and actions of leptin at hypothalamus level.

The activities of leptin are mediated through the transmembrane leptin receptor (ObR) by the activation of JAK/STAT (Janus-activated

kinase/signal transducers and activators of transcription) and MAPK (mitogen-activated protein kinase) pathways (6-9).

The human leptin receptor belongs to the class I cytokine receptor family, and two main isoforms, resulting from an alternative splicing, have been identified. It is now well established that the long form (ObR-l), mainly expressed in the hypothalamus, is responsible for signal transduction through the activation of JAK/STAT, MAPK and PI-3K/Akt pathways (Fig.2). On the other hand, the short isoform (ObR-s), which is more abundant in peripheral tissues, mainly activates the MAPK and seems to be responsible for mitogenic activity (8, 9).

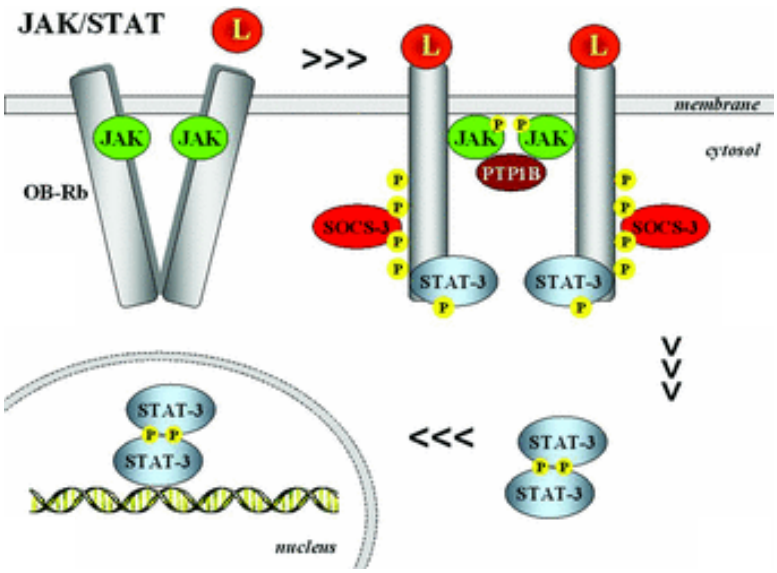

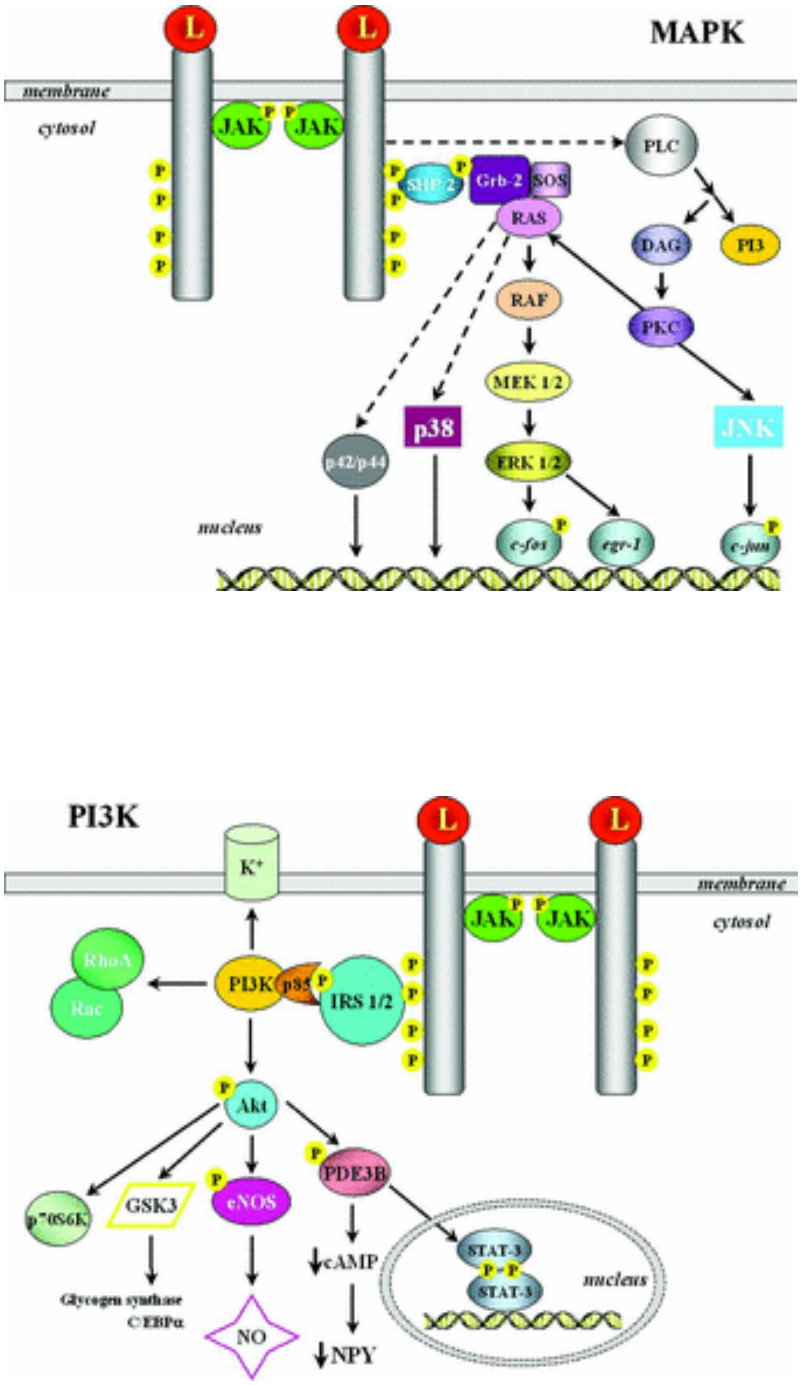

Figure 2. Transductional pathways activated by leptin.

Epidemiological studies demonstrate a positive association between obesity and an increased risk of developing different cancers, such as

pancreatic, colon, prostate, ovarian, endometrial, lung, adrenal and breast cancer (10, 11).

Several lines of evidence suggest that leptin and ObR are involved in the development of normal mammary gland as well as in mammary carcinogenesis (12-14). Hu et al. (12) reported that genetically obese leptin-deficient $Lep^{ob}Lep^{ob}$ and leptin receptor–deficient $Lep^{db}Lep^{db}$ mice have minimal epithelial development in the mature mammary gland compared with their lean counterparts. Moreover, leptin- or leptin receptor–deficient mouse overexpressing transforming growth factor-α mice do not develop mammary tumors (13, 14). Although many studies suggested that leptin might be involved in mammary carcinogenesis, the mechanisms through which this hormone influences the primary breast cancer development is still not known. It has been recently reported that in primary breast tumors leptin was detected in 86.4% of cases examined. Besides, it is worth to mention how the expression of leptin in primary tumors is highly correlated with ObR, while in lymph node metastases the expression of leptin was not significantly associated with ObR expression. This indicates that leptin can influence breast cancer cells not only by endocrine and/or paracrine actions but also through an autocrine leptin loop (15).

In epithelium and epithelium-derived tumors, cell-cell adhesion and tumor mass mostly depend on E-cadherin, a 120-kDa transmembrane molecule (16,17). E-cadherin can establish calcium-dependent homophilic interaction through their extracellular domain and these binding are stabilized by the association of the intracellular domain with α-, β- and γ-catenins, which are linked to F actin to form functional adherens junctions (Fig.3) (16, 17).

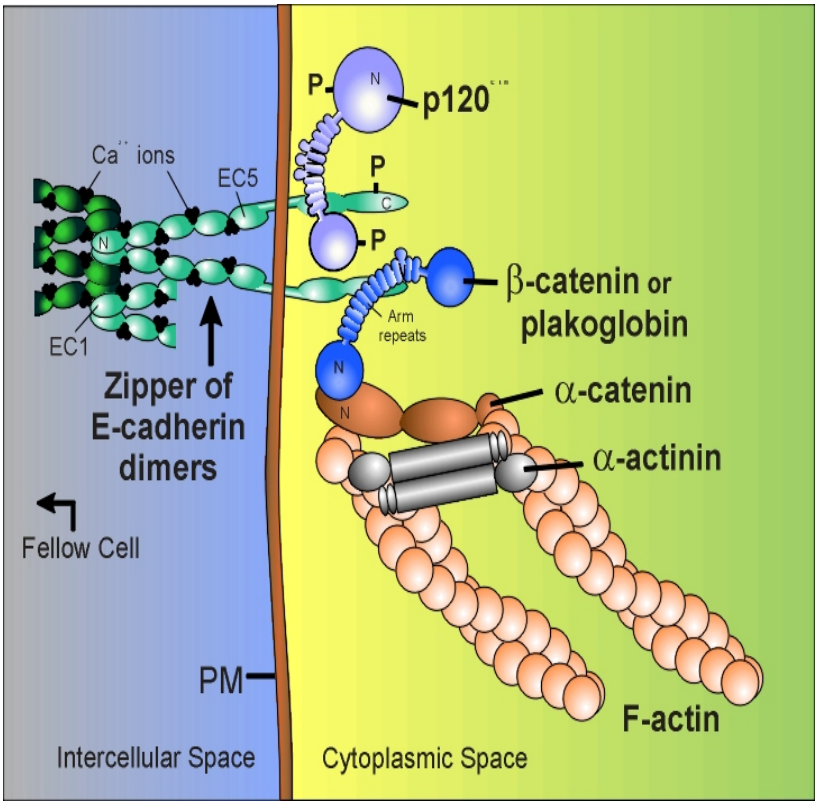

Figure 3. E-cadherin/catenins complex.

As it might be expected, E-cadherin appears to have a major influence on primary cancer development and evolution. Alteration in the function of E-cadherin and the cadherin-catenin complex have been implicated in cancer progression (18) invasion (19-21) and metastasis (22,23).

In this study, we explored a new aspect of the involvement of leptin in initial steps of mammary tumorigenesis. Specifically, we asked whether leptin can affect primary tumor mass either *in vivo* in MCF-7 cell tumor xenograft or *in vitro* in MCF-7 three-dimensional cultures. Our results demonstrated that leptin is able to promote tumor cell proliferation and homotypic tumor cell adhesion via an increase of E-cadherin expression. These combined effects may give reasonable emphasis to the important role of this cytokine in stimulating local primary breast tumor cell growth and progression, particularly in obese women.

Materials and Methods

Plasmids

The plasmids containing the human E-cadherin promoter or its deletions were given by Dr. Y. S. Chang (Chang-Gung University, Republic of China) (24). pHEGO plasmid, containing the full length of ERα cDNA was provided by Dr. D. Picard (University of Geneva). pSG5 vector containing the cDNA encoding dominant negative STAT3, which is a variant of the transcription factor STAT3 lacking an internal domain of 50 base pairs located near the C terminus ($STAT^-$) was given by Dr. J. Turkson (University of South Florida, College of Medicine, Tampa). pCMV5myc vector containing the cDNA encoding dominant negative ERK2 K52R ($ERK2^-$) was provided by Dr. M. Cobb (Southwestern Medical Center, Dallas).

Site-directed mutagenesis

The E-cadherin promoter plasmid bearing CREB mutated site (CREB mut) was created by site-directed mutagenesis using Quick Change kit (Stratagene). We used as template human E-cadherin promoter and the mutagenic primers were the following:

5'-AGGGTGGATCACCTGAtacCAGGAGTTCCAGACCAGC-3' and 5'-GCTGGTCTGGAACTCCTGgtaTCAGGTGATCCACCCT-3'. The constructed reporter vector was confirmed by DNA sequencing.

Cell Lines and Culture Conditions

MCF-7, HeLa and BT-20 cells were obtained from the American Type Culture Collection (ATCC) (Manassas, VA). MCF-7 and HeLa cells were maintained in DMEM/F-12 containing 5% CS, and BT-20 cells were cultured in MEM supplemented with 10% FBS, 1% Eagle's non-essential amino acids and 1% sodium pyruvate (Sigma). Cells were cultured in phenol-red-free DMEM (SFM), containing 0.5% bovine serum albumin, 24h before each experiment. All media were supplemented with 1% L-glutamine and 1% penicillin/streptomycin (Sigma).

In vivo studies

The experiments *in vivo* were performed in 45 days old female nude mice (*nu/nu Swiss*; Charles River). At day 0, the animals were fully anaesthetized, by intramuscular injection of 1.0 mg/kg Zoletil (Virbac)

and 0.12% Xylor (Xylazine), to allow the subcutaneous implantation of estradiol pellets (1.7 mg/pellet 60 days release, Innovative Research of America) into the intrascapular region of mice. The day after, exponentially growing MCF-7 cells ($5.0x10^6$ cells/mouse) were inoculated subcutaneously in 0.1ml of matrigel (BD biosciences). Leptin treatment was started 24h later, when animals were injected intraperitoneally with either solutions: -recombinant human leptin (230μg/kg) diluted in saline + 0.3% bovine serum albumin (BSA) or - saline + 0.3% BSA only, control. The treatment was performed for five days a week until the 13^{th}. Tumor development was followed twice a week by caliper measurements along two orthogonal axes, length (L) and width (W). The volume (V) of tumors was estimated by the formula: V = L x (W2)/2. At the time of killing (13 weeks) tumors were dissected out from the neighboring connective tissue, frozen in nitrogen and stored at -80°C. All the procedures involving animals and their care have been conducted, in conformity with the institutional guidelines, at the Laboratory of Molecular Oncogenesis, Regina Elena Cancer Institute in Rome.

Three-dimensional spheroid culture and cell growth

The cells were plated in single-cell suspension in 2%-agar-coated plates and untreated or treated with 1000 ng/ml leptin and/or 100 nM E_2 for 48h. To block E-cadherin function, the medium was supplemented with E-cadherin antibody (1:100 dilution; Chemicon International) or EGTA to a final concentration of 4 mM. To generate three-dimensional spheroids, the plates were rotated for 4h at 37°C. The three-dimensional cultures were photographed using a phase-contrast microscope (Olympus). The extent of aggregation was scored by measuring the spheroids with an ocular micrometer. The spheroids between 25 and 50, 50 and 100, and >100 μm (in the smallest cross-section) were counted in 10 different fields under ×10 magnification. Cell number was determined, after trypsinization of spheroids, by direct cell counting at 48h of treatments.

E-cadherin adhesion assay

MCF-7 cells were pretreated with leptin (1000 ng/ml) and/or E_2 (100 nM) for 48h and then plated on 6-well plates coated with 1.5 μg/ml recombinant human E-cadherin/Fc chimeric. Before the experiment,

the wells were blocked with 1% BSA for 3h at 37°C and then washed with PBS.

After washing out nonadherent cells, adherent cells were incubated 3h in medium containing 500 μg/ml MTT solution. The reaction product was measured at 570 nm.

Total RNA extraction and Reverse Transcription-PCR Assay

Total RNA was extracted using TRIzol reagent (Invitrogen). Reverse transcription was done using RETROscript kit (Ambion). The cDNAs were amplified by PCR using the following primers:

5'-TCTAAGATGAAGGAGACCATC-3' and

5'-GCGGTAGTAGGACAGGAAGTTGTT-3' (cyclin D1),

5'-TGGAATCCAAGCAGAATTGC-3' and

5'-TATGTGGCAATGCGTTCTCTATCCA-3' (E-cadherin), and

5'-CTCAACATCTCCCCCTTCTC-3' and

5'-CAAATCCCATATCCTCGT-3' (36B4). The PCR was performed for 30 cycles for cyclin D1 (94°C 1 min, 60°C 1 min, 72°C 2 min) and E-cadherin (94°C 1 min, 55°C 1 min, 72°C 2 min) and 15 cycles (94°C 1 min, 59°C 1 min, 72°C 2 min) to amplify 36B4, in the presence of 1 μl of first strand cDNA, 1 μM each of the primers

mentioned above, dNTP (0.5 mM), Taq DNA polymerase (2 units/tube) (Promega) in final volume of 25 µl.

Western blot analysis

Equal amounts of total protein were resolved on an 8-10% SDS-polyacrylamide gel. Proteins were transferred to a nitrocellulose membrane and probed with the appropriated antibody. The antigen-antibody complex was detected by incubation of the membrane at room temperature with a peroxidase-coupled goat anti-mouse or anti-rabbit IgG and revealed using the ECL system (Amersham).

Transfection assay

MCF-7 cells were transfected using the FuGENE 6 reagent (Promega) with the mixture containing 0.5 µg of human E-cadherin promoter constructs. HeLa cells were transfected with E-cadherin promoter (0.5 µg/well) in the presence or absence of HEGO (0.2 µg/well) or cotransfected with STAT3 or ERK2 dominant negative (0.5 µg/well). Twenty-four hours after transfection, the cells were treated with 1000 ng/ml leptin and/or 100 nM E_2 for 48h. Empty vectors were used to ensure that DNA concentrations were constant in each transfection.

TK *Renilla* luciferase plasmid (5 ng/well) was used. Firefly and *Renilla* luciferase activities were measured by Dual Luciferase kit. The firefly luciferase data for each sample were normalized on the basis of transfection efficiency measured by *Renilla* luciferase activity.

Electrophoretic mobility shift assay

Nuclear extracts were prepared from MCF-7 as previously described (25). The probe was generated by annealing single stranded oligonucleotides and labeled with [γ^{32}P] ATP and T4 polynucleotide kinase, and then purified using Sephadex G50 spin columns. The DNA sequences used as probe or as cold competitors are the following:

CRE: 5'-TGGATCACCTGAGGTCAGGAGTTCCAGACC-3',

Sp1: 5'-ATCAGCGGTACGGGGGGCGGTGCTCCGGGG-3'.

In vitro transcribed and translated CREB protein was synthesized using the T7 polymerase in the rabbit reticulocyte lysate system (Promega). The protein binding reactions were carried out in 20 μl of buffer (20 mM HEPES pH 8, 1 mM EDTA, 50 mM KCl, 10 mM DTT, 10% glycerol, 1 mg/ml BSA, 50 μg/ml poli dI/dC) with 50000 cpm of labeled probe, 20 μg of MCF-7 nuclear protein or an

appropriate amount of CREB protein or Sp1 human recombinant protein (Promega), and 5 μg of poly (dI-dC). The mixtures were incubated at room temperature for 20 minutes in the presence or absence of unlabeled competitor oligonucleotides. The specificity of the binding was tested by adding to the mixture reactions specific antibodies (anti-CREB and anti-Sp1). Mithramycin A 100 μM (ICN Biomedicals Inc.) was incubated with the labelled probe for 30 minutes a 4°C before the addition of nuclear extracts. The entire reaction mixture was electrophoresed through a 6% polyacrylamide gel in 0.25 X Tris borate-EDTA for 3h at 150 V.

Chromatin immunoprecipitation assay

We followed ChIP methodology described by Morelli et al. (26). MCF-7 cells were untreated or treated with 1000 ng/ml leptin and/or 100 nM E_2 for 1h. The cells were then cross-linked with 1% formaldehyde and sonicated. Supernatants were immunocleared with sonicated salmon DNA/protein A agarose (Upstate Biotechnology Inc.) and immunoprecipitated with anti-CREB or anti-Sp1 antibodies (Santa Cruz). Pellets were washed as reported (26), eluted with elution buffer (1% SDS and 0.1 M $NaHCO_3$) and digested with proteinase K

(26). DNA was obtained by phenol/chloroform extractions and precipitated with EtOH. 5 μl of each sample were used for PCR with the CREB primers: 5'-TGTAATCCAACACTTCAGGAGG-3', and 5'-TTGAGACGGAGTCTCGCTCT-3', and Sp1 primers:
5'-TAGCAACTCCAGGCTAGAGG-3', and
5'-AACTGACTTCCGCAAGCTCACA-3'.
The PCR conditions were: 94°C 1 min, 56°C 2 min, 72°C 2 min for 30 cycles.

Statistical Analysis

Data were analyzed by analysis of variance using the STATPAC computer program. Statistical comparisons for *in vivo* studies were made by Wilcoxon-Mann-Whitney test.

Results

Effects of leptin on breast cancer cell tumor growth

To determine *in vivo* the influence of leptin on breast cancer cell tumor growth we utilized 45 days old female nude mice bearing, into the intrascapular region, MCF-7 cell tumor xenografts with or without estrogen pellets. Tumors were obtained only in animals with estrogen pellet implants, which were in general larger in animals treated with leptin at the dose of 230 μg/Kg (Fig. 4A). Particularly, 13 weeks of leptin parenteral administration increased the tumor volume to 100% the size of E_2 treatment. Besides, leptin significantly enhanced phosphorylation of tumor derived MAPK and STAT3, suggesting that concentration and dosing schedule of leptin were appropriated for *in vivo* stimulation (Fig. 4B and C).

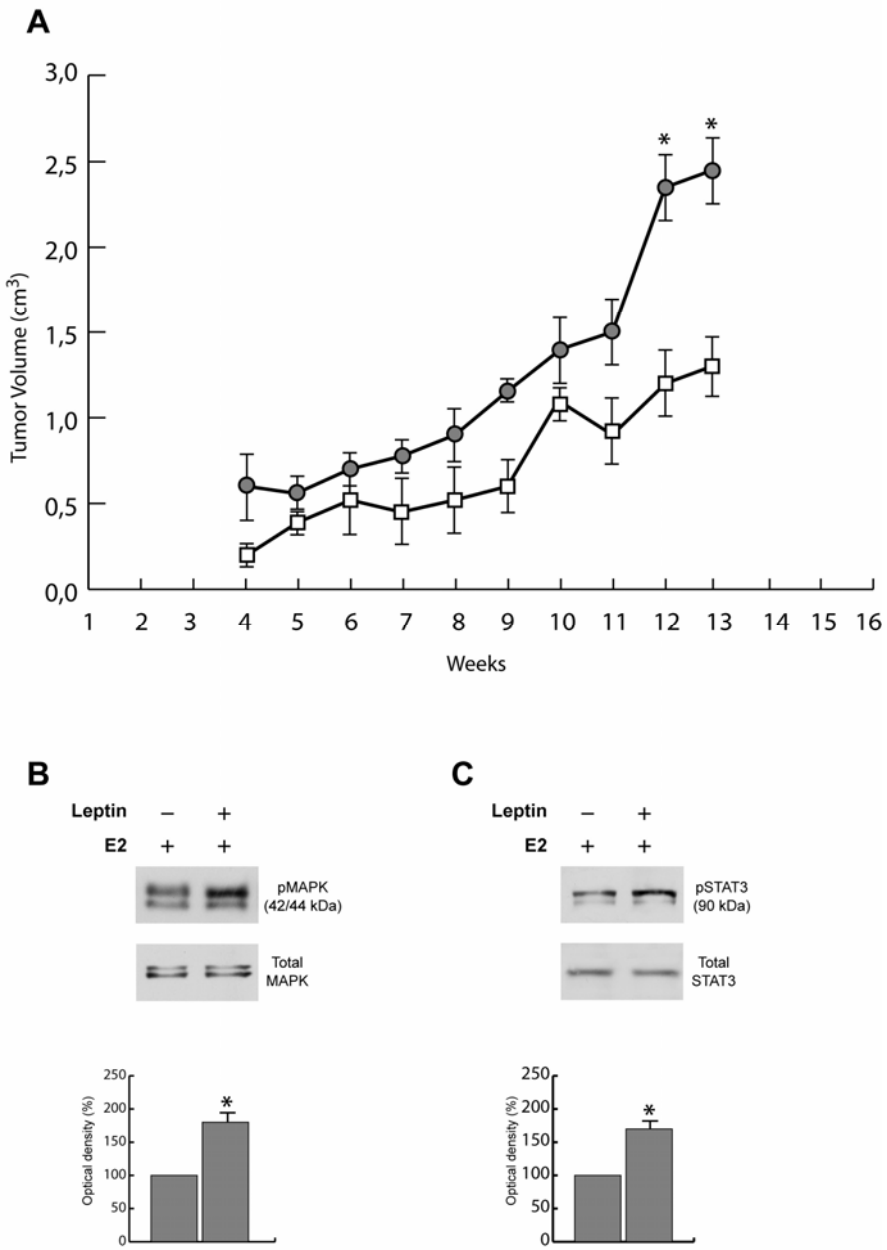

Figure 4: Effect of leptin on growth of MCF-7 cell tumor xenografts.

A. Xenografts were established with MCF-7 cells in female mice implanted with estradiol pellet. One group was treated with 230 μg/Kg leptin (●; n = 5) and a second group with vehicle (□; n = 5). * $p < 0.05$ treated versus control group. Representative western blot on protein extracts from xenografts excised from control mice and mice treated with leptin showing MAPK (**B**) and STAT3 (**C**) activation. The immunoblots were stripped and reprobed with total MAPK and STAT3 which serve as the loading control. The histograms represent the mean ± S.E. of three separate experiments in which the band intensities were evaluated in terms of optical density arbitrary units and expressed as the percentage of the control assumed as 100%. * $p < 0.05$

Leptin enhances cell-cell adhesion and cell proliferation

We performed three-dimensional MCF-7 cultures to evaluate *in vitro* the effects of leptin on cell aggregation. It has been reported that multicellular spheroid culture can more closely mimic some *in vivo* biological features of tumors and improve the relevance of *in vitro* studies (27-30). Our results evidenced that leptin and/or E_2 treatment for 48h enhances cell-cell adhesion of MCF-7 cells compared with untreated cells (Fig. 5A). The combined exposure to both hormones switches cell aggregation towards the formation of spheroids exhibiting prevalently a diameter larger than 100 μm (Tab. 1).

E-cadherin is a major type of adhesion molecule, which forms Ca^{2+}-dependent homophilic ligations to facilitate cell-cell contact in epithelial cells (16,17). Thus, to study whether E-cadherin was responsible for leptin-enhanced cell-cell adhesion, we supplemented the cell culture medium with function-blocking E-cadherin antibody or EGTA, a calcium-chelating agent. As shown in Fig. 5A, in the presence of the antibody MCF-7 cells formed small aggregates demonstrating limited intercellular contact, while EGTA treatment prevented cell-cell adhesion and cells remained rounded and singled

suspended. In addition, the role of E-cadherin was confirmed using an adhesion assay in which cells were allowed to adhere to E-cadherin/Fc protein-coated dishes.

This assay demonstrated a greater binding of cells pretreated with leptin and/or E_2 for 48h with respect to untreated cells (Fig. 5B). Thus, the increased aggregation observed in the presence of leptin and/or E_2 was dependent on E-cadherin. In three-dimensional cultures we also observed a significant increase of cell growth upon leptin and/or E_2 treatment. The leptin-induced cell proliferation was completely abrogated when E-cadherin function was blocked (Fig. 5C).

Table 1: Effect of leptin on cell aggregation in MCF-7 breast cancer cells.

MCF-7	Spheroids		
	25 ≤ 50 μm	50 ≤ 100 μm	> 100 μm
Control	30 ± 1.2	0.6 ± 0.2	0.0 ± 0.0
Leptin	6 ± 0.8	26 ± 1.8	85 ± 2.5
Estradiol	7 ± 0.6	32± 2.1	78 ± 3.2
Leptin + Estradiol	3 ± 0.9	40.5 ± 2.3*	80.7 ± 2.9

MCF-7 cells were cultured as three-dimensional spheroids in SFM. The extent of aggregation was scored by measuring the spheroid diameters with an ocular micrometer. The values represent a sum of spheroids in 10 optical fiels under ×10 magnification. The results are mean ± S.E. from at least three experiments. Representative three-dimensional cultures are shown in Fig. 2A.

* $p < 0.05$ versus leptin and E_2.

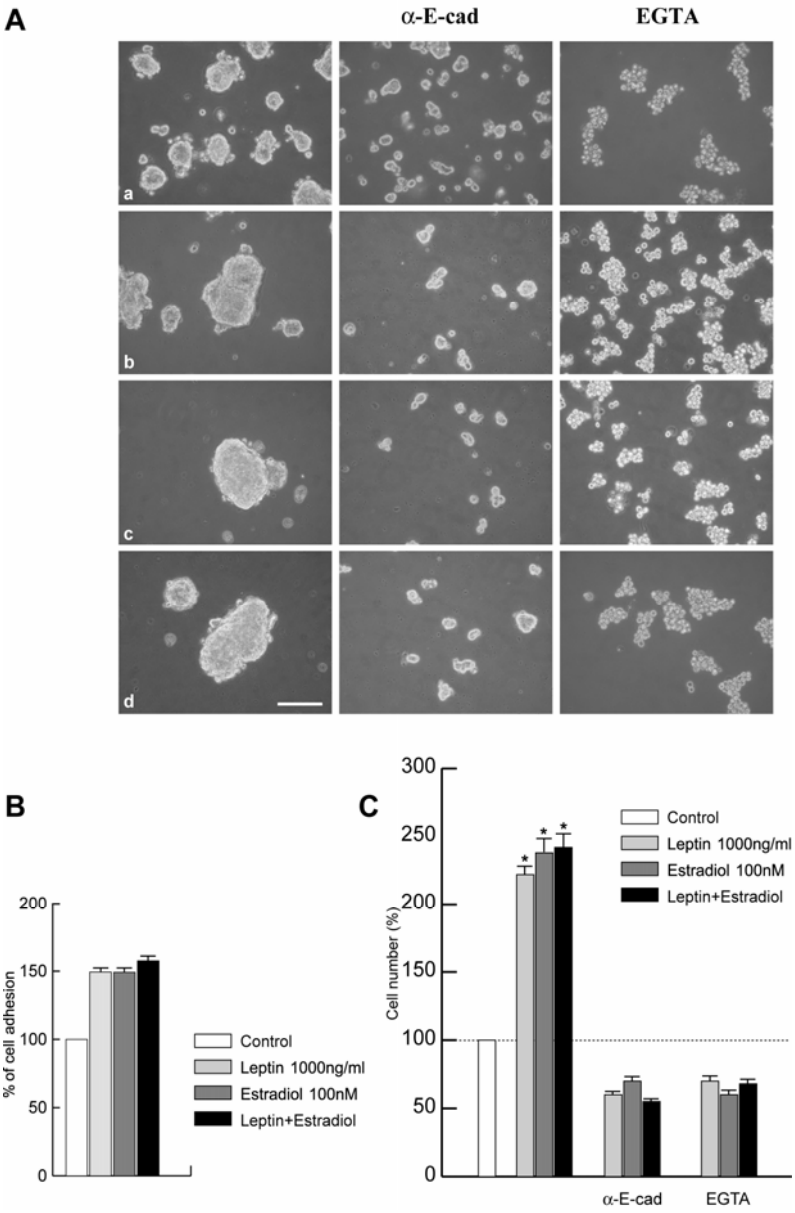

Figure 5: Leptin-enhanced cell-cell adhesion and proliferation depend on E-cadherin function.

A. E-cadherin positive MCF-7 cells were seeded in 2%-agar-coated plates and cultured as three-dimensional spheroids (a-d). To block E-cadherin function, the medium was supplemented with E-cadherin antibody (1:100 dilution; α-E-cad) or EGTA (4 mM). Cells were untreated (a) or treated with leptin (b), E_2 (c) and leptin plus E_2 (d) for 48h and then photographed under phase contrast microscopy. The bar in d equals 50 μm. **B.** 6-well plates were coated with E-cadherin/Fc recombinant protein and binding of cells were measured by the MTT assay. Each bar is the mean of five wells. **C.** Proliferation of MCF-7 cells treated with leptin and/or E_2 for 48h in the absence or presence of E-cadherin antibody (1:100 dilution; α-E-cad) or EGTA (4 mM). The results are average of three experiments. Rapresentative results are shown. * $p < 0.05$.

Furthermore, in MCF-7 spheroids and in xenografts, we observed an increase of cyclin D1, a regulator of cell cycle progression, in terms of mRNA and protein content in the presence of leptin and/or E_2 (Fig.6A and B).

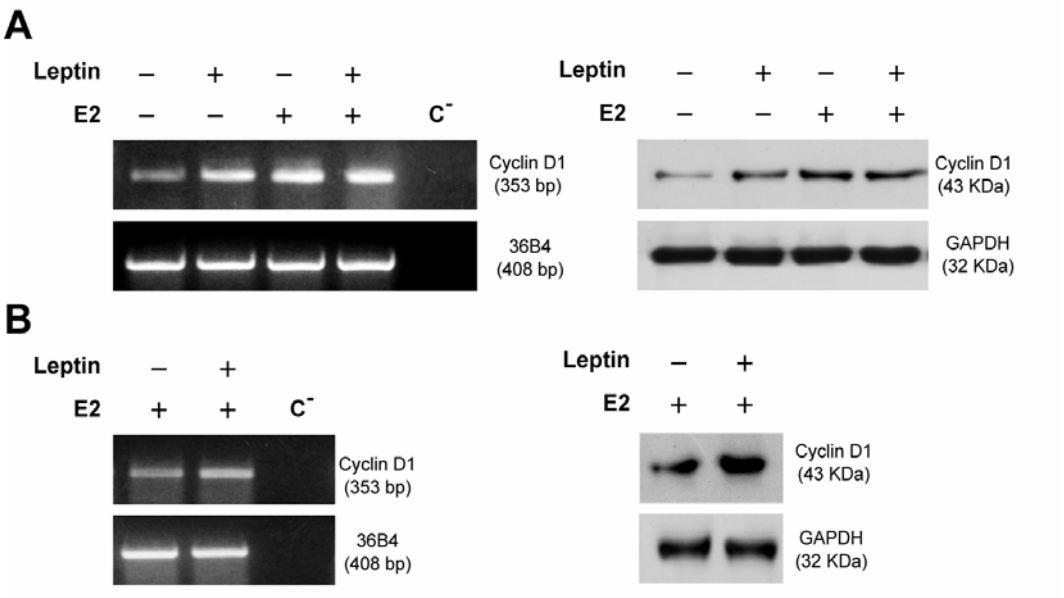

Figure 6: Leptin increases cyclin D1 expression.

Total RNA was isolated from MCF-7 three-dimensional cultures (**A**) or xenografts (**B**) and reversed transcribed. cDNA was subjected to PCR using primers specific for cyclin D1 (30 cycles) or 36B4 (15 cycles). C^-, RNA sample without the addition of reverse transcriptase (negative control). Protein extracts obtained from MCF-7 spheroids (**A**) and xenografts (**B**) were immunoblotted with a specific antibody against human cylin D1. Rapresentative results are shown.

Leptin upregulates E-cadherin expression

To investigate if an enhanced expression of E-cadherin occurred in the above mentioned conditions, we performed RT-PCR and western

blotting analysis. Our results demonstrated that either leptin or E_2 and in higher extent the exposure to both hormones increased expression of E-cadherin in terms of mRNA and protein content (Fig 7A). The latter results were also evident in MCF-7 xenografts (Fig. 7B).

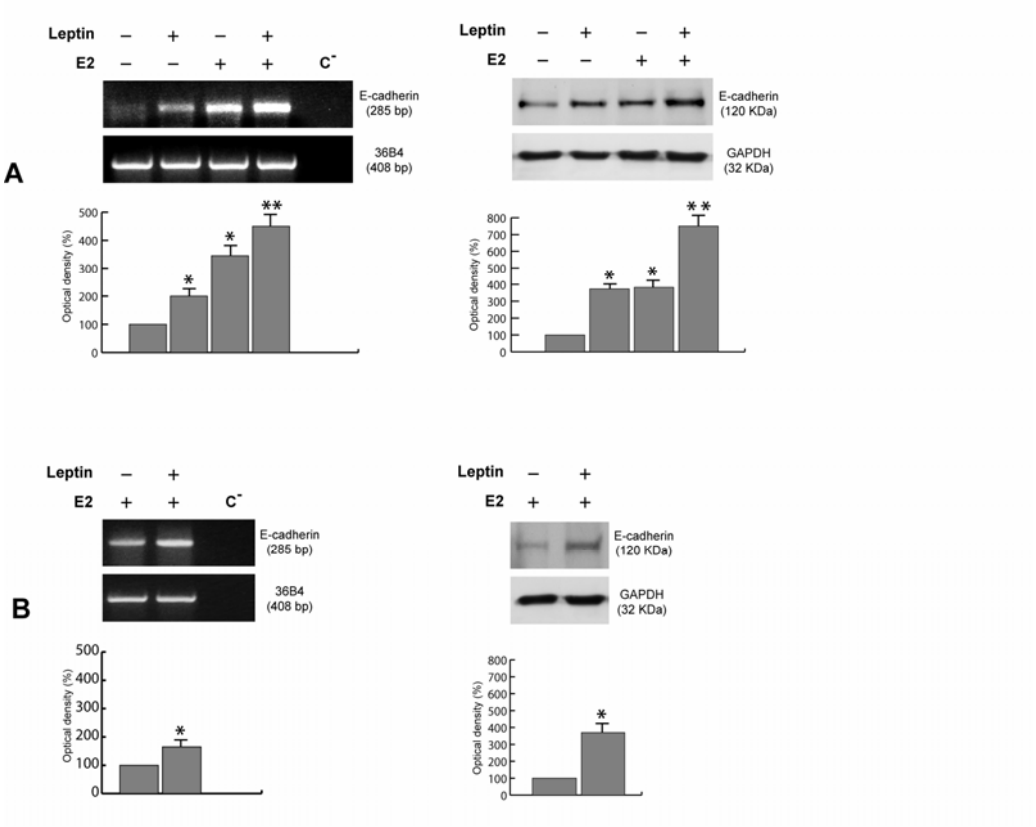

Figure 7: Leptin upregulates E-cadherin expression in MCF-7 spheroids and xenografts.
RT-PCR of E-cadherin mRNA was performed in MCF-7 three-dimensional cultures stimulated for 48h with 1000 ng/ml leptin and/or 100 nM E_2 (**A**) as well as in xenografts (**B**). 36B4 mRNA levels were determined as a control. C^-, RNA sample without the addition of reverse transcriptase (negative control). Protein extracts obtained from MCF-7 spheroids (**A**) and xenografts (**B**) were immunoblotted with a specific antibody against human E-cadherin. Representative results are shown. The histograms represent the mean ± S.E. of three separate experiments in which the band intensities were evaluated in terms of optical density arbitrary units and expressed as the percentage of the control assumed as 100%.

To evaluate whether both hormones were able to activate E-cadherin promoter, we transiently transfected MCF-7 cells with human E-cadherin promoter plasmid (p-1008/+49).

A significant increase in promoter activity was observed in the transfected cells exposed to leptin and/or E_2 for 48h (Fig. 8A).

In contrast, we observed that leptin was unable to activate the constructs containing different deleted segments of human E-cadherin promoter (p-164/+49 and p-83/+49) with respect to the full length, while E_2 induced activation in the presence of p-164/+49 construct (Fig. 8B and C).

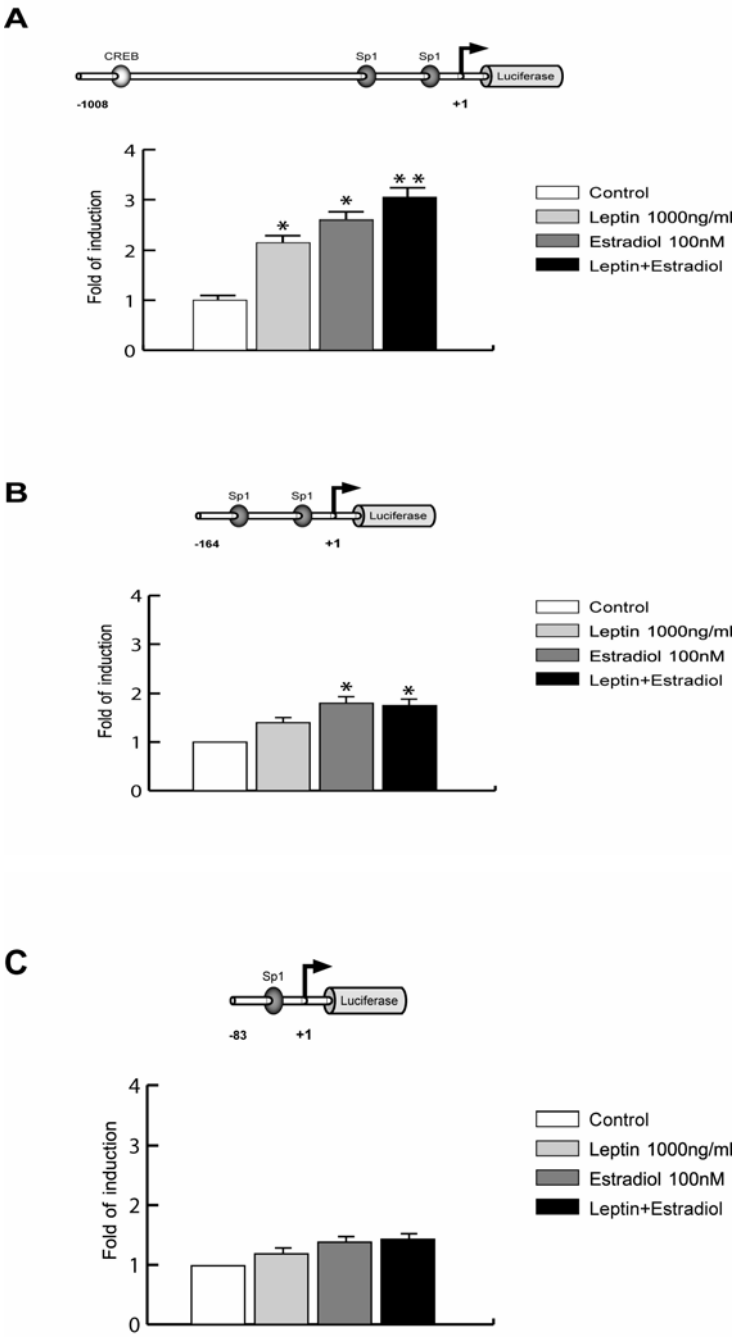

Figure 8: Leptin upregulates E-cadherin full length promoter activity in MCF-7 cells.

MCF-7 cells were transiently transfected with a luciferase reporter plasmids containing the human E-cadherin promoter full length p-1008/+49 (**A**) or deleted segments of human E-cadherin promoter p-164/+49 (**B**) and p-83/+49 (**C**). Schematic representation of human E-cadherin promoter constructs are shown. The +1 position represent the transcriptional initiation site. The cells were left untreated (control) or treated in the presence of 1000 ng/ml of leptin and/or 100 nM of E_2. The values represent the means ± S.E. of three separate experiments. In each experiment, the activities of the transfected plasmid was assayed in triplicate transfections. * $p < 0.05$, ** $p < 0.01$ compared with control.

Leptin enhances CREB- and Sp1-DNA binding activity to E-cadherin promoter

The role of leptin and E_2 on the trascriptional activity of E-cadherin gene, was explored analyzing the nucleotide sequence of the E-cadherin gene promoter. We evidenced, upstream to the initiation transcription site, one CRE (-925/-918) and two Sp-1 (-144/-132 and -51/-39) as putative effectors of leptin and estrogens (Fig. 9).

Figure 9: Nucleotide sequence of the E-cadherin gene promoter.

For instance, in MCF-7 cells transiently transfected with E-cadherin promoter plasmid bearing CREB mutated site (CREB mut), we observed that the stimulatory effect of leptin was abrogated, while the activation of E_2 still persisted, even though in a lower extent with respect to the intact promoter (Fig. 10).

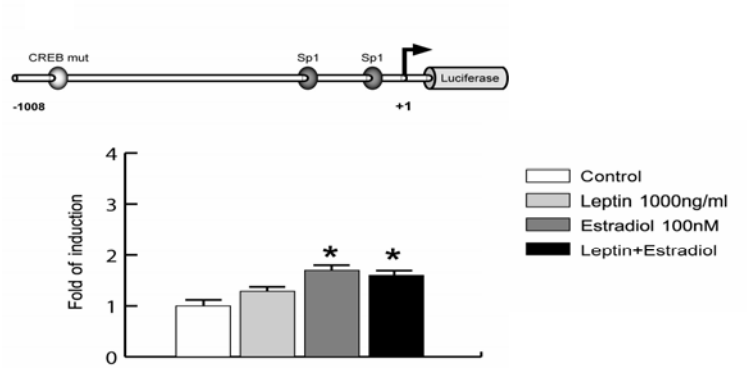

Figure 10: Leptin upregulates E-cadherin promoter activity through CREB site.

MCF-7 cells were transiently transfected with a luciferase reporter plasmid containing the human E-cadherin promoter full-length mutated in the CREB site (CREB mut). Schematic representation of human E-cadherin promoter constructs. The +1 position represents the transcriptional initiation site. The cells were left untreated (control) or treated in the presence of 1,000 ng/mL leptin and/or 100 nmol/L E_2. Columns, mean of three separate experiments; bars, SE. In each experiment, the activities of the transfected plasmid were assayed in triplicate transfections. *, $P < 0.05$ compared with control.

To characterize the role of these motifs in modulating E-cadherin promoter activity, we performed EMSA. Nuclear extracts from MCF-7 cells, using as probe a CRE responsive element, showed two protein-DNA complexes (Fig. 11A lane 1), which were abolished by the addition of a non-radiolabeled competitor (Fig. 11A lane 2). Leptin treatment induced a strong increase in CREB DNA-binding activity (Fig. 11A lane 3), which was immunodepleted in the presence of CREB antibody (Fig. 11A lane 4). Using transcribed and translated *in vitro* CREB protein, we obtained two bands migrating at the same level as that of MCF-7 nuclear extracts (Fig. 11A lane 9). In the presence of the MAPK inhibitor PD98059, the complex induced by leptin treatment was reduced (Fig. 11B lanes 5 and 9). These findings addressed a specific involvement of leptin signalling in the up-regulation of E-cadherin expression.

Using a DNA probe containing an Sp1 site, we observed in MCF-7 nuclear extracts, a specific protein-DNA complex that was slightly enhanced by leptin, increased upon E_2 exposure and furthermore by the combined treatments (Fig. 11C lanes 1, 3, 5 and 7). In the presence of Sp1 human recombinant protein we observed a single complex that causes the same shift with respect to the band revealed in MCF-7

nuclear extracts (Fig. 11C lane 10). The addition of mithramycin A (100 μM), that binds to GC boxes and prevents sequential Sp1 binding, to nuclear extracts treated with leptin and E_2, blocked the formation of DNA-Sp1 complexes (Fig. 11C lane 9). The original band DNA-protein complex was supershifted by Sp1 antibody (Fig. 11C lanes 4, 6 and 8). In all hormonal treatments performed, the pure antiestrogen ICI 182,780 reduced the Sp1-DNA binding complex (Fig. 11D lanes 5, 7 and 9) evidencing that leptin induced an activation of ERα, as we previously demonstrated (25).

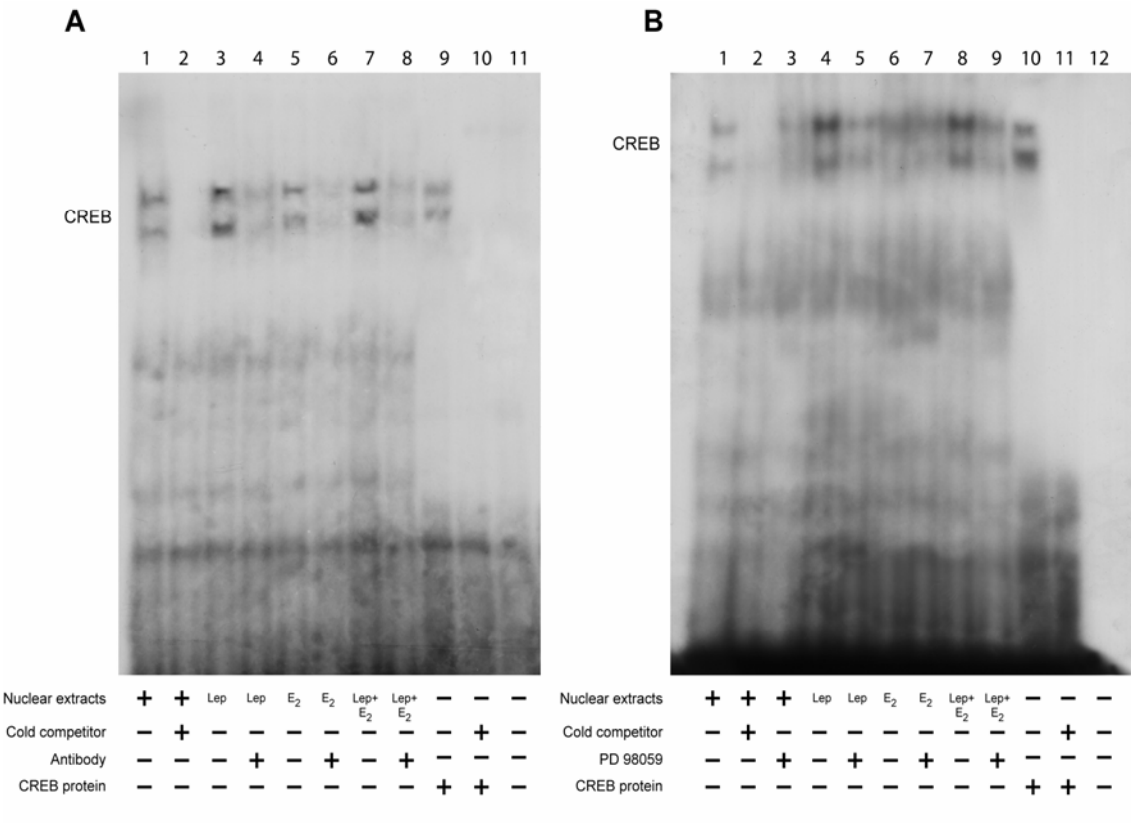

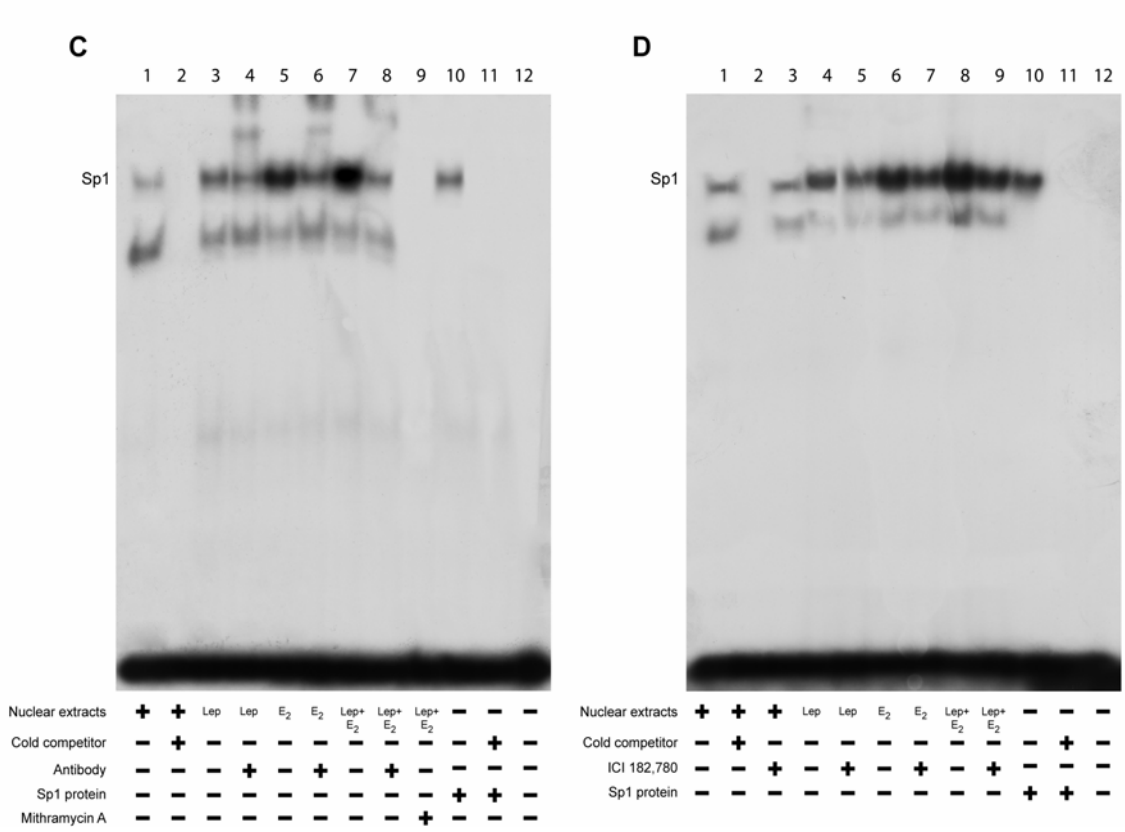

Figure 11: Effects of *in vitro* leptin treatment on CREB and Sp1 DNA-binding activity in MCF-7 cells.

Nuclear extracts from MCF-7 cells were incubated with a double-stranded CREB- (**A** and **B**) or Sp1- (**C** and **D**) specific consensus sequence probe labelled with [γ-^{32}P]ATP and subjected to electrophoresis in a 6% polyacrylamide gel (lane 1). **A**. We used as positive control a transcribed and translated *in vitro* CREB protein (lane 9). Competition experiments were performed by adding as competitor a 100-fold molar excess of unlabeled probe (lanes 2 and 10). MCF-7 nuclear extracts treated with 1000 ng/ml of leptin and/or 100 nM of E_2 for 48h incubated with probe are shown in lanes 3, 5 and 7 respectively. The specificity of the binding was tested by adding to the reaction mixture a CREB antibody (lanes 4, 6 and 8). **B**. MCF-7 cells were serum-starvated overnight with 10 μM PD 98059 (lanes 3, 5, 7 and 9). Lanes 11 (A) and 12 (B) contain probe alone. **C.** Sp1 human recombinant protein was used as positive control (lane 10). Competition experiments were performed by adding as competitor a 100-fold molar excess of unlabeled probe (lanes 2 and 11). MCF-7 nuclear extracts treated with 1000 ng/ml of leptin and/or 100 nM of E_2 for 48h incubated with probe are shown in lanes 3, 5 and 7 respectively. The specificity of the binding was tested by adding to the reaction mixture a Sp1 antibody (lanes 4, 6 and 8). The formation of DNA-Sp1 complexes was blocked by the addition of 100 μM mithramycin A (lane 9). **D.** The pure antiestrogen ICI 182,780 (1 μM) was added in leptin- (lane 5) and/or E_2-treated (lanes 7 and 9) MCF-7 nuclear extracts. Lanes 12 contain probe alone.

Effects of leptin on CREB and Sp1 recruitment to the E-cadherin promoter

To corroborate EMSA results, we performed ChIP assay. We found that the stimulation of MCF-7 cells with leptin increased the recruitment of CREB to E-cadherin gene promoter (Fig. 12A). Furthermore, we observed that leptin or E_2 stimulated the recruitment of Sp1 to the E-cadherin promoter and the combined treatment induced an additive effect (Fig. 12B).

The latter event suggests that leptin and E_2 may converge in activating ERα to recruit Sp1 on E-cadherin promoter.

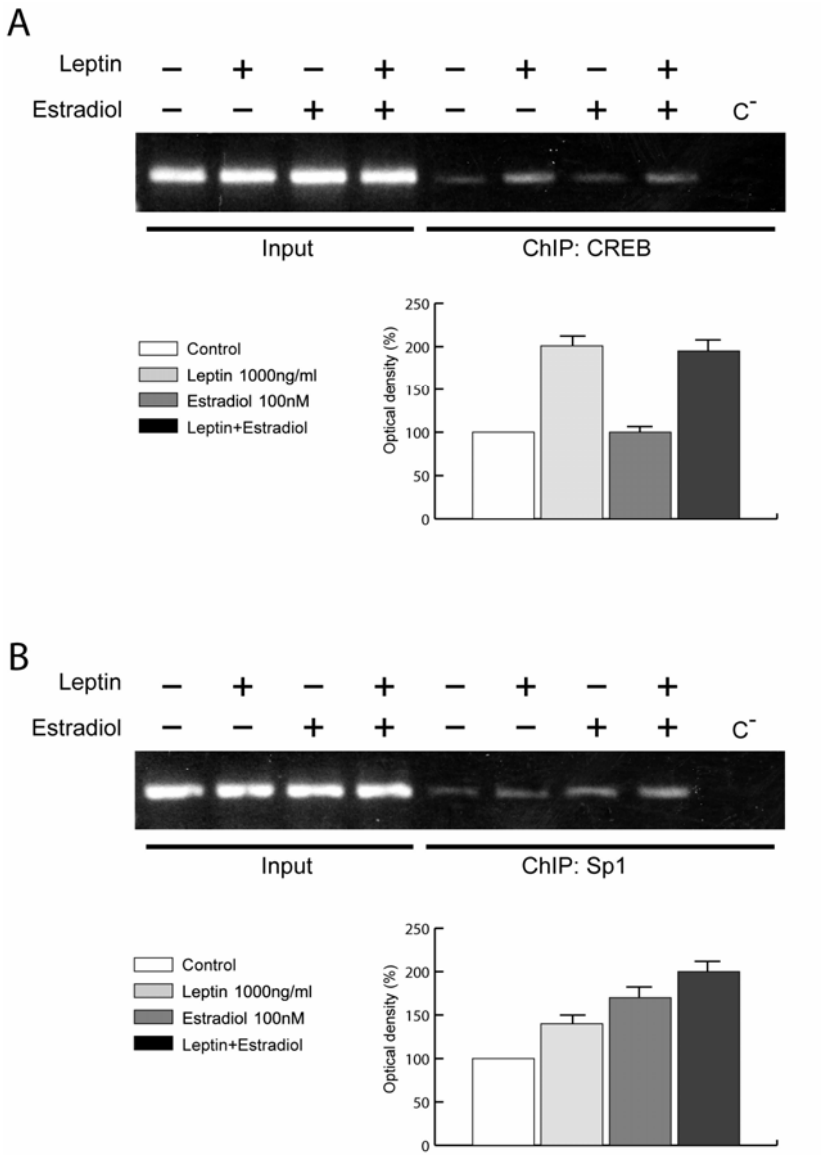

Figure 12: Recruitment of CREB and Sp1 to the E-cadherin promoter in MCF-7 cells.

The cells were treated for 1h with 1000 ng/ml leptin and/or 100 nM E_2 or left untreated. The precleared chromatin was immunoprecipitated with specific antibodies, namely, anti-CREB for CREB IPs (**A**) or anti-Sp1 for Sp1 IPs (**B**). E-cadherin promoter sequences containing CREB or Sp1 sites were detected by PCR with specific primers, as detailed in Materials and Methods. To determine input DNA, the E-cadherin promoter fragment was amplified from 5 µl purified soluble chromatin before immunoprecipitation. PCR products obtained at 30 cycles are shown. ChIP with non-immune IgG was used as negative control (C^-). This experiment was repeated three times with similar results and the most representative experiment is shown. The histograms represent the mean ± S.E. of three separate experiments in which the band intensities were evaluated in terms of optical density arbitrary units and expressed as the percentage of the control assumed as 100%.

Involvement of ERα in the leptin-induced upregulation of E-cadherin expression

Stemming from the data provided by EMSA and ChIP assays, we evaluated the involvement of ERα in the enhanced E-cadherin expression induced by leptin. Our results demonstrated that, in three-dimensional cultures, in the presence of the pure antiestrogen ICI 182,780 the upregulatory effect of leptin on E-cadherin protein expression still persisted, while the stimulatory effects of E_2 was abrogated (Fig. 13A).

In addition, the specific role of leptin signalling in upregulating E-cadherin expression, was also confirmed by functional studies in ERα negative HeLa cells. We evidenced that leptin was able to activate E-cadherin promoter (Fig. 13B) which was abrogated in the presence of ERK2 and STAT3 dominant negative (Fig. 13C), sustaining furthermore the involvement of leptin signalling. It is worth to note how the ectopic expression of ERα in HeLa cells was able to potentiate the effect of leptin (Fig. 13B).

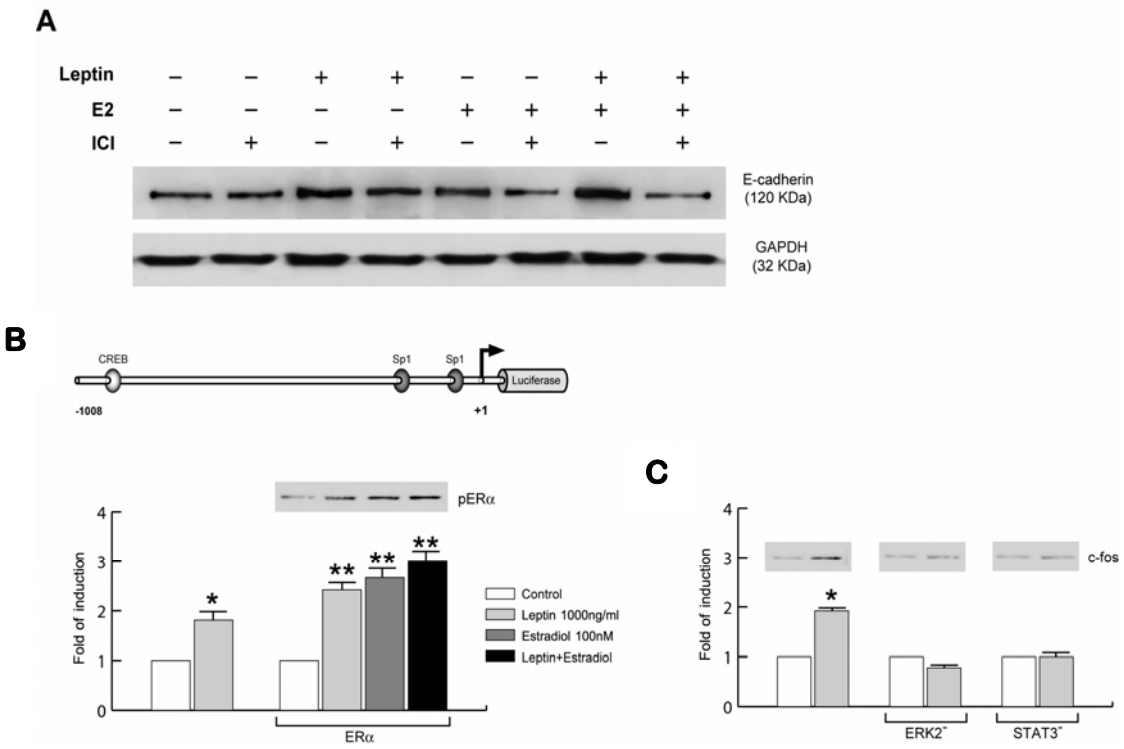

Figure 13: Influence of ERα on leptin-induced upregulation of E-cadherin expression.

A. MCF-7 spheroids were preincubated with 1 μM ICI 182,780 for 1h and then treated with leptin (1000 ng/ml) and/or E_2 (100 nM) for 48h. Total proteins (50 μg) were immunoblotted with a specific antibody against human E-cadherin. GAPDH serves as loading control.

B. Estrogen receptor negative HeLa cells were transfected with a plasmid containing E-cadherin promoter or cotransfected with E-cadherin promoter and pHEGO. Transfected cells were treated with leptin (1000 ng/ml) and/or E_2 (100 nM) for 48h. The values represent the means ± S.E. of three separate experiments. In each experiment, the activities of the transfected plasmids were assayed in triplicate transfections. Small square shows western blot analysis for phosphorylated ERα using anti-phospho-ERα (ser 118). * $p < 0.05$, ** $p < 0.01$ compared with control.

C. HeLa cells were transiently transfected with dominant negative ERK2 or STAT3 plasmid and then treated for 48h with leptin. In each experiment, the activities of the transfected plasmids were assayed in triplicate transfections. Small squares show western blot analysis for c-fos. * $p < 0.05$ compared with control.

To test the activity of the transfected ERα we performed western blotting analysis for phosphorylated ERα, while for dominant negative ERK2 and STAT3 genes we evaluated the expression of c-fos, as target of both pathways (31-33). Moreover, in BT-20 cells lacking of ERα, leptin-enhanced E-cadherin protein content was reduced in the presence of either ERK2 or STAT3 dominant negative. In the same cells, cotransfected with ERα and ERK2 or STAT3 dominant negative, E_2 alone or in combination with leptin was unable to maintain the upregulatory effect on E-cadherin expression (Fig. 14).

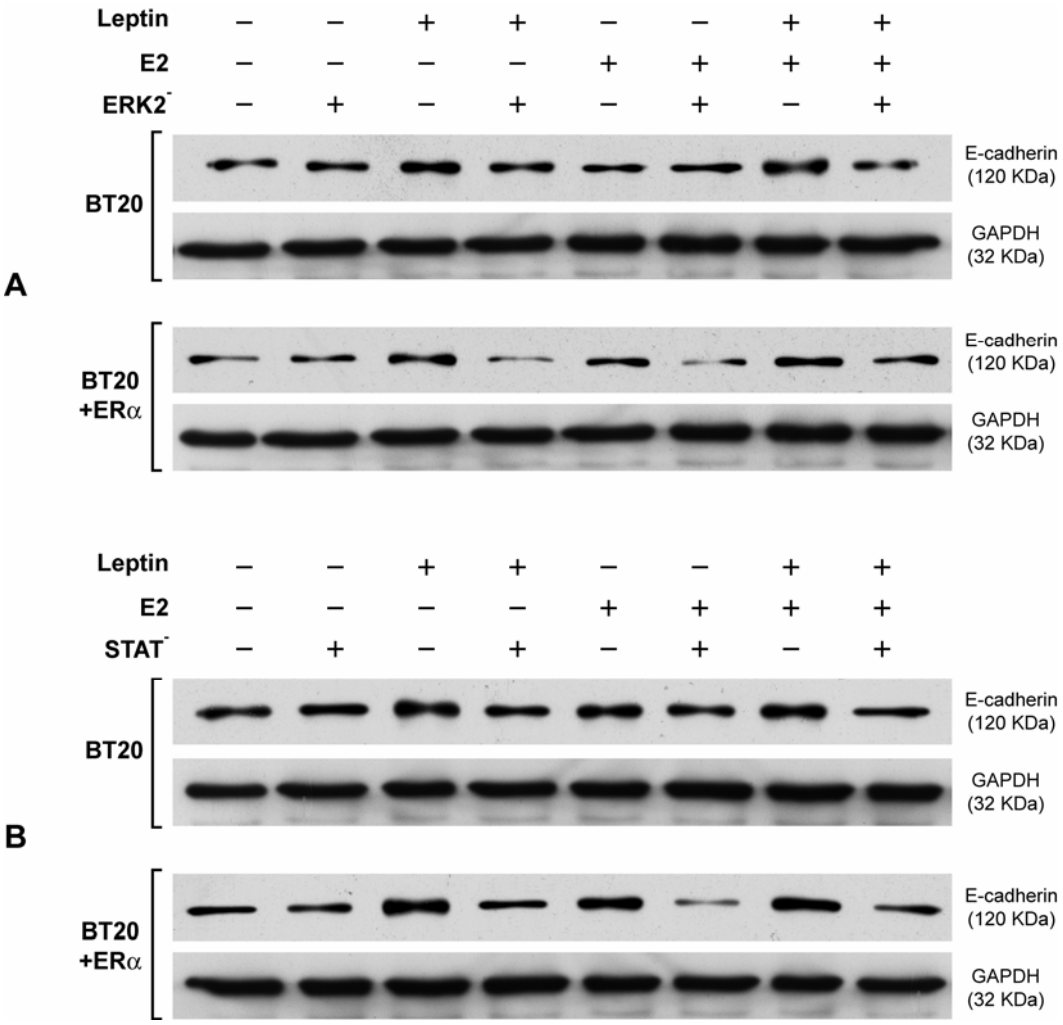

Figure 14: Role of ERα on leptin-induced E-cadherin expression.

BT-20 cells were transfected with ERK2 dominant negative (**A**) or with STAT3 dominant negative (**B**) in the presence or absence of ERα and then treated with leptin (1000 ng/ml) and/or E_2 (100 nM). Total proteins (50 μg) were immunoblotted with a specific antibody against human E-cadherin. GAPDH serves as loading control. Results are representative of three independent experiments.

Discussion

Leptin stimulates cell growth, counteracts apoptosis, and induces migration and angiogenic factors in different cellular cancer models (10). For instance, hyperleptinemia is a common feature of obese women, who have a higher risk of breast cancer than women with normal weight (34), but the association between circulating leptin and breast cancer is still not clear. It has been reported that in interstitial fluid of adipose tissue, leptin concentration is higher than the circulating levels (35). Thus, we may reasonably assume that in the presence of an abundant adipose tissue surrounding epithelial breast cancer cells, the paracrine leptin effects become crucial in affecting local and primary tumor progression.

The aim of this study was to evaluate whether leptin can influence local primary breast cancer development and progression, using an *in vivo* model of MCF-7 xenografts implanted in female nude mice, and an *in vitro* system represented by MCF-7 three-dimensional cultures. Our results showed in MCF-7 xenografts that leptin treatment significantly potentiated the E_2-increased tumor size. In the same view, *in vitro* studies revealed that the combined exposure to both

hormones enhanced cell-cell aggregation with respect to the separate treatments.

E-cadherin is an intercellular adhesion molecule generally implicated as tumor suppressor in several types of epithelial tumors, based on findings that the expression of this homotypic adhesion molecule is frequently lost in human epithelial cancers (18,20,21). However, it has well been demonstrated in ovarian epithelial tumors, that E-cadherin expression is much more elevated than normal ovaries, suggesting that E-cadherin can play a role in the development of ovarian carcinomas (36). For instance, it is worth to mention that E-cadherin may serve not only as an intercellular adhesion molecule, but it may trigger intracellular activation of proliferation and survival signals (37).

In our study, the increased cell-cell aggregation, observed in MCF-7 three-dimensional cultures upon leptin and/or E_2 treatments, appears to be dependent on E-cadherin molecule that has an indispensable role in this process. Indeed, the addition of a function-blocking E-cadherin antibody or a calcium chelating agent, EGTA, blocked cell-cell adhesion induced by both hormones. Besides, we demonstrated by adhesion assay a greater binding of cells pretreated with leptin and/or E_2 on E-cadherin/Fc protein-coated dishes.

In the same experimental conditions an increased proliferative rate was observed upon leptin or E_2 exposure, which was completely abrogated when E-cadherin function was blocked.

An important cell cycle regulator, such as cyclin D1, resulted to be upregulated in three-dimensional cultures as well as in xenografts.

Besides, in both models we demonstrated that leptin and/or E_2 enhanced E-cadherin expression in terms of mRNA, protein content and promoter activity.

The analysis of E-cadherin promoter sequence, revealed the presence of CRE and Sp1 sites, as potential target of leptin and E_2 signals. It is well documented how leptin and E_2 through non genomic effects are able to activate MAPK pathway that induces activation of CREB kinase, a member of the $p90^{RSK}$ family that corresponds to RSK2 and thereby phosphorylates CREB serine 133 (38-40). This well fits with our functional studies demonstrating that leptin was no longer able to activate the E-cadherin gene promoter mutated in the CREB site, while E_2 maintained an activatory effect even though in a lower extent with respect to the intact promoter. The latter data suggest that the activatory effect of E_2 may persist through its binding to Sp1-DNA complex.

The important role of Sp1 responsive element in activating E-cadherin promoter was demonstrated by EMSA and ChIP assays. Our results evidenced that E_2, as extensively documented, acts in a nonclassic way through the interaction of ERα with Sp1 (41-45). It is worth to note that upon leptin exposure we also observed an increase in Sp1-DNA binding activity, clearly reduced in the presence of the pure antiestrogen ICI 182,780, as well as an enhanced recruitment of Sp1 to E-cadherin promoter. These observations are supported by our previous findings reporting that leptin is able to transactivate, in a unliganded-dependent manner, ERα through MAPK signal (25).

A cross-talk between leptin and E_2 has been well documented in neoplastic mammary tissues and breast cancer cell lines (15,25,46,47). For instance, E_2 upregulates leptin expression in MCF-7 cells (15), while leptin is an amplifier of E_2 signalling through a double mechanism: an enhanced aromatase gene expression (46) and a direct transactivation of ERα (25). Thus, we investigated whether the upregolatory effect induced by leptin on E-cadherin expression can be modulated by ERα. We found that E-cadherin protein appears still upregulated by leptin in the presence of the pure antiestrogen ICI 182,780. Moreover, in HeLa cells, leptin was able to activate E-

cadherin promoter, which was abrogated in the presence of ERK2 or STAT3 dominant negative, suggesting that leptin signalling is involved in enhancing E-cadherin expression. These latter data are supported by western blotting analysis performed in BT-20 cells lacking of ERα in which ERK2 and STAT3 dominant negative reversed leptin-enhanced E-cadherin protein content. The upregulatory effect induced by E_2 on E-cadherin expression in the presence of ectopic ERα appeared inhibited in the presence of ERK2 and STAT3 dominant negative. The latter findings may be a consequence of the enhanced expression of leptin receptor upon E_2 exposure (15), which may have an impaired signalling on E-cadherin expression. An additional explanation, which could coexist with the previous one, may be that both ERK2 and STAT3 dominant negative could interfere with ERα/Sp1 interaction at level of E-cadherin gene transcription (48).

A hypothetical model of the possible mechanism through which leptin and E_2 may functionally interact in modulating E-cadherin expression in breast cancer is shown in Scheme 1. Leptin through MAPK activation may phosphorylate CREB and induce its transactivation. For instance, CREB phosphorylated at serine 133 is often reported not

only as an index of PKA but also as an effector of MAPK activation (49). Concomitantly, leptin in the presence of E_2 may potentiate the transactivation of ERα, which in turn may interact with Sp1 and bind DNA in a nonclassic way. On the other hand it is well known that ERα, in the presence of its natural ligand, interacts with Sp1.

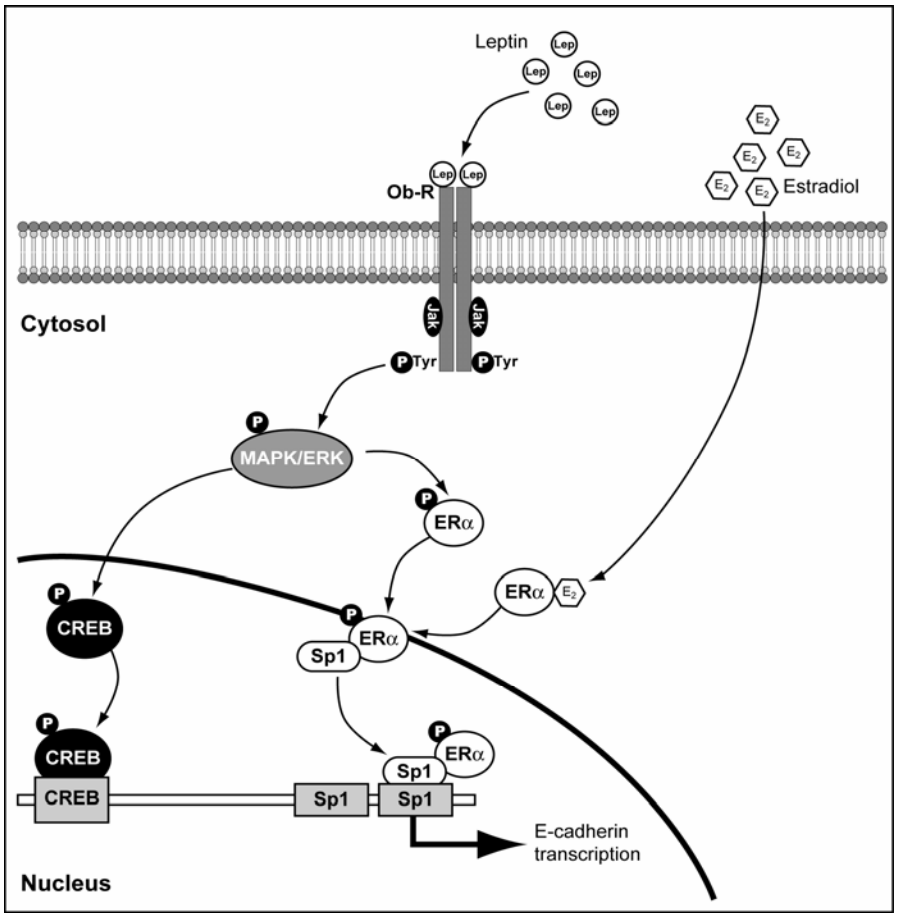

Scheme 1. Hypothesized model of leptin signalling in modulating E-cadherin expression in breast cancer.

Interaction of leptin with its specific receptor (ObR) induces, through MAPK activation, phosphorylation of CREB and its transactivation. Leptin may potentiate the transactivation of ERα, which in turn may interact with Sp1 and bind DNA in a nonclassic way. Both CREB and Sp1 transcriptional factors bind on E-cadherin promoter at specific responsive sequences and induce an enhanced E-cadherin expression.

Thus, we may reasonably propose that, upon leptin exposure, the increased E-cadherin-mediated cellular adhesion and activation of proliferation signals may enhance the transformation of normal epithelial cells to neoplastic cells, and then stimulate the growth of tumor mass. Distinct from its role as a tumor suppressor, E-cadherin may function as tumor enhancer in the development of primary breast cancer.

In conclusion, all these data address how leptin and E_2 signalling may represent a target of combined pharmacological tools to be exploited in the novel therapeutical adjuvant strategies for breast cancer treatment particularly in obese women.

In the latter concern, according to our on going results, derivate of thiazolidinediones (TZDs) are intriguing molecule exhibiting both the capability to inhibit leptin gene expression as well as to antagonized estrogen signalling. The latter effects appear to occur through a double mechanism: a) down regulation of aromatase expression, b) antagonistic action on ERα at genomic level (50). Besides we should taking into account how these substances may play important metabolic action leading at a reduction of insulin-resistance generally associated to the obesity (51). On the basis of these observation the

derivate of TZDs may be implemented in the adjuvant strategies for breast cancer treatment, particular in postmenopausal obese women.

References

(1) **Zhang Y, Proenca R, Maffei M, Barone M, Leopold L, Friedman JM.** Positional cloning of the mouse obese gene and its human homologue. Nature 1994;372:425-32.

(2) **Halaas JL, Gajiwala KS, Maffei M, et al.** Weight-reducing effects of the plasma protein encoded by the obese gene. Science 1995;269:543-6.

(3) **Bray GA.** The underlying basis for obesity: relationship to cancer. J Nutr 2002;132:3451-5S.

(4) **Bonnet M, Delavaud C, Laud K, et al.** Mammary leptin synthesis, milk leptin and their putative physiological roles. Reprod Nutr Dev 2002; 42(5):399-413.

(5) **Ahima RS, Flier JS.** Adipose tissue as an endocrine organ. Trends Endocrinol Metab 2000;11:327-32.

(6) **Tartaglia LA.** The leptin receptor. J Biol Chem 1997;272(10):6093-6.

(7) **White DW, Kuropatwinski KK, Devos R, Baumann H, Tartaglia LA.** Leptin receptor (OB-R) signaling. Cytoplasmic domain mutational analysis and evidence for receptor homo-oligomerization. J Biol Chem 1997;272(7):4065-71.

(8) **Bjorbaek C, Uotani S, da Silva B, Flier JS.** Divergent signaling capacities of the long and short isoforms of the leptin receptor. J Biol Chem 1997;272:32686-95.

(9) **Yamashita T, Murakami T, Otani S, Kuwajima M, Shima K.** Leptin receptor signal transduction: OBRa and OBRb of fa type. Biochem Biophys Res Commun 1998;246:752-9.

(10) **Garofalo C, Surmacz E.** Leptin and cancer. J Cell Physiol 2006;207:12-22.

(11) **Calle EE, Kaaks R.** Overweight, obesity and cancer: epidemiological evidence and proposed mechanisms. Nat Rev Cancer 2004;4:579-91.

(12) **Hu X, Juneja SC, Maihle NJ, Cleary MP.** Leptin - growth factor in normal and malignant breast cells and for normal mammary gland development. J Natl Cancer Inst 2002;94:1704-11.

(13) **Cleary MP, Phillips FC, Getzin SC, et al.** Genetically obese MMTV-TGF-/$Lep^{ob}Lep^{ob}$ do not develop mammary tumors. Breast Cancer Res Treat 2003;77:205-15.

(14) **Cleary MP, Juneja SC, Phillips FC, Hu X, Grande JP, Maihle NJ.** Leptin receptor-deficient MMTV-TGF-/$Lep^{db}Lep^{db}$ female mice do not develop oncogene-induced mammary tumors. Exp Biol Med (Maywood) 2004;229:182-93.

(15) **Garofalo C, Koda M, Cascio S, et al.** Increased expression of leptin and the leptin receptor as a marker of breast cancer progression: possible role of obesity-related stimuli. Clin Cancer Res 2006;12(5):1447-53.

(16) **Takeichi M.** Cadherin cell adhesion receptors as a morphogenetic regulator. Science 1991;251:1451-55.

(17) **Takeichi M.** Morphogenetic roles of classic cadherins. Curr Opin Cell Biol 1995;7:619-27.

(18) **Perl AK, Wilgenbus P, Dahl U, Semb H, Christofori G.** A causal role for E-cadherin in the transition from adenoma to carcinoma. Nature 1998;392(6672):190-3.

(19) **Behrens J, Mareel MM, Van Roy FM, Birchmeier W.** Dissecting tumor cell invasion: epithelial cells acquire invasive properties after the loss of uvomorulin-mediated cell-cell adhesion. J Cell Biol 1989;108(6):2435-47.

(20) **Frixen UH, Behrens J, Sachs M, et al.** E-cadherin-mediated cell-cell adhesion prevents invasiveness of human carcinoma cells. J Cell Biol 1991;113(1):173-85.

(21) **Vleminckx K, Vakaet L Jr, Mareel M, Fiers W, van Roy F.** Genetic manipulation of E-cadherin expression by epithelial tumor cells reveals an invasion suppressor role. Cell 1991;66(1):107-19.

(22) **Dorudi S, Sheffield JP, Poulsom R, Northover JM, Hart IR.** E-cadherin expression in colorectal cancer. An immunocytochemical and in situ hybridization study. Am J Pathol 1993;142(4):981-6.

(23) **Mbalaviele D, Dunstan CR, Sasaki A, Williams PJ, Mundy GR, Yoneda T.** E-cadherin expression in human breast cancer cells suppresses the development of osteolytic bone metastases in an experimental metastasis model. Cancer Res 1996;56:4063-70.

(24) **Tsai CN, Tsai CL, Tse KP, Chang HY, Chang YS.** The Epstein-Barr virus oncogene product, latent membrane protein 1, induces the downregulation of E-cadherin gene expression via activation of DNA methyltransferases. Proc Natl Acad Sci USA 2002; 99(15):10084-9.

(25) **Catalano S, Mauro L, Marsico S, et al.** Leptin induces, via ERK1/ERK2 signal, functional activation of estrogen receptor alpha in MCF-7 cells. J Biol Chem 2004;279(19):19908-15.

(26) **Morelli C, Garofalo C, Sisci D, et al.** Nuclear insulin receptor substrate 1 interacts with estrogen receptor alpha at ERE promoters. Oncogene 2004; 23: 7517–26.

(27) **Dangles V, Femenia F, Laine V, et al.** Two- and three-dimensional cell structures govern epidermal growth factor survival function in human bladder carcinoma cell lines. Cancer Res 1997;57(16):3360-4.

(28) **Kunz-Schughart LA, Kreutz M, Knuechel R.** Multicellular spheroids: a three-dimensional in vitro culture system to study tumour biology. Int J Exp Phatol 1998;79(1):1-23.

(29) **Santini MT, Rainaldi G.** Three-dimensional spheroid model in tumor biology. Pathobiology 1999;67(3):148-57.

(30) **Sutherland RM.** Cell and environment interactions in tumor microregions: the multicell spheroid model. Science 1988;240(4849):177-84.

(31) **Maggiolini M, Vivacqua A, Fasanella G, et al.** The G protein-coupled receptor GPR30 mediates c-fos up-regulation by 17beta-estradiol and phytoestrogens in breast cancer cells. J Biol Chem 2004;279(26):27008-16.

(32) **De Sousa LP, Brasil BS, Silva BM, et al.** Plasminogen/plasmin regulates c-fos and egr-1 expression via the MEK/ERK pathway. Biochem Biophys Res Commun 2005;329(1):237-45.

(33) **Darnel JE.** The JAK-STAT pathway: summary of initial studies and recent advances. Recent Prog Horm Res 1996;51:391-403.

(34) **Lorincz AM, Sukumar S.** Molecular links between obesity and breast cancer. Endocr Relat Cancer 2006;13(2):279-92.

(35) **Orban Z, Remaley AT, Sampson M, Trajanoski Z, Chrousos GP.** The differential effect of food intake and beta-adrenergic stimulation on adipose-derived hormones and cytokines in man. J Clin Endocrinol Metab 1999;84(6):2126-33.

(36) **Reddy P, Lui L, Ren C, et al.** Formation of E-cadherin-mediated cell-cell adhesion activates AKT and mitogen activated protein kinase via phosphatidylinositol 3 kinase and ligand-independent activation of epidermal growth factor receptor in ovarian cancer cells. Mol Endocrinol 2005;19(10):2564-78.

(37) **Steinberg MS, McNutt PM.** Cadherins and their connections: adhesion junctions have broader functions. Curr Opin Cell Biol 1999;11:554-60.

(38) **Xing, J, Ginty, DD, Greenberg, ME.** Coupling of the RAS-MAPK pathway to gene activation by RSK2, a growth factor-regulated CREB kinase. Science 1996;273:959-63.

(39) **Dalby KN., Morrice N, Caudwell FB, Avruch J, Cohen P.** Identification of regulatory phosphorylation sites in mitogen-activated protein kinase (MAPK)-activated protein kinase-1a/p90rsk that are inducible by MAPK. J Biol Chem 1998;273:1496-505.

(40) **Bannister AJ, Oehler T, Wilheim D, Angel P, Kouzarides T.** Stimulation of c-Jun activity by CBP: c-jun residues Ser63/73 are required for CBP induced stimulation in vivo and CBP binding in vitro. Oncogene 1995;11:2509-14.

(41) **Krishnan V, Wang X, Safe S.** Estrogen receptor-Sp1 complexes mediate estrogen-induced cathepsin D gene expression in MCF-7 human breast cancer cells. J Biol Chem 1994;269(22):15912-7.

(42) **Porter W, Saville B, Hoivik D, Safe S.** Functional synergy between the transcription factor Sp1 and the estrogen receptor. Mol Endocrinol 1997;11(11):1569-80.

(43) **Petz LN, Nardulli AM.** Sp1 binding sites and an estrogen response element half-site are involved in regulation of the human progesterone receptor A promoter. Mol Endocrinol 2000;14(7):972-85.

(44) **Saville B, Wormke M, Wang F, et al.** Ligand-, cell-, and estrogen receptor subtype (alpha/beta)-dependent activation at GC-rich (Sp1) promoter elements. J Biol Chem 2000;275(8):5379-87.

(45) **Panno ML, Mauro L, Marsico S, et al.** Evidence that the mouse insulin receptor substrate-1 belongs to the gene family on which the promoter is activated by estrogen receptor alpha through its interaction with Sp1. J Mol Endocrinol 2006;36(1):91-105.

(46) **Catalano S, Marsico S, Giordano C, et al.** Leptin enhances, via AP-1, expression of aromatase in the MCF-7 cell line. J Biol Chem 2003;278(31):28668-76.

(47) **Garofalo C, Sisci D, Surmacz E.** Leptin interferes with the effects of the antiestrogen ICI 182,780 in MCF-7 breast cancer cells. Clin Cancer Res 2004;10(19):6466-75.

(48) **De Miguel F, Lee SO, Onate SA, Gao AC.** Stat3 enhances transactivation of steroid hormone receptors. Nucl Recept 2003;1:3-10.

(49) **Houslay MD, Kolch W.** Cell-type specific integration of cross-talk between extracellular signal-regulated kinase and cAMP signalling. Mol Pharmacol 2000;58:659-68.

(50) **Bonofiglio D, Gabriele S, Aquila S, et al.** Estrogen receptor alpha binds to peroxisome proliferator-activated receptor response element and negatively interferes with peroxisome proliferator-activated receptor gamma signaling in breast cancer cells. Clin Cancer Res 2005;11(17):6139-47.

(51) **Bonofiglio D, Aquila S, Catalano S, et al.** Peroxisome proliferator-activated receptor-gamma activates p53 gene promoter binding to the nuclear factor-kappaB sequence in human MCF7 breast cancer cells. Mol Endocrinol 2006;20(12):3083-92.

Full Papers

Evidences that leptin upregulates E-cadherin expression in breast cancer: effects on tumor growth and progression.
Mauro L, Catalano S, Bossi G, Pellegrino M, Barone I, Morales S, Giordano C, Bartella V, Casaburi I, Andò S.
Cancer Research, 2007, 67 (7): 3412-3421.

Fas ligand expression in TM4 sertoli cells is enhanced by estradiol "in situ" production.
Catalano S, Rizza P, Gu G, Barone I, Giordano C, Marsico S, Casaburi I, Middea E, Lanzino M, Pellegrino M, Andò S.
Journal of Cellular Physiology, 2007, 211: 448-56.

Evidence that low doses of Taxol enhance the functional transactivatory properties of p53 on p21 waf promoter in MCF-7 breast cancer cells.
Panno ML, Giordano F, Mastroianni F, Morelli C, Brunelli E, Palma MG, Pellegrino M, Aquila S, Miglietta A, Mauro L, Andò S.
FEBS Letters, vol.580:2371-2380, 2006.

Peroxisome Proliferator-Activated Receptor (PPAR)gamma is expressed by human spermatozoa: its potential role on the sperm physiology.
Aquila S, Bonofiglio D, Gentile M, Middea E, Gabriele S, Belmonte M, Catalano S, Pellegrino M, Andò S.
Journal of Cellular Physiology, 2006, 209(3):977-86.

Abstracts

Fas Ligand in TM4 cells is up-regulated by estradiol through Estrogen Receptor α interaction with Sp-1.
Casaburi I, Catalano S, Rizza P, Marsico S, Gu G, Barone I, Giordano C, Middea E, Lanzino M, Pellegrino M**,** Andò S.
VIII Congresso A.I.B.G., 15-17 Settembre 2005, Sirolo (AN).

Molecular mechanism through which leptin upregulates E-cadherin expression in breast cancer. *In vitro* and *in vivo* effects in tumor cell growth and progression.
Mauro L, Pellegrino M**,** Catalano S, Bossi G, Barone I, Morales S, Giordano C, Giordano F, Bartella V, Panno ML, S. Andò.
The Endocrine Society's 88th Annual Meeting, Boston, MA, June 24-27, 2006.

Molecular mechanism through wich leptin upregulates E-cadherin expression and influences breast cancer cell growth and progression.
Mauro L, PellegrinoM, Catalano S, Bossi G, Barone I, Morales S, GiordanoC, GiordanoF, Bartella V, Salerno M, Panno ML, Andò S.
XXVIII Congresso Nazionale della Società Italiana di Patologia, SIP 2006, Pavia 19-22 Settembre 2006. Oral communication.

The modulatory role of IRS-1 on cell adhesion in human breast cancer cells.
Salerno M, Panno ML, Mauro L, Pellegrino M, Cadavero ML, Morelli C, Garofalo C, Casaburi I, Andò S.
XXVIII Congresso Nazionale della Società Italiana di Patologia, SIP 2006, Pavia 19-22 Settembre 2006. Oral communication.

Evidences that leptin upregulates E-cadherin gene expression in breast cancer and promotes tumor cell growth and progression.
Mauro L, Catalano S, Pellegrino M, Bossi G, Barone I, Morales S, Giordano C, Giordano F, Bartella V, Panno ML, Andò S.
29th Annual San Antonio Breast Cancer Symposium, San Antonio, TX. December 14 - 17, 2006**.** Breast Cancer Research and Treatment, 2006. Abstract #P3109.

PI3-kinase/Akt pathway is involved in the short non genomic autocrine loop between 17-β estradiol and aromatase activity in MCF-7 cells.
Catalano S, Barone I, Giordano C, Casaburi I, Gu G, Rizza P, Pellegrino M, Bonofiglio D, Andò S.
Keystone Symposia, Santa Fe, New Mexico, February 15-20, 2007.

Evidences that leptin upregulates E-cadherin expression in breast cancer: effects on tumor growth and progression
Andò S, Catalano S, Pellegrino M, Bossi G, Barone I, Morales S, Giordano C, Giordano F, Bartella V, Panno ML, Mauro L.
American Society for Investigative Pathology. 2007 Annual Meeting at Experimental Biology. Washington April 28 – May 2, 2007

Evidences that Leptin Up-regulates E-Cadherin Expression in Breast Cancer: Effects on Tumor Growth and Progression

Loredana Mauro,[1] Stefania Catalano,[2] Gianluca Bossi,[5] Michele Pellegrino,[2] Ines Barone,[2] Sara Morales,[1] Cinzia Giordano,[1] Viviana Bartella,[2] Ivan Casaburi,[2] and Sebastiano Andò[1,3,4]

Departments of [1]Cellular Biology and [2]Pharmaco-Biology, [3]Centro Sanitario, and [4]Faculty of Pharmacy, University of Calabria, Rende, Italy and [5]Laboratory of Molecular Oncogenesis, Regina Elena Cancer Institute, Rome, Italy

Abstract

Leptin, a cytokine mainly produced by adipocytes, seems to play a crucial role in mammary carcinogenesis. In the present study, we explored the mechanism of leptin-mediated promotion of breast tumor growth using xenograft MCF-7 in 45-day-old female nude mice, and an *in vitro* model represented by MCF-7 three-dimensional cultures. Xenograft tumors, obtained only in animals with estradiol (E_2) pellet implants, doubled control value after 13 weeks of leptin exposure. In three-dimensional cultures, leptin and/or E_2 enhanced cell-cell adhesion. This increased aggregation seems to be dependent on E-cadherin because it was completely abrogated in the presence of function-blocking E-cadherin antibody or EGTA, a calcium-chelating agent. In three-dimensional cultures, leptin and/or E_2 treatment significantly increased cell growth, which was abrogated when E-cadherin function was blocked. These findings well correlated with an increase of mRNA and protein content of E-cadherin in three-dimensional cultures and in xenografts. In MCF-7 cells both hormones were able to activate E-cadherin promoter. Mutagenesis studies, electrophoretic mobility shift assay, and chromatin immunoprecipitation assays revealed that cyclic AMP–responsive element binding protein and Sp1 motifs, present on E-cadherin promoter, were important for the up-regulatory effects induced by both hormones on E-cadherin expression in breast cancer MCF-7 cells. In conclusion, the present study shows how leptin is able to promote tumor cell proliferation and homotypic tumor cell adhesion via an increase of E-cadherin expression. This combined effect may give reasonable emphasis to the important role of this cytokine in stimulating primary breast tumor cell growth and progression, particularly in obese women. [Cancer Res 2007;67(7):3412–21]

Introduction

Leptin is an adipocyte-derived hormone (1) that, in addition to the control weight homeostasis by regulating food intake and energy expenditure (2, 3), is implicated in the modulation of many other processes such as reproduction, lactation, hematopoiesis, immune responses, cell differentiation, and proliferation (4, 5). The activities of leptin are mediated through the transmembrane leptin receptor (ObR; refs. 6, 7) by activation of the Janus-activated kinase/signal transducers and activators of transcription (STAT) and mitogen-activated protein kinase (MAPK) pathways (8, 9).

Epidemiologic studies show a positive association between obesity and an increased risk of developing different cancers (10, 11). Several lines of evidence suggest that leptin and ObR are involved in the development of normal mammary gland and in mammary carcinogenesis (12–14). It has been recently reported that in primary breast tumors, leptin was detected in 86.4% of cases examined, and its expression was highly correlated with ObR (15). This indicates that leptin can influence breast cancer cells not only by endocrine and/or paracrine actions but also through autocrine pathways.

In epithelium and epithelium-derived tumors, cell-cell adhesion and tumor mass mostly depend on E-cadherin, a 120-kDa transmembrane molecule (16, 17). As it might be expected, E-cadherin seems to have a major influence on primary cancer development and evolution. Alteration in the function of E-cadherin and the cadherin-catenin complex has been implicated in cancer progression (18), invasion (19–21), and metastasis (22, 23).

In this study, we explored a new aspect of the involvement of leptin in initial steps of mammary tumorigenesis. Specifically, we asked whether leptin can affect primary tumor mass either *in vivo* in MCF-7 cell tumor xenograft or *in vitro* in MCF-7 three-dimensional cultures. Our results showed that leptin is able to promote tumor cell proliferation and homotypic tumor cell adhesion via an increase of E-cadherin expression. These combined effects may give reasonable emphasis to the important role of this cytokine in stimulating local primary breast tumor cell growth and progression, particularly in obese women.

Materials and Methods

Plasmids. The plasmids containing the human E-cadherin promoter or its deletions were given by Dr. Y.S. Chang (Chang-Gung University, Republic of China; ref. 24). pHEGO plasmid containing the full length of estrogen receptor α (ERα) cDNA was provided by Dr. D. Picard (University of Geneva). pSG5 vector containing the cDNA-encoding dominant-negative STAT3, which is a variant of the transcription factor STAT3 lacking an internal domain of 50 bp located near the COOH terminus ($STAT^-$), was given by Dr. J. Turkson (University of South Florida, College of Medicine, Tampa, FL). pCMV5myc vector containing the cDNA-encoding dominant-negative extracellular signal-regulated kinase 2 K52R ($ERK2^-$) was provided by Dr. M. Cobb (Southwestern Medical Center, Dallas, TX).

Site-directed mutagenesis. The E-cadherin promoter plasmid-bearing cyclic AMP–responsive element binding protein (CREB)–mutated site (CREB mut) was created by site-directed mutagenesis using Quick Change kit (Stratagene, La Jolla, CA). We used as template the human E-cadherin

Note: Supplementary data for this article are available at Cancer Research Online (http://cancerres.aacrjournals.org/).

L. Mauro and S. Catalano contributed equally to this work.

Requests for reprints: Sebastiano Andò, Department of Cellular Biology, University of Calabria, Via Pietro Bucci, cubo 4c, 87036 Arcavacata, Rende (CS), Italy. Phone: 39-984-496201; Fax: 39-984-492929-496203; E-mail: sebastiano.ando@unical.it.

doi:10.1158/0008-5472.CAN-06-2890

promoter, and the mutagenic primers were as follows: 5′-AGGGTGGATCACCTGAtacCAGGAGTTCCAGACCAGC-3′ and 5′-GCTGGTCTGGAACTCCTGgtaTCAGGTGATCCACCCT-3′. The constructed reporter vector was confirmed by DNA sequencing.

Cell lines and culture conditions. MCF-7, HeLa, and BT-20 cells were obtained from the American Type Culture Collection (Manassas, VA). MCF-7 and HeLa cells were maintained in DMEM/F-12 containing 5% calf serum and BT-20 cells were cultured in MEM supplemented with 10% fetal bovine serum, 1% Eagle's nonessential amino acids, and 1% sodium pyruvate (Sigma, Milan, Italy). Cells were cultured in phenol red–free DMEM (serum-free medium), containing 0.5% bovine serum albumin, 24 h before each experiment. All media were supplemented with 1% L-glutamine and 1% penicillin/streptomycin (Sigma).

***In vivo* studies.** The experiments *in vivo* were done in 45-day-old female nude mice (*nu/nu Swiss*; Charles River, Milan, Italy). At day 0, the animals were fully anesthetized by i.m. injection of 1.0 mg/kg Zoletil (Virbac) and 0.12% Xylor (Xylazine) to allow the s.c. implantation of estradiol (E_2) pellets (1.7 mg per pellet, 60-day release; Innovative Research of America, Sarasota, FL) into the intrascapular region of mice. The day after, exponentially growing MCF-7 cells (5.0×10^6 per mouse) were inoculated s.c. in 0.1 mL of Matrigel (BD Biosciences, Bedford, MA). Leptin treatment was started 24 h later, when animals were injected i.p. with either solutions: recombinant human leptin (230 μg/kg) diluted in saline + 0.3% bovine serum albumin (BSA) or saline + 0.3% BSA only (control). The treatment was done for 5 days a week until the 13th week. Tumor development was followed twice a week by caliper measurements along two orthogonal axes: length (L) and width (W). The volume (V) of tumors was estimated by the following formula: $V = L \times (W^2) / 2$. At the time of killing (13 weeks), tumors were dissected out from the neighboring connective tissue, frozen in nitrogen, and stored at −80°C. All the procedures involving animals and their care have been conducted in conformity with the institutional guidelines at the Laboratory of Molecular Oncogenesis, Regina Elena Cancer Institute in Rome.

Three-dimensional spheroid culture and cell growth. The cells were plated in single-cell suspension in 2% agar–coated plates and untreated or treated with 1,000 ng/mL leptin and/or 100 nmol/L E_2 for 48 h. To block E-cadherin function, the medium was supplemented with E-cadherin antibody (1:100 dilution; Chemicon International, Temecula, CA) or EGTA to a final concentration of 4 mmol/L. To generate three-dimensional spheroids, the plates were rotated for 4 h at 37°C. The three-dimensional cultures were photographed using a phase-contrast microscope (Olympus, Milan, Italy). The extent of aggregation was scored by measuring the spheroids with an ocular micrometer. The spheroids between 25 and 50, 50 and 100, and >100 μm (in the smallest cross-section) were counted in 10 different fields under ×10 magnification.

Cell number was determined, after trypsinization of spheroids, by direct cell counting at 48 h of treatments.

E-cadherin adhesion assay. MCF-7 cells were pretreated with leptin (1,000 ng/mL) and/or E_2 (100 nmol/L) for 48 h and then plated on six-well plates coated with 1.5 μg/mL recombinant human E-cadherin/Fc chimeric. Before the experiment, the wells were blocked with 1% BSA for 3 h at 37°C and then washed with PBS.

After washing out nonadherent cells, adherent cells were incubated 3 h in medium containing 500 μg/mL 3-(4,5-dimethylthiazol-2-yl)-2,5-diphenyltetrazolium bromide solution. The reaction product was measured at 570 nm.

Total RNA extraction and reverse transcription-PCR assay. Total RNA was extracted using TRIzol reagent (Invitrogen, San Diego, CA). Reverse transcription was done using RETROscript kit (Ambion, Austin, TX). The cDNAs were amplified by PCR using the following primers: 5′-TCTAAGATGAAGGAGACCATC-3′ and 5′-GCGGTAGTAGGACAGGAAGTTGTT-3′ (cyclin D1), 5′-TGGAATCCAAGCAGAATTGC-3′ and 5′-TATGTGGCAATGCGTTCTCTATCCA-3′ (E-cadherin), and 5′-CTCAACATCTCCCCCTTCTC-3′ and 5′-CAAATCCCATATCCTCGT-3′ (36B4). The PCR was done for 30 cycles for cyclin D1 (94°C for 1 min, 60°C for 1 min, and 72°C for 2 min) and E-cadherin (94°C for 1 min, 55°C for 1 min, and 72°C for 2 min) and 15 cycles (94°C for 1 min, 59°C for 1 min, and 72°C for 2 min) to amplify 36B4, in the presence of 1 μL of first-strand cDNA, 1 μmol/L each of the primers mentioned above, deoxynucleotide triphosphate (0.5 mmol/L), Taq DNA polymerase (2 units per tube; Promega, Madison, WI) in a final volume of 25 μL.

Western blot analysis. Equal amounts of total protein were resolved on an 8% to 10% SDS-polyacrylamide gel. Proteins were transferred to a nitrocellulose membrane and probed with the appropriated antibody. The antigen-antibody complex was detected by incubation of the membrane at room temperature with a peroxidase-coupled goat anti-mouse or anti-rabbit IgG and revealed using the enhanced chemiluminescence system (Amersham, Buckinghamshire, United Kingdom).

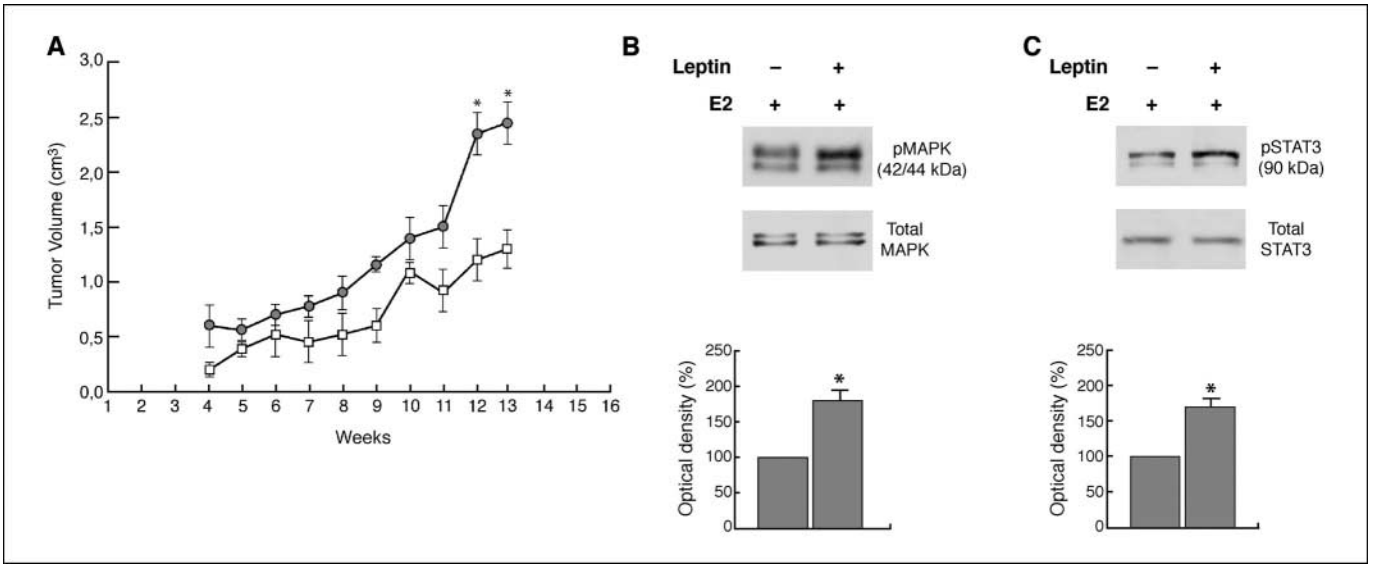

Figure 1. Effect of leptin on growth of MCF-7 cell tumor xenografts. *A,* xenografts were established with MCF-7 cells in female mice implanted with E_2 pellet. One group was treated with 230 μg/kg leptin (●, $n = 5$) and a second group with vehicle (□, $n = 5$). *, $P < 0.05$, treated versus control group. Representative Western blot on protein extracts from xenografts excised from control mice and mice treated with leptin showing MAPK (*B*) and STAT3 (*C*) activation. The immunoblots were stripped and reprobed with total MAPK and STAT3, which serve as the loading control. *pMAPK,* phosphorylated MAPK; *pSTAT,* phosphorylated STAT. *Columns,* mean of three separate experiments in which the band intensities were evaluated in terms of optical density arbitrary units and expressed as the percentage of the control assumed as 100%; *bars,* SE. *, $P < 0.05$.

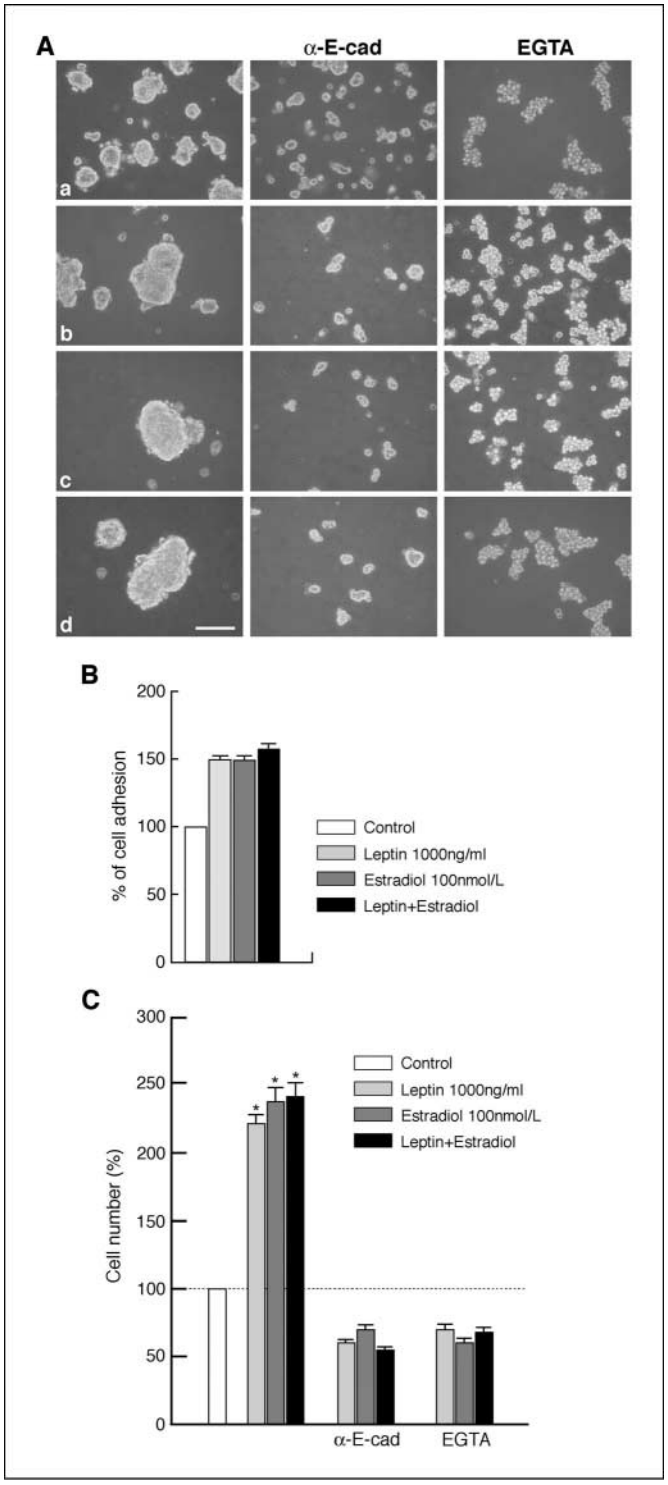

Figure 2. Leptin-enhanced cell-cell adhesion and proliferation depend on E-cadherin function. *A,* E-cadherin–positive MCF-7 cells were seeded in 2% agar–coated plates and cultured as three-dimensional spheroids (*a–d*). To block E-cadherin function, the medium was supplemented with E-cadherin antibody (1:100 dilution; α-E-cad) or EGTA (4 mmol/L). Cells were untreated (*a*) or treated with leptin (*b*), E_2 (*c*), and leptin plus E_2 (*d*) for 48 h and then photographed under phase-contrast microscopy. Bar, 50 μm. *B,* six-well plates were coated with E-cadherin/Fc recombinant protein, and binding of cells were measured by the 3-(4,5-dimethylthiazol-2-yl)-2,5-diphenyltetrazolium bromide assay. *Columns,* mean of five wells; *bars,* SE. *C,* proliferation of MCF-7 cells treated with leptin and/or E_2 for 48 h in the absence or presence of E-cadherin antibody (1:100 dilution; α-E-cad) or EGTA (4 mmol/L). *Columns,* average of three experiments; *bars,* SE. Representative results. *, $P < 0.05$.

Transfection assay. MCF-7 cells were transfected using the FuGENE 6 reagent (Promega) with the mixture containing 0.5 μg of human E-cadherin promoter constructs. HeLa cells were transfected with E-cadherin promoter (0.5 μg per well) in the presence or absence of HEGO (0.2 μg per well) or cotransfected with STAT3 or ERK2 dominant negative (0.5 μg per well). Twenty-four hours after transfection, the cells were treated with 1,000 ng/mL leptin and/or 100 nmol/L E_2 for 48 h. Empty vectors were used to ensure that DNA concentrations were constant in each transfection. TK *Renilla* luciferase plasmid (5 ng per well) was used. Firefly and *Renilla* luciferase activities were measured by Dual Luciferase kit. The firefly luciferase data for each sample were normalized based on the transfection efficiency measured by *Renilla* luciferase activity.

Electrophoretic mobility shift assay. Nuclear extracts were prepared from MCF-7 as previously described (25). The probe was generated by annealing single-stranded oligonucleotides, labeled with [γ^{32}P]ATP and T4 polynucleotide kinase, and then purified using Sephadex G50 spin columns. The DNA sequences used as probe or as cold competitors are as follows: CRE, 5′-TGGATCACCTGAGGTCAGGAGTTCCAGACC-3′; Sp1, 5′-ATCAGC-GGTACGGGGGGCGGTGCTCCGGGG-3′. *In vitro* transcribed and translated CREB protein was synthesized using the T7 polymerase in the rabbit reticulocyte lysate system (Promega). The protein-binding reactions were carried out in 20 mL of buffer [20 mmol/L HEPES (pH 8), 1 mmol/L EDTA, 50 mmol/L KCl, 10 mmol/L DTT, 10% glycerol, 1 mg/mL BSA, 50 μg/mL poly(dI/dC) with 50,000 cpm] of labeled probe, 20 μg of MCF-7 nuclear protein or an appropriate amount of CREB protein or Sp1 human recombinant protein (Promega), and 5 μg of poly(dI-dC). The mixtures were incubated at room temperature for 20 min in the presence or absence of unlabeled competitor oligonucleotides. The specificity of the binding was tested by adding to the mixture reaction–specific antibodies (anti-CREB and anti-Sp1). Mithramycin A (100 μmol/L; ICN Biomedicals, Inc., Costa Mesa, CA) was incubated with the labeled probe for 30 min at 4°C before the addition of nuclear extracts. The entire reaction mixture was electrophoresed through a 6% polyacrylamide gel in 0.25× Tris borate-EDTA for 3 h at 150 V.

Chromatin immunoprecipitation assay. We followed chromatin immunoprecipitation (ChIP) methodology described by Morelli et al. (26). MCF-7 cells were untreated or treated with 1,000 ng/mL leptin and/or 100 nmol/L E_2 for 1 h. The cells were then cross-linked with 1% formaldehyde and sonicated. Supernatants were immunocleared with sonicated salmon DNA/protein A agarose (Upstate Biotechnology, Inc., Lake Placid, NY) and immunoprecipitated with anti-CREB or anti-Sp1 antibodies (Santa Cruz Biotechnology, Santa Cruz, CA). Pellets were washed as reported (26), eluted

Table 1. Effect of leptin on cell aggregation in MCF-7 breast cancer cells

MCF-7	Spheriods		
	25 ≤ 50 μm	50 ≤ 100 μm	>100 μm
Control	30 ± 1.2	0.6 ± 0.2	0.0 ± 0.0
Leptin	6 ± 0.8	26 ± 1.8	85 ± 2.5
E_2	7 ± 0.6	32 ± 2.1	78 ± 3.2
Leptin + E_2	3 ± 0.9	40.5 ± 2.3*	80.7 ± 2.9

NOTE: MCF-7 cells were cultured as three-dimensional spheroids in serum-free medium. The extent of aggregation was scored by measuring the spheroid diameters with an ocular micrometer. The values represent a sum of spheroids in 10 optical fields under ×10 magnification. The results are mean ± SE from at least three experiments. Representative three-dimensional cultures are shown in Fig. 2*A*.

*$P < 0.05$ versus leptin and E_2.

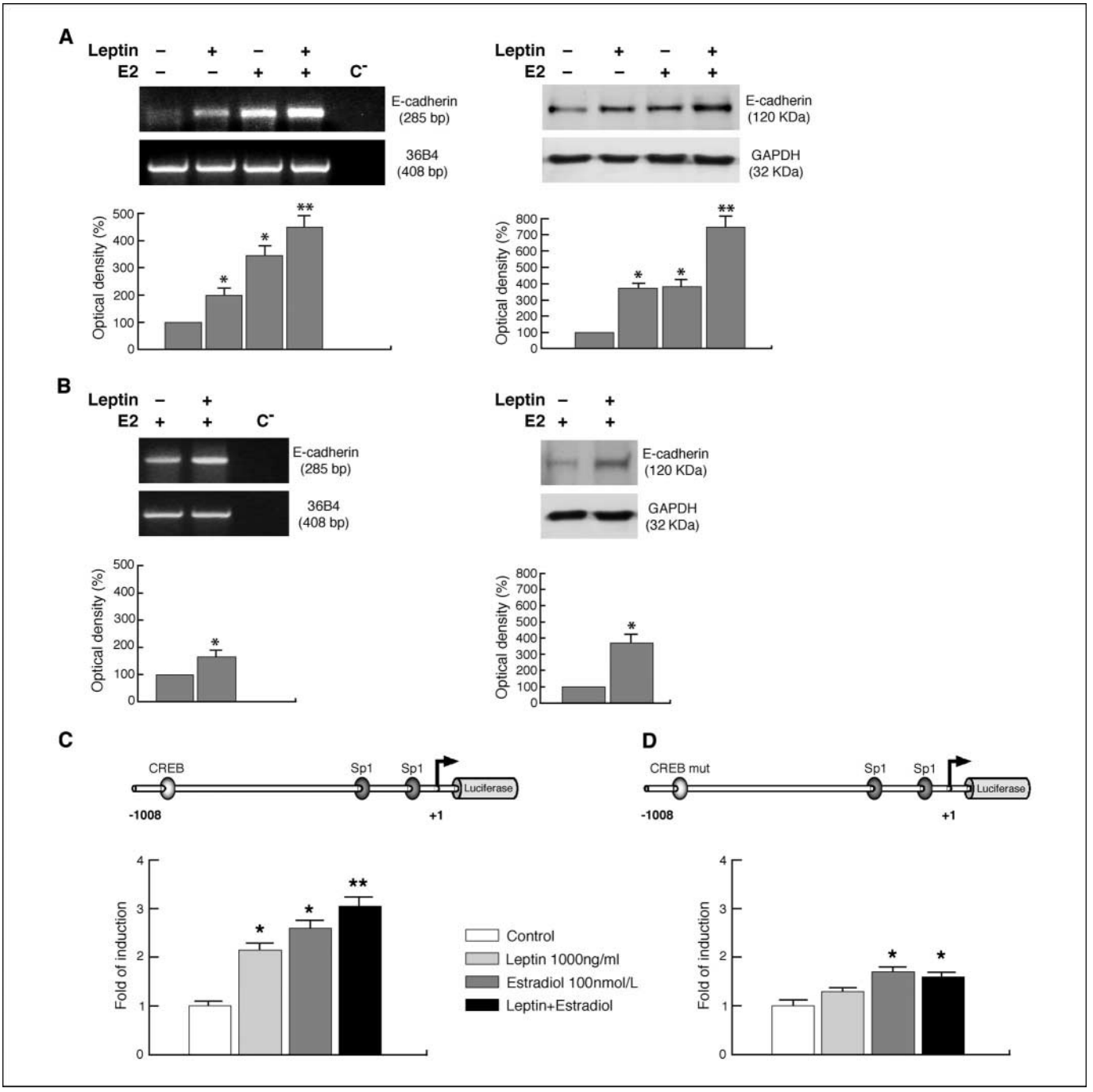

Figure 3. Leptin up-regulates E-cadherin expression in MCF-7 spheroids and xenografts. Reverse transcription-PCR of E-cadherin mRNA was done in MCF-7 three-dimensional cultures stimulated for 48 h with 1,000 ng/mL leptin and/or 100 nmol/L E_2 (*A*) as well as in xenografts (*B*). 36B4 mRNA levels were determined as a control. *C*$^-$, RNA sample without the addition of reverse transcriptase (negative control). Protein extracts obtained from MCF-7 spheroids (*A*) and xenografts (*B*) were immunoblotted with a specific antibody against human E-cadherin. Representative results. *GAPDH,* glyceraldehyde-3-phosphate dehydrogenase. *Columns,* mean of three separate experiments in which the band intensities were evaluated in terms of optical density arbitrary units and expressed as the percentage of the control assumed as 100%; *bars,* SE. MCF-7 cells were transiently transfected with a luciferase reporter plasmid containing the human E-cadherin promoter full-length p-1008/+49 (*C*) or mutated in the CREB site (CREB mut; *D*). Schematic representation of human E-cadherin promoter constructs. The +1 position represents the transcriptional initiation site. The cells were left untreated (control) or treated in the presence of 1,000 ng/mL leptin and/or 100 nmol/L E_2. *Columns,* mean of three separate experiments; *bars,* SE. In each experiment, the activities of the transfected plasmid were assayed in triplicate transfections. *, $P < 0.05$; **, $P < 0.01$ compared with control.

with elution buffer (1% SDS and 0.1 mol/L $NaHCO_3$), and digested with proteinase K (26). DNA was obtained by phenol/chloroform extractions and precipitated with ethanol; 5 μL of each sample were used for PCR with CREB primers (5′-TGTAATCCAACACTTCAGGAGG-3′ and 5′-TTGAGACG-GAGTCTCGCTCT-3′) and Sp1 primers (5′-TAGCAACTCCAGGCTAGAGG-3′ and 5′-AACTGACTTCCGCAAGCTCACA-3′). The PCR conditions were 94°C for 1 min, 56°C for 2 min, and 72°C for 2 min for 30 cycles.

Statistical analysis. Data were analyzed by ANOVA using the STATPAC computer program. Statistical comparisons for *in vivo* studies were made by Wilcoxon-Mann-Whitney test.

Results

Effects of leptin on breast cancer cell tumor growth. To determine *in vivo* the influence of leptin on breast cancer cell tumor growth, we used 45-day-old female nude mice bearing, into the intrascapular region, MCF-7 cell tumor xenografts with or without estrogen pellets. Tumors were obtained only in animals with estrogen pellet implants, which were in general larger in animals treated with leptin at the dose of 230 μg/kg (Fig. 1*A*). Particularly, 13 weeks of leptin parenteral administration increased the tumor volume to 100% the size of E_2 treatment. Besides, leptin significantly enhanced phosphorylation of tumor-derived MAPK and STAT3, suggesting that concentration and dosing schedule of leptin were appropriated for *in vivo* stimulation (Fig. 1*B* and *C*).

Leptin enhances cell-cell adhesion and cell proliferation. We did three-dimensional MCF-7 cultures to evaluate *in vitro* the effects of leptin on cell aggregation. It has been reported that multicellular spheroid culture can more closely mimic some *in vivo* biological features of tumors and improve the relevance of *in vitro* studies (27–30).

Our results evidenced that leptin and/or E_2 treatment for 48 h enhances cell-cell adhesion of MCF-7 cells compared with untreated cells (Fig. 2*A*). The combined exposure to both hormones switches cell aggregation towards the formation of spheroids exhibiting prevalently a diameter larger than 100 μm (Table 1).

E-cadherin is a major type of adhesion molecule, which forms Ca^{2+}-dependent homophilic ligations to facilitate cell-cell contact in epithelial cells (16, 17). Thus, to study whether E-cadherin was responsible for leptin-enhanced cell-cell adhesion, we supplemented the cell culture medium with function-blocking E-cadherin antibody or EGTA, a calcium-chelating agent. As shown in Fig. 2*A*, in the presence of the antibody, MCF-7 cells formed small aggregates showing limited intercellular contact, whereas EGTA treatment prevented cell-cell adhesion, and cells remained rounded and singled suspended.

In addition, the role of E-cadherin was confirmed using an adhesion assay in which cells were allowed to adhere to E-cadherin/Fc protein–coated dishes. This assay showed a greater binding of cells pretreated with leptin and/or E_2 for 48 h with respect to untreated cells (Fig. 2*B*). The adhesion was blocked using either a function-blocking E-cadherin antibody or EGTA (data not shown). Thus, the increased aggregation observed in the presence of leptin and/or E_2 was dependent on E-cadherin.

In three-dimensional cultures, we also observed a significant increase of cell growth upon leptin and/or E_2 treatment. The leptin-induced cell proliferation was completely abrogated when E-cadherin function was blocked (Fig. 2*C*).

Furthermore, in MCF-7 spheroids and in xenografts, we observed an increase of cyclin D1, a regulator of cell cycle progression, in terms of mRNA and protein content in the presence of leptin and/or E_2 (Supplementary Fig. S1).

Leptin up-regulates E-cadherin expression. To investigate if an enhanced expression of E-cadherin occurred in the above-mentioned conditions, we did reverse transcription-PCR and Western blotting analysis. Our results showed that either leptin or E_2 and, in higher extent, the exposure to both hormones increased expression of E-cadherin in terms of mRNA and protein content (Fig. 3*A*). The latter results were also evident in MCF-7 xenografts (Fig. 3*B*).

To evaluate whether both hormones were able to activate E-cadherin promoter, we transiently transfected MCF-7 cells with human E-cadherin promoter plasmid (p-1008/+49). A significant increase in promoter activity was observed in the transfected cells exposed to leptin and/or E_2 for 48 h (Fig. 3*C*).

In contrast, we observed that leptin was unable to activate the constructs containing different deleted segments of human E-cadherin promoter (p-164/+49 and p-83/+49) with respect to the full length, whereas E_2 induced activation in the presence of p-164/+49 construct (Supplementary Fig. S2).

Leptin enhances CREB-DNA and Sp1-DNA binding activity to E-cadherin promoter. The role of leptin and E_2 on the transcriptional activity of the *E-cadherin* gene was explored analyzing the nucleotide sequence of the *E-cadherin* gene promoter. We evidenced, upstream to the initiation transcription site, one CRE (−925/−918) and two Sp1 (−144/−132 and −51/−39) as putative effectors of leptin and estrogens. For instance, in MCF-7 cells transiently transfected with E-cadherin promoter plasmid-bearing CREB-mutated site (CREB mut), we observed that the stimulatory effect of leptin was abrogated, whereas the activation of E_2 still persisted, although in a lower extent with respect to the intact promoter (Fig. 3*D*).

To characterize the role of these motifs in modulating E-cadherin promoter activity, we did electrophoretic mobility shift assay (EMSA). Nuclear extracts from MCF-7 cells, using as probe a CRE-responsive element, showed two protein-DNA complexes (Fig. 4*A, lane 1*), which were abolished by the addition of a nonradiolabeled competitor (Fig. 4*A, lane 2*). Leptin treatment induced a strong increase in CREB DNA-binding activity (Fig. 4*A, lane 3*), which was immunodepleted in the presence of CREB antibody (Fig. 4*A, lane 4*). Using transcribed and translated *in vitro* CREB protein, we obtained two bands migrating at the same level as that of MCF-7 nuclear extracts (Fig. 4*A, lane 9*). In the presence of the MAPK inhibitor PD98059, the complex induced by leptin treatment was reduced (Fig. 4*B, lanes 5* and *9*). These findings addressed a specific involvement of leptin signaling in the up-regulation of E-cadherin expression.

Using a DNA probe containing an Sp1 site, we observed in MCF-7 nuclear extracts, a specific protein-DNA complex that was slightly enhanced by leptin, increased upon E_2 exposure and furthermore by the combined treatments (Fig. 4*C, lanes 1, 3, 5*, and *7*). In the presence of Sp1 human recombinant protein, we observed a single complex that causes the same shift with respect to the band revealed in MCF-7 nuclear extracts (Fig. 4*C, lane 10*). The addition

Figure 4. Effects of *in vitro* leptin treatment on CREB-DNA and Sp1-DNA binding activity in MCF-7 cells. Nuclear extracts from MCF-7 cells were incubated with a double-stranded CREB-specific (*A* and *B*) or Sp1-specific (*C* and *D*) consensus sequence probe labeled with [γ-^{32}P]ATP and subjected to electrophoresis in a 6% polyacrylamide gel (*lane 1*). *A,* we used as positive control a transcribed and translated *in vitro* CREB protein (*lane 9*). Competition experiments were done by adding as competitor a 100-fold molar excess of unlabeled probe (*lanes 2* and *10*). MCF-7 nuclear extracts treated with 1,000 ng/mL leptin (*Lep*) and/or 100 nmol/L E_2 for 48 h incubated with probe (*lanes 3, 5*, and *7*, respectively). The specificity of the binding was tested by adding to the reaction mixture a CREB antibody (*lanes 4, 6*, and *8*). *B,* MCF-7 cells were serum starved overnight with 10 μmol/L PD 98059 (*lanes 3, 5, 7*, and *9*). *Lanes 11* (*A*) and *12* (*B*) contain probe alone. *C,* Sp1 human recombinant protein was used as positive control (*lane 10*). Competition experiments were done by adding as competitor a 100-fold molar excess of unlabeled probe (*lanes 2* and *11*). MCF-7 nuclear extracts treated with 1,000 ng/mL leptin and/or 100 nmol/L E_2 for 48 h incubated with probe (*lanes 3, 5*, and *7*, respectively). The specificity of the binding was tested by adding to the reaction mixture a Sp1 antibody (*lanes 4, 6*, and *8*). The formation of DNA-Sp1 complexes was blocked by the addition of 100 μmol/L mithramycin A (*lane 9*). *D,* the pure antiestrogen ICI 182,780 (1 μmol/L) was added in leptin-treated (*lane 5*) and/or E_2-treated (*lanes 7* and *9*) MCF-7 nuclear extracts. *Lane 12* contain probe alone.

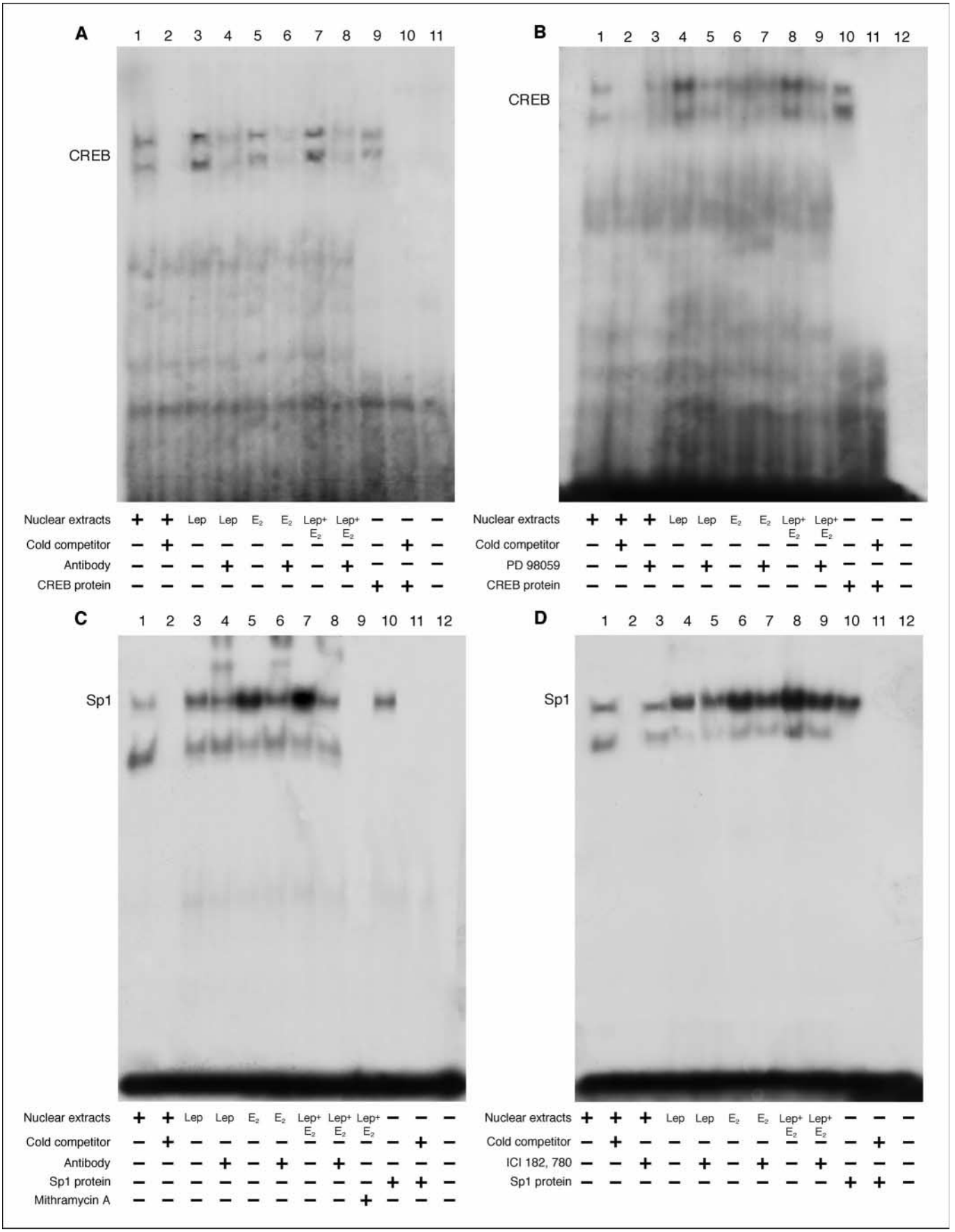
A
1 2 3 4 5 6 7 8 9 10 11
CREB
Nuclear extracts + + Lep Lep E2 E2 Lep+ E2 Lep+ E2 – – –
Cold competitor – + – – – – – – – + –
Antibody – – – + – + – + – – –
CREB protein – – – – – – – – + + –
B
1 2 3 4 5 6 7 8 9 10 11 12
CREB
Nuclear extracts + + + Lep Lep E2 E2 Lep+ E2 Lep+ E2 – – –
Cold competitor – + – – – – – – – – + –
PD 98059 – – + – + – + – + – – –
CREB protein – – – – – – – – – + + –
C
1 2 3 4 5 6 7 8 9 10 11 12
Sp1
Nuclear extracts + + Lep Lep E2 E2 Lep+ E2 Lep+ E2 Lep+ E2 – – –
Cold competitor – + – – – – – – – – + –
Antibody – – – + – + – + – – – –
Sp1 protein – – – – – – – – – + + –
Mithramycin A – – – – – – – – + – – –
D
1 2 3 4 5 6 7 8 9 10 11 12
Sp1
Nuclear extracts + + + Lep Lep E2 E2 Lep+ E2 Lep+ E2 – – –
Cold competitor – + – – – – – – – – + –
ICI 182, 780 – – + – + – + – + – – –
Sp1 protein – – – – – – – – – + + –

of mithramycin A (100 μmol/L), which binds to GC boxes and prevents sequential Sp1 binding, to nuclear extracts treated with leptin and E_2 blocked the formation of DNA-Sp1 complexes (Fig. 4*C, lane 9*). The original band DNA-protein complex was supershifted by Sp1 antibody (Fig. 4*C, lanes 4, 6*, and *8*). In all hormonal treatments done, the pure antiestrogen ICI 182,780 reduced the Sp1-DNA binding complex (Fig. 4*D, lanes 5, 7*, and *9*), evidencing that leptin induced an activation of ERα, as we previously showed (25).

Effects of leptin on CREB and Sp1 recruitment to the E-cadherin promoter. To corroborate EMSA results, we did ChIP assay. We found that the stimulation of MCF-7 cells with leptin increased the recruitment of CREB to *E-cadherin* gene promoter (Fig. 5*A*). Furthermore, we observed that leptin or E_2 stimulated the recruitment of Sp1 to the E-cadherin promoter, and the combined treatment induced an additive effect (Fig. 5*B*). The latter event suggests that leptin and E_2 may converge in activating ERα to recruit Sp1 on E-cadherin promoter.

Involvement of ERα in the leptin-induced up-regulation of E-cadherin expression. Stemming from the data provided by EMSA and ChIP assays, we evaluated the involvement of ERα in the enhanced E-cadherin expression induced by leptin. Our results showed that in three-dimensional cultures, in the presence of the pure antiestrogen ICI 182,780, the up-regulatory effect of leptin on E-cadherin protein expression still persisted, whereas the stimulatory effects of E_2 was abrogated (Fig. 6*A*).

In addition, the specific role of leptin signaling in up-regulating E-cadherin expression was also confirmed by functional studies in ERα-negative HeLa cells. We evidenced that leptin was able to activate E-cadherin promoter (Fig. 6*B*), which was abrogated in the presence of ERK2 and STAT3 dominant negative (Fig. 6*C*), sustaining furthermore the involvement of leptin signaling. It is worth to note how the ectopic expression of ERα in HeLa cells was able to potentiate the effect of leptin (Fig. 6*B*). To test the activity of the transfected ERα, we did Western blotting analysis for phosphorylated ERα, whereas for dominant-negative *ERK2* and *STAT3* genes, we evaluated the expression of c-*fos*, as target of both pathways (31–33). Moreover, in BT-20 cells lacking of ERα, leptin-enhanced E-cadherin protein content was reduced in the presence of either ERK2 or STAT3 dominant negative. In the same cells, cotransfected with ERα and ERK2 or STAT3 dominant negative, E_2 alone or in combination with leptin was unable to maintain the up-regulatory effect on E-cadherin expression (Supplementary Fig. S3).

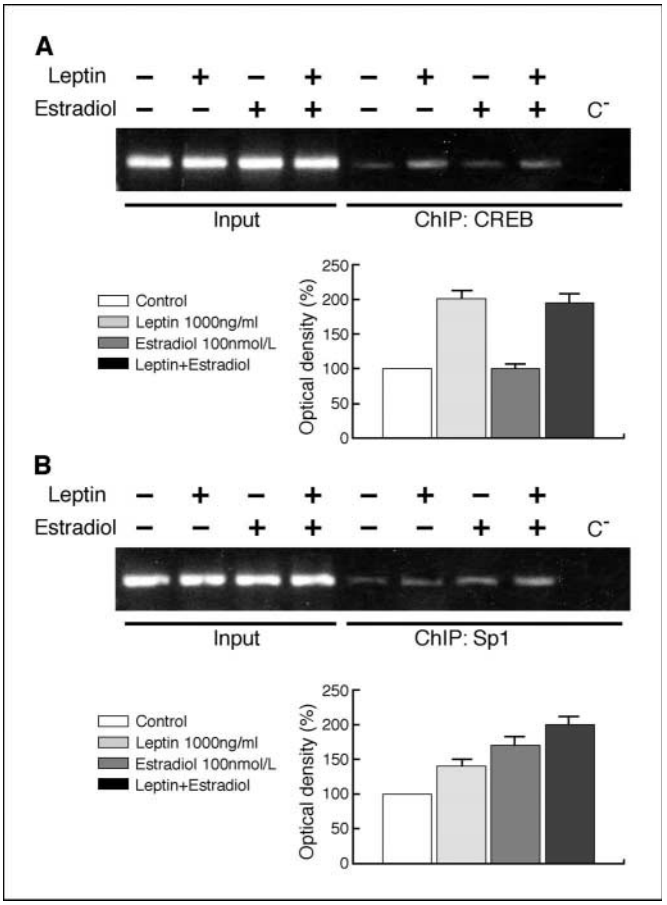

Figure 5. Recruitment of CREB and Sp1 to the E-cadherin promoter in MCF-7 cells. The cells were treated for 1 h with 1,000 ng/mL leptin and/or 100 nmol/L E_2 or left untreated. The precleared chromatin was immunoprecipitated with specific antibodies [i.e., anti-CREB for CREB immunoprecipitates (*A*) or anti-Sp1 for Sp1 immunoprecipitates (*B*)]. E-cadherin promoter sequences containing CREB or Sp1 sites were detected by PCR with specific primers, as detailed in Materials and Methods. To determine input DNA, the E-cadherin promoter fragment was amplified from 5 μL purified soluble chromatin before immunoprecipitation. PCR products obtained at 30 cycles. ChIP with non-immune IgG was used as negative control (*C*⁻). This experiment was repeated three times with similar results. Most representative experiment. *Columns,* mean of three separate experiments in which the band intensities were evaluated in terms of optical density arbitrary units and expressed as the percentage of the control assumed as 100%; *bars,* SE.

Discussion

Leptin stimulates cell growth, counteracts apoptosis, and induces migration and angiogenic factors in different cellular cancer models (10). For instance, hyperleptinemia is a common feature of obese women who have a higher risk of breast cancer than women with normal weight (34), but the association between circulating leptin and breast cancer is still not clear. It has been reported that in interstitial fluid of the adipose tissue, leptin concentration is higher than the circulating levels (35). Thus, we may reasonably assume that in the presence of an abundant adipose tissue surrounding epithelial breast cancer cells, the paracrine leptin effects become crucial in affecting local and primary tumor progression.

The aim of this study was to evaluate whether leptin can influence local primary breast cancer development and progression, using an *in vivo* model of MCF-7 xenografts implanted in female nude mice and an *in vitro* system represented by MCF-7 three-dimensional cultures. Our results showed in MCF-7 xenografts that leptin treatment significantly potentiated the E_2-increased tumor size. In the same view, *in vitro* studies revealed that the combined exposure to both hormones enhanced cell-cell aggregation with respect to the separate treatments.

E-cadherin is an intercellular adhesion molecule generally implicated as tumor suppressor in several types of epithelial tumors, based on findings that the expression of this homotypic adhesion molecule is frequently lost in human epithelial cancers (18, 20, 21). However, it has well been shown in ovarian epithelial tumors that E-cadherin expression is much more elevated than normal ovaries, suggesting that E-cadherin can play a role in the development of ovarian carcinomas (36). For instance, it is worth to mention that E-cadherin may serve not only as an intercellular adhesion molecule, but it may also trigger intracellular activation of proliferation and survival signals (37).

In our study, the increased cell-cell aggregation, observed in MCF-7 three-dimensional cultures upon leptin and/or E_2 treatments, seems to be dependent on E-cadherin molecule that has an indispensable role in this process. Indeed, the addition of a function-blocking E-cadherin antibody or a calcium-chelating agent (EGTA) blocked cell-cell adhesion induced by both hormones. Besides, we showed by adhesion assay a greater binding of cells pretreated with leptin and/or E_2 on E-cadherin/Fc protein–coated dishes.

In the same experimental conditions, an increased proliferative rate was observed upon leptin or E_2 exposure, which was completely abrogated when E-cadherin function was blocked.

An important cell cycle regulator, such as cyclin D1, resulted to be up-regulated in three-dimensional cultures and in xenografts.

Besides, in both models, we showed that leptin and/or E_2 enhanced E-cadherin expression in terms of mRNA, protein content, and promoter activity.

The analysis of E-cadherin promoter sequence revealed the presence of CRE and Sp1 sites as potential target of leptin and E_2 signals. It is well documented how leptin and E_2 through nongenomic effects are able to activate the MAPK pathway that induces activation of CREB kinase, a member of the $p90^{RSK}$ family that corresponds to RSK2 and thereby phosphorylates CREB Ser^{133} (38–40). This well fits with our functional studies showing that leptin was no longer able to activate the *E-cadherin* gene promoter mutated in the CREB site, whereas E_2 maintained an activatory effect although in a lower extent with respect to the intact promoter. The latter data suggest that the activatory effect of E_2 may persist through its binding to Sp1-DNA complex.

The important role of the Sp1-responsive element in activating E-cadherin promoter was shown by EMSA and ChIP assays. Our results evidenced that E_2, as extensively documented, acts in a nonclassic way through the interaction of ERα with Sp1 (41–45). It is worth to note that upon leptin exposure, we also observed an increase in Sp1-DNA binding activity, clearly reduced in the presence of the pure antiestrogen ICI 182,780, as well as an enhanced recruitment of Sp1 to E-cadherin promoter. These observations are supported by our previous findings reporting that leptin is able to transactivate, in a unliganded-dependent manner, ERα through MAPK signal (25).

A cross-talk between leptin and E_2 has been well documented in neoplastic mammary tissues and breast cancer cell lines (15, 25, 46, 47). For instance, E_2 up-regulates leptin expression in MCF-7 cells (15), whereas leptin is an amplifier of E_2 signaling through a double mechanism: an enhanced aromatase gene expression (46) and a direct transactivation of ERα (25). Thus, we investigated whether the up-regulatory effect induced by leptin on E-cadherin expression can be modulated by ERα. We found that E-cadherin protein seems up-regulated still by leptin in the presence of the pure antiestrogen ICI 182,780. Moreover, in HeLa cells, leptin was able to activate E-cadherin promoter, which was abrogated in the presence of ERK2 or STAT3 dominant negative, suggesting that

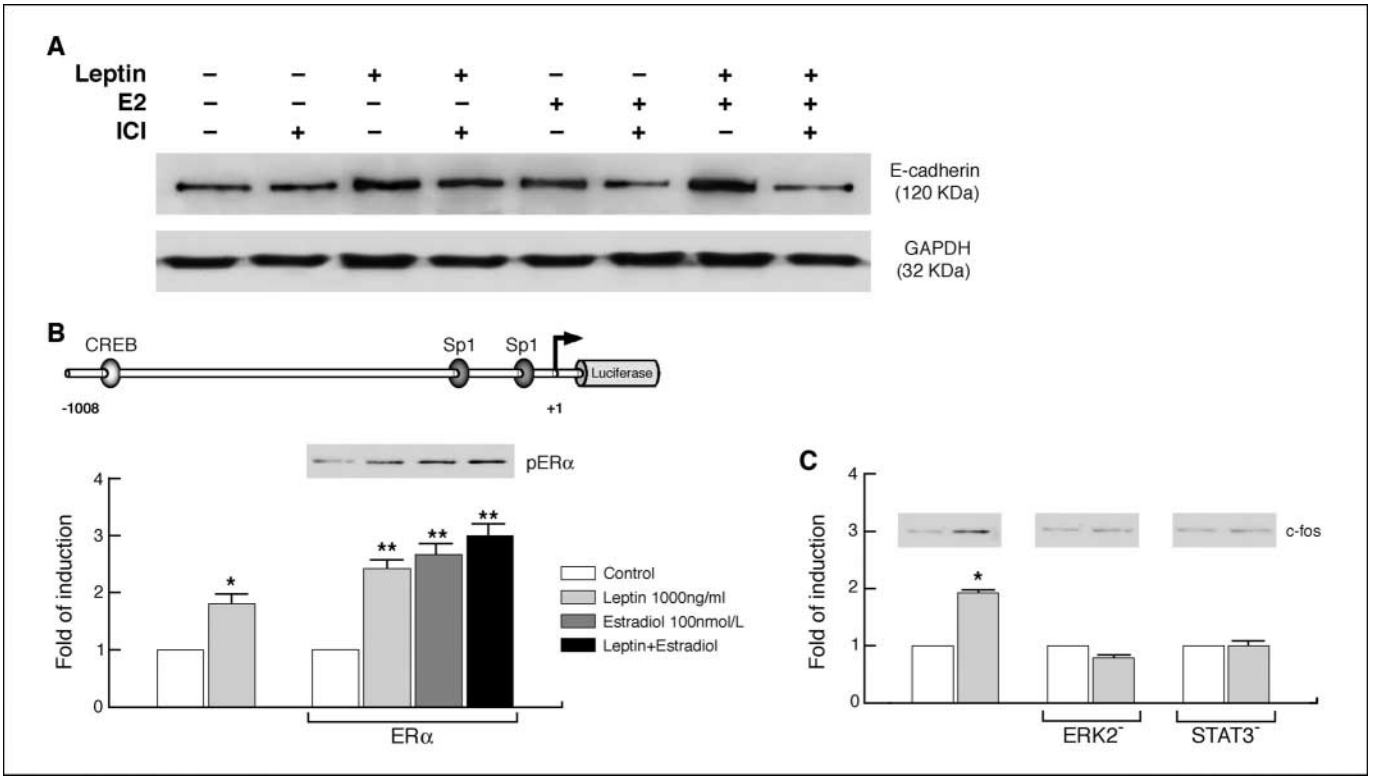

Figure 6. Influence of ERα on leptin-induced upregulation of E-cadherin expression. *A,* MCF-7 spheroids were preincubated with 1 μmol/L ICI 182,780 (*ICI*) for 1 h and then treated with leptin (1,000 ng/mL) and/or E_2 (100 nmol/L) for 48 h. Total proteins (50 μg) were immunoblotted with a specific antibody against human E-cadherin. GAPDH serves as loading control. *B,* ER-negative HeLa cells were transfected with a plasmid containing E-cadherin promoter or cotransfected with E-cadherin promoter and pHEGO. Transfected cells were treated with leptin (1,000 ng/mL) and/or E_2 (100 nmol/L) for 48 h. *Columns,* means of three separate experiments; *bars,* SE. In each experiment, the activities of the transfected plasmids were assayed in triplicate transfections. *Inset,* Western blot analysis for phosphorylated ERα (*pERα*) using anti–phosphorylated ERα (Ser^{118}). *, $P < 0.05$; **, $P < 0.01$, compared with control. *C,* HeLa cells were transiently transfected with dominant-negative ERK2 or STAT3 plasmid and then treated for 48 h with leptin. In each experiment, the activities of the transfected plasmids were assayed in triplicate transfections. *Inset,* Western blot analysis for c-*fos*. *, $P < 0.05$, compared with control.

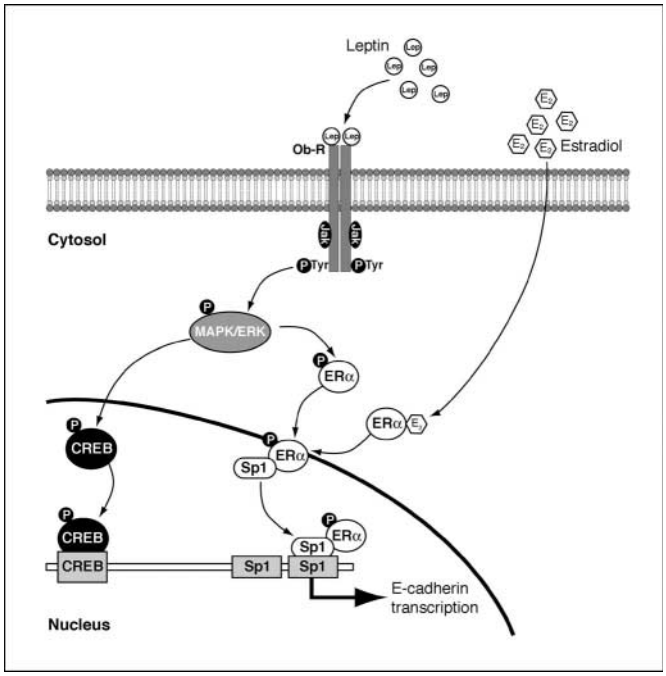

Figure 7. Hypothesized model of leptin signaling in modulating E-cadherin expression in breast cancer. Interaction of leptin (*Lep*) with its specific receptor (ObR) induces, through MAPK activation, phosphorylation of CREB and its transactivation. Leptin may potentiate the transactivation of ERα, which in turn may interact with Sp1 and bind DNA in a nonclassic way. Both CREB and Sp1 transcriptional factors bind on E-cadherin promoter at specific responsive sequences and induce an enhanced E-cadherin expression.

leptin signaling is involved in enhancing E-cadherin expression. These latter data are supported by Western blotting analysis done in BT-20 cells lacking of ERα in which ERK2 and STAT3 dominant negative reversed leptin-enhanced E-cadherin protein content. The up-regulatory effect induced by E_2 on E-cadherin expression in the presence of ectopic ERα seemed inhibited in the presence of ERK2 and STAT3 dominant negative. The latter findings may be a consequence of the enhanced expression of leptin receptor upon E_2 exposure (15), which may have an impaired signaling on E-cadherin expression. An additional explanation, which could coexist with the previous one, may be that both ERK2 and STAT3 dominant negative could interfere with ERα-Sp1 interaction at level of *E-cadherin* gene transcription (48).

A hypothetical model of the possible mechanism through which leptin and E_2 may functionally interact in modulating E-cadherin expression in breast cancer is shown in Fig. 7. Leptin through MAPK activation may phosphorylate CREB and induce its transactivation. For instance, CREB phosphorylated at Ser^{133} is often reported not only as an index of PKA but also as an effector of MAPK activation (49). Concomitantly, leptin in the presence of E_2 may potentiate the transactivation of ERα, which in turn may interact with Sp1 and bind DNA in a nonclassic way. On the other hand, it is well known that ERα, in the presence of its natural ligand, interacts with Sp1.

Thus, we may reasonably propose that upon leptin exposure, the increased E-cadherin–mediated cellular adhesion and activation of proliferation signals may enhance the transformation of normal epithelial cells to neoplastic cells and then stimulate the growth of tumor mass. Distinct from its role as a tumor suppressor, E-cadherin may function as tumor enhancer in the development of primary breast cancer.

In conclusion, all these data address how leptin and E_2 signaling may represent a target of combined pharmacologic tools to be exploited in the novel therapeutic adjuvant strategies for breast cancer treatment particularly in obese women.

Acknowledgments

Received 8/4/2006; revised 1/17/2007; accepted 1/23/2007.

Grant support: Associazione Italiana per la Ricerca sul Cancro grants 2005 and 2006 and Spanish Ministry of Education Postdoctoral Research Grant (S. Morales).

The costs of publication of this article were defrayed in part by the payment of page charges. This article must therefore be hereby marked *advertisement* in accordance with 18 U.S.C. Section 1734 solely to indicate this fact.

We thank Dr. Domenico Sturino for the English revision of the article and Dr. Pasquale Cicirelli for technical assistance.

References

1. Zhang Y, Proenca R, Maffei M, Barone M, Leopold L, Friedman JM. Positional cloning of the mouse obese gene and its human homologue. Nature 1994; 372:425–32.
2. Halaas JL, Gajiwala KS, Maffei M, et al. Weight-reducing effects of the plasma protein encoded by the obese gene. Science 1995;269:543–6.
3. Bray GA. The underlying basis for obesity: relationship to cancer. J Nutr 2002;132:3451–5S.
4. Bonnet M, Delavaud C, Laud K, et al. Mammary leptin synthesis, milk leptin and their putative physiological roles. Reprod Nutr Dev 2002;42:399–413.
5. Ahima RS, Flier JS. Adipose tissue as an endocrine organ. Trends Endocrinol Metab 2000;11:327–32.
6. Tartaglia LA. The leptin receptor. J Biol Chem 1997; 272:6093–6.
7. White DW, Kuropatwinski KK, Devos R, Baumann H, Tartaglia LA. Leptin receptor (OB-R) signaling. Cytoplasmic domain mutational analysis and evidence for receptor homo-oligomerization. J Biol Chem 1997;272: 4065–71.
8. Bjorbaek C, Uotani S, da Silva B, Flier JS. Divergent signaling capacities of the long and short isoforms of the leptin receptor. J Biol Chem 1997;272: 32686–95.
9. Yamashita T, Murakami T, Otani S, Kuwajima M, Shima K. Leptin receptor signal transduction: OBRa and OBRb of fa type. Biochem Biophys Res Commun 1998; 246:752–9.
10. Garofalo C, Surmacz E. Leptin and cancer. J Cell Physiol 2006;207:12–22.
11. Calle EE, Kaaks R. Overweight, obesity and cancer: epidemiological evidence and proposed mechanisms. Nat Rev Cancer 2004;4:579–91.
12. Hu X, Juneja SC, Maihle NJ, Cleary MP. Leptin: growth factor in normal and malignant breast cells and for normal mammary gland development. J Natl Cancer Inst 2002;94:1704–11.
13. Cleary MP, Phillips FC, Getzin SC, et al. Genetically obese MMTV-TGF-/$Lep^{ob}Lep^{ob}$ do not develop mammary tumors. Breast Cancer Res Treat 2003;77:205–15.
14. Cleary MP, Juneja SC, Phillips FC, Hu X, Grande JP, Maihle NJ. Leptin receptor-deficient MMTV-TGF-/$Lep^{db}Lep^{db}$ female mice do not develop oncogene-induced mammary tumors. Exp Biol Med (Maywood) 2004;229:182–93.
15. Garofalo C, Koda M, Cascio S, et al. Increased expression of leptin and the leptin receptor as a marker of breast cancer progression: possible role of obesity-related stimuli. Clin Cancer Res 2006;12:1447–53.
16. Takeichi M. Cadherin cell adhesion receptors as a morphogenetic regulator. Science 1991;251:1451–5.
17. Takeichi M. Morphogenetic roles of classic cadherins. Curr Opin Cell Biol 1995;7:619–27.
18. Perl AK, Wilgenbus P, Dahl U, Semb H, Christofori G. A causal role for E-cadherin in the transition from adenoma to carcinoma. Nature 1998;392:190–3.
19. Behrens J, Mareel MM, Van Roy FM, Birchmeier W. Dissecting tumor cell invasion: epithelial cells acquire invasive properties after the loss of uvomorulin-mediated cell-cell adhesion. J Cell Biol 1989;108:2435–47.
20. Frixen UH, Behrens J, Sachs M, et al. E-cadherin-mediated cell-cell adhesion prevents invasiveness of human carcinoma cells. J Cell Biol 1991;113:173–85.
21. Vleminckx K, Vakaet L, Jr., Mareel M, Fiers W, van Roy F. Genetic manipulation of E-cadherin expression by epithelial tumor cells reveals an invasion suppressor role. Cell 1991;66:107–19.
22. Dorudi S, Sheffield JP, Poulsom R, Northover JM, Hart IR. E-cadherin expression in colorectal cancer. An immunocytochemical and *in situ* hybridization study. Am J Pathol 1993;142:981–6.
23. Mbalaviele D, Dunstan CR, Sasaki A, Williams PJ, Mundy GR, Yoneda T. E-cadherin expression in human breast cancer cells suppresses the development of osteolytic bone metastases in an experimental metastasis model. Cancer Res 1996;56:4063–70.
24. Tsai CN, Tsai CL, Tse KP, Chang HY, Chang YS. The Epstein-Barr virus oncogene product, latent membrane

protein 1, induces the downregulation of E-cadherin gene expression via activation of DNA methyltransferases. Proc Natl Acad Sci U S A 2002;99:10084–9.
25. Catalano S, Mauro L, Marsico S, et al. Leptin induces, via ERK1/ERK2 signal, functional activation of estrogen receptor α in MCF-7 cells. J Biol Chem 2004;279:19908–15.
26. Morelli C, Garofalo C, Sisci D, et al. Nuclear insulin receptor substrate 1 interacts with estrogen receptor α at ERE promoters. Oncogene 2004;23:7517–26.
27. Dangles V, Femenia F, Laine V, et al. Two- and three-dimensional cell structures govern epidermal growth factor survival function in human bladder carcinoma cell lines. Cancer Res 1997;57:3360–4.
28. Kunz-Schughart LA, Kreutz M, Knuechel R. Multicellular spheroids: a three-dimensional *in vitro* culture system to study tumour biology. Int J Exp Pathol 1998;79:1–23.
29. Santini MT, Rainaldi G. Three-dimensional spheroid model in tumor biology. Pathobiology 1999;67:148–57.
30. Sutherland RM. Cell and environment interactions in tumor microregions: the multicell spheroid model. Science 1988;240:177–84.
31. Maggiolini M, Vivacqua A, Fasanella G, et al. The G protein-coupled receptor GPR30 mediates c-*fos* up-regulation by 17β-estradiol and phytoestrogens in breast cancer cells. J Biol Chem 2004;279:27008–16.
32. De Sousa LP, Brasil BS, Silva BM, et al. Plasminogen/plasmin regulates c-*fos* and egr-1 expression via the MEK/ERK pathway. Biochem Biophys Res Commun 2005;329:237–45.
33. Darnel JE. The JAK-STAT pathway: summary of initial studies and recent advances. Recent Prog Horm Res 1996;51:391–403.
34. Lorincz AM, Sukumar S. Molecular links between obesity and breast cancer. Endocr Relat Cancer 2006;13:279–92.
35. Orban Z, Remaley AT, Sampson M, Trajanoski Z, Chrousos GP. The differential effect of food intake and β-adrenergic stimulation on adipose-derived hormones and cytokines in man. J Clin Endocrinol Metab 1999;84:2126–33.
36. Reddy P, Lui L, Ren C, et al. Formation of E-cadherin-mediated cell-cell adhesion activates AKT and mitogen activated protein kinase via phosphatidylinositol 3 kinase and ligand-independent activation of epidermal growth factor receptor in ovarian cancer cells. Mol Endocrinol 2005;19:2564–78.
37. Steinberg MS, McNutt PM. Cadherins and their connections: adhesion junctions have broader functions. Curr Opin Cell Biol 1999;11:554–60.
38. Xing J, Ginty DD, Greenberg ME. Coupling of the RAS-MAPK pathway to gene activation by RSK2, a growth factor-regulated CREB kinase. Science 1996;273:959–63.
39. Dalby KN, Morrice N, Caudwell FB, Avruch J, Cohen P. Identification of regulatory phosphorylation sites in mitogen-activated protein kinase (MAPK)-activated protein kinase-1a/p90rsk that are inducible by MAPK. J Biol Chem 1998;273:1496–505.
40. Bannister AJ, Oehler T, Wilheim D, Angel P, Kouzarides T. Stimulation of c-Jun activity by CBP: c-*jun* residues $Ser^{63/73}$ are required for CBP induced stimulation *in vivo* and CBP binding *in vitro*. Oncogene 1995;11:2509–14.
41. Krishnan V, Wang X, Safe S. Estrogen receptor-Sp1 complexes mediate estrogen-induced cathepsin D gene expression in MCF-7 human breast cancer cells. J Biol Chem 1994;269:15912–7.
42. Porter W, Saville B, Hoivik D, Safe S. Functional synergy between the transcription factor Sp1 and the estrogen receptor. Mol Endocrinol 1997;11:1569–80.
43. Petz LN, Nardulli AM. Sp1 binding sites and an estrogen response element half-site are involved in regulation of the human progesterone receptor A promoter. Mol Endocrinol 2000;14:972–85.
44. Saville B, Wormke M, Wang F, et al. Ligand-, cell-, and estrogen receptor subtype (α/β)-dependent activation at GC-rich (Sp1) promoter elements. J Biol Chem 2000;275:5379–87.
45. Panno ML, Mauro L, Marsico S, et al. Evidence that the mouse insulin receptor substrate-1 belongs to the gene family on which the promoter is activated by estrogen receptor α through its interaction with Sp1. J Mol Endocrinol 2006;36:91–105.
46. Catalano S, Marsico S, Giordano C, et al. Leptin enhances, via AP-1, expression of aromatase in the MCF-7 cell line. J Biol Chem 2003;278:28668–76.
47. Garofalo C, Sisci D, Surmacz E. Leptin interferes with the effects of the antiestrogen ICI 182,780 in MCF-7 breast cancer cells. Clin Cancer Res 2004;10:6466–75.
48. De Miguel F, Lee SO, Onate SA, Gao AC. Stat3 enhances transactivation of steroid hormone receptors. Nucl Recept 2003;1:3–10.
49. Houslay MD, Kolch W. Cell-type specific integration of cross-talk between extracellular signal-regulated kinase and cAMP signalling. Mol Pharmacol 2000;58:659–68.

Journal of Cellular Physiology

Fas Ligand Expression in TM4 Sertoli Cells is Enhanced by Estradiol "In situ" Production

STEFANIA CATALANO,[1] PIETRO RIZZA,[1] GUOWEI GU,[1] INES BARONE,[1] CINZIA GIORDANO,[2] STEFANIA MARSICO,[1] IVAN CASABURI,[1] EMILIA MIDDEA,[1] MARILENA LANZINO,[1] MICHELE PELLEGRINO,[1] AND SEBASTIANO ANDÒ[2]*

[1]*Department of Pharmaco-Biology, University of Calabria 87036 Arcavacata di Rende (CS), Calabria, Italy*

[2]*Department of Cell Biology Faculty of Pharmacy, University of Calabria 87036 Arcavacata di Rende (CS), Calabria, Italy*

The testis is an immunologically privileged site of the body where Sertoli cells work on to favor local immune tolerance by testicular autoantigens segregation and immunosuppressive factors secretion. Fas/Fas Ligand (FasL) system, expressed prevalently in Sertoli cells, has been considered to be one of the central mechanisms in testis immunological homeostasis. In different cell lines it has been reported that the proapoptotic protein FasL is regulated by 17-β estradiol (E2). Thus, using as experimental model mouse Sertoli cells TM4, which conserve a large spectrum of functional features present in native Sertoli cells, like aromatase activity, we investigated if estradiol "in situ" production may influence FasL expression. Our results demonstrate that an aromatizable androgen like androst-4-ene-3,17-dione (Δ4) enhanced FasL mRNA, protein content and promoter activity in TM4 cells. The treatment with N^6,2′-*O*-dibutyryladenosine-3′-5′-cyclic monophosphate [$(Bu)_2$cAMP] (simulating FSH action), that is well known to stimulate aromatase activity in Sertoli cells, amplified Δ4 induced FasL expression. Functional studies of mutagenesis, electrophoretic mobility shift (EMSA) and chromatin immunoprecipitation (ChIP) assays revealed that the Sp-1 motif on FasL promoter was required for E2 enhanced FasL expression in TM4 cells. These data let us to recruit FasL among those genes whose expression is up-regulated by E2 through a direct interaction of ERα with Sp-1 protein. Finally, evidence that an aromatizable androgen is able to increase FasL expression suggests that E2 production by aromatase activity may contribute to maintain the immunoprivilege status of Sertoli cells.

J. Cell. Physiol. 211: 448–456, 2007.

The immunoprivilege of male gonad lies on blood-testis barrier, prevalently maintained by Sertoli cell functions. This physical barrier between the general circulation and testicular tissue probably conceals antigens from the immune system and prevents effector cell access (Filippini et al., 2001; Bart et al., 2002; Ferguson et al., 2002). This immune protective function together with the secretion of hormonal and nutritive factors produced by Sertoli cells, under FSH control, substain germ cells functional maturation along all spermatogenesis process (Griswold et al., 1988; De Cesaris et al., 1992).

The Fas/FasL system was first identified in T cells (Suda et al., 1993; Lynch et al., 1995) where it plays a key role in eliminating T cell populations following antigenic stimulation and clonal proliferation. This system is also functional in the testis (Bellgrau et al., 1995; Sanberg et al., 1996) and in a variety of other tissues in which these proteins are constitutively expressed to maintain their immunoprivilege, such as eyes (Griffith et al., 1995), placenta (Guller, 1997; Uckman et al., 1997) and brain (Saas et al., 1997).

FasL is a type II trans-membrane protein that belongs to the tumor necrosis factor (TNF) family of cytokines and induces apoptosis in cells expressing Fas receptors (Suda et al., 1993). Fas (CD95, APO-1) is a transmembrane receptor protein, sharing a high degree of homology with the tumor necrosis factor/nerve growth factor receptor family (TNF/NGF-Rs) (Watanabe-Fukunaga et al., 1992; Nagata and Goldstein, 1995). It is characterized by an intracellular domain called "death domain" responsible for the activation of the intracellular signaling pathway following Fas-FasL interaction (Nagata and Goldstein, 1995).

The Fas/FasL expression during testicular development and its cell specific localization within the testis is still a matter of debate, but it is generally assumed that FasL is predominantly expressed in Sertoli cells (Suda et al., 1993; Bellgrau et al., 1995; French et al., 1996; Lee et al., 1997; Francavilla et al., 2000; D'Abrizio et al., 2004).

Among the different factors influencing FasL, it has been reported that 17-β estradiol (E2) is able to regulate the expression of this proapoptotic protein in human endometrial cells (Selam et al., 2001) and human ovarian tissue (Sapi et al., 2002). Moreover, estrogen treatment increases FasL expression in monocytes through the interaction of estrogen receptor with FasL promoter (Mor et al., 2003).

It has been well established that the estrogens biosynthesis, in the testis, is catalyzed by the enzyme complex referred to as aromatase cytochrome P450, which aromatizes the A ring of C19 androgens to the phenolic A ring of C18 estrogens (Armstrong and Dorrington, 1977; Van der Molen et al., 1981). The enzyme aromatase is composed of two polypeptides: an ubiquitous non-specific flavoprotein NADPH-cytochrome P450 reductase and a specific form of cytochrome P450 (P450arom encoded by the CYP 19 gene) (Simpson et al., 1994). In the testis an age-related change has been observed in the cellular localization of the aromatization event, primarily in Sertoli cells in immature animals, but located in Leydig and germ cells in adults (Levallet et al., 1998; Andò et al., 2001). Besides, the synthesis of estrogens is regulated at the level of the

Stefania Catalano and Pietro Rizza contributed equally to this work.

Contract grant sponsor: PRIN-MIUR;
Contract grant number: 2004067227.

*Correspondence to: Sebastiano Andò, Department of Cell Biology University of Calabria, Arcavacata di Rende (CS) Calabria 87036, Italy. E-mail: sebastiano.ando@unical.it

Received 22 June 2006; Accepted 24 October 2006

DOI: 10.1002/jcp.20952

aromatizing enzyme system by Follicole-Stimulating Hormone (FSH) and cyclic AMP (Dorrington and Armstrong, 1975).
In the mouse Sertoli cell line TM4 we previously demonstrated P450arom immunocytochemical localization together with its enzymatic activity (Catalano et al., 2003).
In the present study, we investigated if an aromatizable androgen like androst-4-ene-3,17-dione (Δ4), after its conversion to E2, can modulate FasL expression in TM4 cells. Our results demonstrate that estradiol "in situ" production enhanced FasL mRNA, protein content and promoter activity. Many transcription factors have been reported to regulate FasL promoter by DNA-protein interaction upon diverse biological signals in different cells and tissues (Latinis et al., 1997; Kasihatla et al., 1998; Matsui et al., 1998; Mittelstadt and Ashwell, 1998; Kavurma et al., 2001; Kirschhoff et al., 2002; Kavurma and Khachigian, 2003).
Functional studies of mutagenesis, electrophoretic mobility shift analysis and ChIP assay lead us to demonstrate that the up-regulatory effects induced by E2 on FasL expression are mediated by a direct interaction of Estrogen Receptor alpha (ERα) with Sp-1 protein.

Materials and Methods

Materials

Dulbecco's Modified Eagle's Medium/Nutrient Mixture F-12 Ham (DMEM/F12), Triazol Reagent and 100 bp DNA ladder by Invitrogen (Carlsbad, CA), L-Glutamine, penicillin, horse serum, Eagle's non-essential amino acids, calf serum (CS), streptomycin, bovine serum albumine (BSA), phosphate-buffered saline (PBS) were purchased from Eurobio (Les Ullis Cedex, France). FuGENE 6, Sephadex G50 spin columns and poly (dI-dC) by Roche (Indianapolis, IN). GoTaq DNA polymerase, T4 polynucleotide Kinase, TNT master mix, Dual luciferase kit, Sp-1 human recombinant protein and TK renilla luciferase plasmid were provided by Promega (Madison, WI). The RETROscript kit and DNase I were purchased from Ambion (Austin, TX). Aprotinin, leupeptin, phenylmethylsulfonyl fluoride (PMSF), sodium orthovanadate, androst-4-ene-3,17-dione (Δ4), 7α,19α-dimethyl-19-nortestosterone (mibolerone), formaldehyde, NP-40, proteinase K, tRNA, Tamoxifen (Tam), N^6,2′-*O*-dibutyryladenosine-3′-5′-cyclic monophosphate [$(Bu)_2$cAMP] and 1,3,5-Tris(4-Hydroxyphenyl)-4-propyl-1H-pyrazole (PPT) by Sigma (Milan, Italy). Antibodies against ERα, ERβ, β-actin, Sp-1, and polymerase II (N20) were provided by Santa Cruz Biotechnology (Santa Cruz, CA) whereas anti-FasL antibody by BD biosciences (San Josè, CA). ECL System and [γ^{32}P]ATP were purchased by Amersham Pharmacia (Buckinghamshire, UK). Letrozole was provided by Novartis Pharma AG (Basel, Switzerland), Mithramycin by ICN Biomedicals, (Shelton, CT). Salmon sperm DNA/protein A agarose by UBI (Chicago, IL). Diarylpropionitrile (DPN) and ICI 182,780 were purchased from Tocris chemical (Bristol, UK). ABI Prism 7000 Sequence Detection System, TaqMan Ribosomal RNA Reagent kit, TaqMan Ribosomal RNA Control Reagent kit and SYBR Green Universal PCR Master Mix by Biosystems (Forster City, CA).

Cell cultures

The TM4 cell line, derived from the testis of immature BALB/c mice, was originally characterized based on its morphology, hormone responsiveness, and metabolism of steroids (Mather, 1980). This cell line was obtained from the American Type Culture Collection (ATCC) (Manassas, VA) and cultured in DMEM-F12 containing 2.5% fetal CS, 5% horse serum, 1 mg/ml penicillin–streptomycin. Human uterin cervix adenocarcinoma (HeLa) cells were obtained from the ATCC. HeLa cells were cultured in DMEM/F12 containing 5% CS, 1% L-Glutamine, 1% Eagle's non essential amino acids and 1 mg/ml penicillin–streptomycin.

Western blot analysis

TM4 cells were grown in 10 cm dishes to 70–80% confluence and lysed in 500 μl of 50 mM Hepes (pH 7.5), 150 mM NaCl, 1.5 mM $MgCl_2$, 1 mM EGTA, 10% glycerol, 1% Triton X-100, a mixture of protease inhibitors (Aprotinin, PMSF and Na-orthovanadate). Equal amounts of total proteins were resolved on a 11% SDS-polyacrylamide gel and then electroblotted onto a nitrocellulose membrane. Blots were incubated overnight at 4°C with: (1) mouse monoclonal ERα antibody, (2) rabbit polyclonal ERβ ??antibody, (3) mouse monoclonal FasL antibody, (4) mouse monoclonal β-actin antibody. The antigen-antibody complex was detected by incubation of membranes 1 h at room temperature with peroxidase-coupled goat anti-rabbit IgG or goat anti-mouse IgG and revealed using the ECL System. Blots were then exposed to film and bands of interest were quantified by densitometer (Mod 620 BioRad, USA). The results obtained as optical density arbitrary values were transformed to percentages of the control (percent control) taking the samples from cells not treated as 100%.

Real-time RTPCR

Total cellular RNA was extracted from TM4 cells using "TRIAZOL Reagent" as suggested by the manufacturer. All RNA was treated with DNase I and purity and integrity of the RNA were confirmed spectroscopically and by gel electrophoresis prior to use. Two micrograms of total RNA was reverse transcribed in a final volume of 50 μl using a RETROscript kit as suggested by the manufacturer. cDNA was diluted 1:5 in nuclease free water, aliquoted and stored at −20°C. The cDNAs obtained were further amplified for FasL gene using the following primers: forward 5′-CGAGGAGTGTGGCCCATTT-3′ and reverse 5′-GGTTCCATATGTGTCTTCCCATTC-3′.
PCR reactions were performed in the ABI Prism 7000 Sequence Detection System, using 0.1 μM of each primer, in a total volume of 30 μL reaction mixture following the manufacturer's recommendations. SYBR Green Universal PCR Master Mix for the dissociation protocol was used for FasL and 18S. Negative control contained water instead of first-strand cDNA. Each sample was normalized on the basis of its 18S ribosomal RNA content. The 18S quantification was performed using a TaqMan Ribosomal RNA Reagent kit following the method provided in the TaqMan Ribosomal RNA Control Reagent kit. The relative FasL gene expression levels were normalized to a calibrator that was chosen to be the basal, untreated sample. Final results were expressed as n-fold differences in FasL gene expression relative to 18S rRNA and calibrator, calculated following the ΔΔCt method, as follows:

$$\text{n-fold} = 2^{-(\Delta Ct_{\text{sample}} - \Delta Ct_{\text{calibrator}})}$$

where ΔCt values of the sample and calibrator were determined by subtracting the average Ct value of the 18S rRNA reference gene from the average Ct value of the different genes analyzed.

Transfection assay

Transient transfection experiments were performed using pGL_2 vectors containing different deleted segments of human FasL gene promoter (p-2365: −2365/−2; p-318: −318/−2; p-237: −237/−2) ligated to a luciferase reporter gene (kindly provided by Dr. Paya, Department of Immunology, Mayo Clinic Rochester, Minnesota, USA). Deletion of Sp-1 sequence in FasL gene promoter was generated by PCR using as template p-318 construct. The resulting plasmid encoding the human Fas-L gene promoter containing the desired deletion was designed p-280 Sp-1 and the sequence was confirmed by nucleotide sequence analysis.
FuGENE 6 was used as recommended by the manufacturer to transfect TM4 cells plated in 3.5 cm^2 wells with pGL_2 FasL promoter constructs (0.5 μg/well).
Another set of experiments was performed in HeLa cells cotransfecting p-318 FasL promoter (−318/−2) (0.5 μg/well) and the wild-type human ERα expression vector (HEGO) (0.5 μg/well) (Tora et al., 1989) or pCMV5-hERβ, containing human ERβ gene (0.5 μg/well) (a gift from JA Gustafsson).
Empty vectors were used to ensure that DNA concentrations were constant in each transfection. TK renilla luciferase plasmid (25 ng/well) was used to normalize the efficiency of the transfection. Twenty-four hours after transfection, the medium was changed and TM4 cells were treated in serum free medium (SFM) in the presence of Δ4, $(Bu)_2$cAMP, mibolerone, letrozole, PPT and DPN. HeLa cells, 24 h after transfection, were treated in the presence or absence of E2 for 24 h. The firefly and renilla luciferase activities were measured using Dual Luciferase Kit. The firefly luciferase data for each sample were

normalized on the basis of transfection efficiency measured by renilla luciferase activity.

Electrophoretic mobility shift assay (EMSA)

Nuclear extracts were prepared from TM4 as previously described (Andrews and Faller, 1991). Briefly, TM4 cells plated into 60 mm dishes were scraped into 1.5 ml of cold PBS. Cells were pelleted for 10 sec and resuspended in 400 μl cold buffer A (10 mM HEPES-KOH pH 7.9 at 4°C, 1.5 mM $MgCl_2$, 10 mM KCl, 0.5 mM dithiothreitol, 0.2 mM PMSF, 1 mM leupeptin) by flicking the tube. The cells were allowed to swell on ice for 10 min and then vortexed for 10 sec. Samples were then centrifuged for 10 sec and the supernatant fraction discarded. The pellet was resuspended in 50 μl of cold Buffer B (20 mM HEPES-KOH pH 7.9, 25% glycerol, 1.5 mM $MgCl_2$, 420 mM NaCl, 0.2 mM EDTA, 0.5 mM dithiothreitol, 0.2 mM PMSF, 1 mM leupeptin) and incubated on ice for 20 min for high-salt extraction. Cellular debris was removed by centrifugation for 2 min at 4°C and the supernatant fraction (containing DNA binding proteins) was stored at −70°C. The yield was determined by Bradford method (Bradford, 1976). The probe was generated by annealing single stranded oligonucleotides and labeled with [γ^{32}P] ATP and T4 polynucleotide kinase, and then purified using Sephadex G50 spin columns. The DNA sequences used as probe or as cold competitor are the following (the nucleotide motifs of interest are underlined and mutations are shown as lowercase letters): Sp1 5′-AAATTGTGGGCGGAAACTTCCAGGGG-3′, mutated Sp-1 5′-AAATTGTGttCGGAAACTTCCAGGGG-3′. Oligonucleotides were synthesized by Sigma Genosys. The protein binding reactions were carried out in 20 μl of buffer (20 mM HEPES pH 8, 1 mM EDTA, 50 mM KCl, 10 mM DTT, 10% glicerol, 1 mg/ml BSA, 50 μg/ml poli dI/dC) with 50,000 cpm of labeled probe, 10 μg of TM4 nuclear protein and 5 μg of poly (dI-dC). The above-mentioned mixture was incubated at room temperature for 20 min in the presence or absence of unlabeled competitor oligonucleotide. For experiments involving Sp-1, ERα and ERβ antibodies, the reaction mixture was incubated with these antibodies at 4°C for 12 h. For in vitro mithramycin treatment, mithramycin (100 nM) was incubated with the labeled probe for 30 min at 4°C before the addition of nuclear extract. As positive controls we used Sp-1 human recombinant protein (1 μl) and in vitro transcribed and translated ERα protein (1 μl) synthesized using T7 polymerase in the rabbit reticulocyte lysate system as direct by the manufacturer. The entire reaction mixture was electrophoresed through a 6% polyacrylamide gel in 0.25 X Tris borate-EDTA for 3 h at 150 V. Gel was dried and subjected to autoradiography at −70°C.

Chromatin immunoprecipitation (ChIP)

According to the ChIP assay procedure previously described (Shang et al., 2000), TM4 cells were grown in 60 mm dishes to 50–60% confluence, shifted to SFM for 24 h and then treated with E2 (100 nM), ICI 182,780 (10 μM), E2 + ICI for 1 h. Thereafter, the cells were washed twice with PBS and crosslinked with 1% formaldehyde at 37°C for 10 min. Next, cells were washed twice with PBS at 4°C, collected and resuspended in 200 μl of lysis buffer (1% SDS, 10 mM EDTA, 50 mM Tris-HCl pH 8.1) and left on ice for 10 min. Then, cells were sonicated four times for 10 sec at 30% of maximal power (Sonics, Vibra Cell 500W) and collected by centrifugation at 4°C for 10 min at 14,000 rpm. The supernatants were diluted in 1.3 ml of IP buffer (0.01% SDS, 1.1% Triton X-100, 1.2 mM EDTA, 16.7 mM Tris-HCl pH 8.1, 16.7 mM NaCl) and immunocleared with 80 μl of sonicated salmon sperm DNA/protein A agarose for 1 h at 4°C. The precleared chromatin was immunoprecipitated with a specific anti-Sp-1, anti ERα and anti polymerase II antibodies and with a normal mouse serum IgG (Nms) as negative control. At this point, 60 μl of salmon sperm DNA/protein A agarose were added and precipitation was further continued for 2 h at 4°C. After pelleting, precipitates were washed sequentially for 5 min with the following buffers: Wash A (0.1% SDS, 1% Triton X-100, 2 mM EDTA, 20 mM Tris-HCl pH 8.1, 150 mM NaCl), Wash B (0.1% SDS, 1% Triton X-100, 2 mM EDTA, 20 mM Tris-HCl pH 8.1, 500 mM NaCl), and Wash C (0.25 M LiCl, 1% NP-40, 1% sodium deoxycholate, 1 mM EDTA, 10 mM Tris-HCl pH 8.1), and then twice with TE buffer (10 mM Tris, 1 mM EDTA). The immunocomplexes were eluated with elution buffer (1% SDS, 0.1 M $NaHCO_3$), reverse crosslinked by heating at 65°C and digested with proteinase K (0.5 mg/ml) at 45°C for 1 h. DNA was obtained by phenol/chloroform/isoamyl alcohol extraction. Two microliters of 10 mg/ml yeast tRNA were added to each sample and DNA was precipitated with 70% EtOH for 24 h at −20°C, and then washed with 95% EtOH and resuspended in 20 μl of TE buffer. One microlitre of each sample was used for PCR amplification with the following primers flanking Sp-1 sequence present in the Fas-L promoter region: 5′-GCAACTGAGGCCTTGAAGGC-3′ (forward) and 5′-GCAGCTGGTGAGTCAGGCCAG-3′ (reverse). The PCR conditions were 1 min at 94°C, 1 min at 65°C, and 2 min at 72°C. The amplification products obtained in 25 cycles were analyzed in a 2% agarose gel and visualized by ethidium bromide staining.

Statistical analysis

Each datum point represents the mean ± SE of three different experiments. Data were analyzed by ANOVA test using the STATPAC computer program.

Results

Estradiol "in situ" production, by aromatase activity, enhances FasL expression in TM4 cell line

In TM4 cells, which exibit a spectrum of features in common with native Sertoli cells, like the presence of aromatase activity, we investigated if an aromatizable androgen Δ4, through its conversion into E2, may influence FasL mRNA and protein content by Real-time RT-PCR and Western blot analysis. Since aromatase expression and activity, in Sertoli cells, is under FSH control (Dorrington and Armstrong, 1975) we also evaluated the treatment with $(Bu)_2$cAMP (simulating FSH action) on FasL expression.

As shown in Figure 1A the treatment with Δ4 (100 nM) for 24 h resulted in an increase of FasL mRNA expression more than 1.9-fold. The simultaneous treatment with $(Bu)_2$cAMP (1 mM) and Δ4, further enhanced FasL mRNA expression compared with Δ4 treatment alone (2.4-fold), suggesting that $(Bu)_2$cAMP stimulates E2 "in situ" production by its action on aromatase activity. These up-regulatory effects were reversed by addition of the aromatase inhibitor letrozole (1 μM) (90%), while no significant difference was observed in the presence of a non-aromatizable androgen mibolerone (100 nM) with or without $(Bu)_2$cAMP.

Next, we performed Western blot analysis using a monoclonal antibody anti FasL. We detected a band of 37 kDa which intensity was increased upon Δ4 treatment. Exposure to $(Bu)_2$cAMP combined with Δ4 enhanced the effect induced by Δ4 alone. The addition of letrozole reversed these up-regulatory effects (Fig. 1B,C).

To evaluate whether E2 "in situ" production was able to activate FasL promoter we transiently transfected TM4 cells with vector containing human FasL promoter fused to the luciferase reporter gene. The treatment for 24 h with Δ4 or Δ4 + $(Bu)_2$cAMP displayed a significant increase of the basal promoter activity that was reversed by letrozole (Fig. 1D).

Effects of Δ4 on expression of human FasL promoter/luciferase reporter gene constructs in TM4 cells

To delimit the *cis*-elements involved in FasL transcriptional activation by Δ4, we transiently transfected TM4 cells with plasmids containing different deleted segments of human FasL promoter. Schematic representation of constructs is shown in Figure 2A. Transfected cells were untreated (C) or treated with 100 nM of Δ4 and 1 μM of letrozole.

p-318 plasmid showed a higher basal activity when compared with the other plasmids (p-2365, p-237) (Fig. 2B) suggesting the presence of a DNA sequences upstream from −318 to which transcription factors with repressor activity bind. These data well fit with previous results demonstrating that FasL gene promoter region, located between −318 and −237, plays a major role in promoting basal transcription in TM4 Sertoli cells (McClure et al., 1999).

In TM4 cells transfected with p-2365 and p-318 plasmids the treatment with Δ4 induced a significant increase of the basal

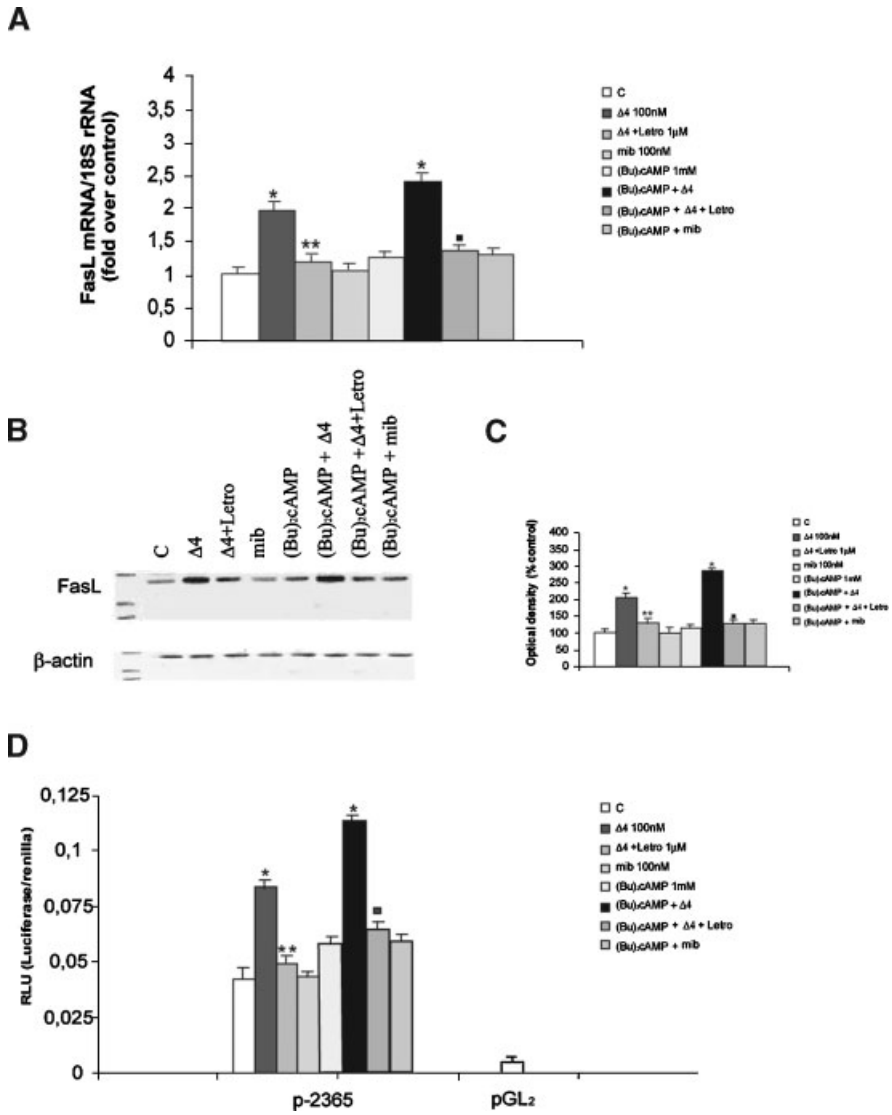

Fig. 1. Effects of Δ4 on FasL expression. A: Total RNA was obtained from TM4 cells untreated (control, C) or treated for 24 h with Δ4 (100 nM) mibolerone (mib 100 nM), $(Bu)_2$cAMP (1 mM), $(Bu)_2$cAMP + Δ4 and $(Bu)_2$cAMP + mib. One micromolar of aromatase inhibitor letrozole (Letro) was used. Real time RT-PCR was performed to analyze mRNA levels of FasL. Data represent the mean ± SE of values from three separate RNA samples. Each sample was normalized to its 18S ribosomal RNA content. Final results are expressed as n-fold differences of gene expression relative to calibrator (control) calculated with the ΔΔCt method as indicated in the "Material and Methods" section. *$P < 0.01$ compared to control. **$P < 0.01$ compared to Δ_4 treated samples; ■ $P < 0.01$ compared to $(Bu)_2$cAMP + Δ4 treated samples. B: Immunoblot of FasL from TM4 cells treated in the absence (C) or in the presence of the above-mentioned treatments. C: The histograms represent the mean ± SE of three separate experiments in which band intensities were evaluated in term of optical density arbitrary units and expressed as percentage of the control assumed as 100%. *$P < 0.01$ compared to control; **$P < 0.01$ compared to Δ_4 treated samples; ■ $P < 0.01$ compared to $(Bu)_2$cAMP + Δ4 treated samples. D: Transcriptional activity of TM4 cells transfected with p-2365 construct is shown. TM4 cells were treated in the absence (C) or in the presence of Δ4 (100 nM), mibolerone (mib 100 nM), $(Bu)_2$cAMP (1 mM), $(Bu)_2$cAMP + Δ4 and $(Bu)_2$cAMP + mib. One micromolar of aromatase inhibitor letrozole was used. The values represent the means ± SE of three different experiments. In each experiment, the activities of the transfected plasmids were assayed in triplicate transfections. pGL_2: basal activity measured in cells transfected with pGL_2 basal vector. *$P < 0.01$ compared to control. **$P < 0.01$ compared to Δ4 treated samples; ■ $P < 0.01$ compared to $(Bu)_2$cAMP + Δ4 treated samples.

promoter activity that was completely reversed by letrozole. In contrast, Δ4 was unable to activate p-237 construct eliciting, in the region from −318 to −237, the presence of *cis*-element involved in estrogen responsiveness. In fact, this region contains Sp-1 site, a potential target of ER. In order to explore the role of the Sp-1 binding site in the regulation of FasL expression by Δ4, functional experiments were performed using the Sp-1 deleted plasmid (p-280 Sp-1). Luciferase assay revealed that the inducibility by Δ4 on FasL promoter was totally lost (Fig. 2D). These results suggest that the up-regulatory effects of estradiol production by aromatase activity require Sp-1 sequence motif.

ERβ is not involved in E2-modulating FasL expression

Before exploring more closely the possible interaction between E2/ER complex to Sp-1 and the role of this binding in modulating FasL expression, we set out to determine which functional ER(s) isoform was present in TM4 cells. By Western blotting

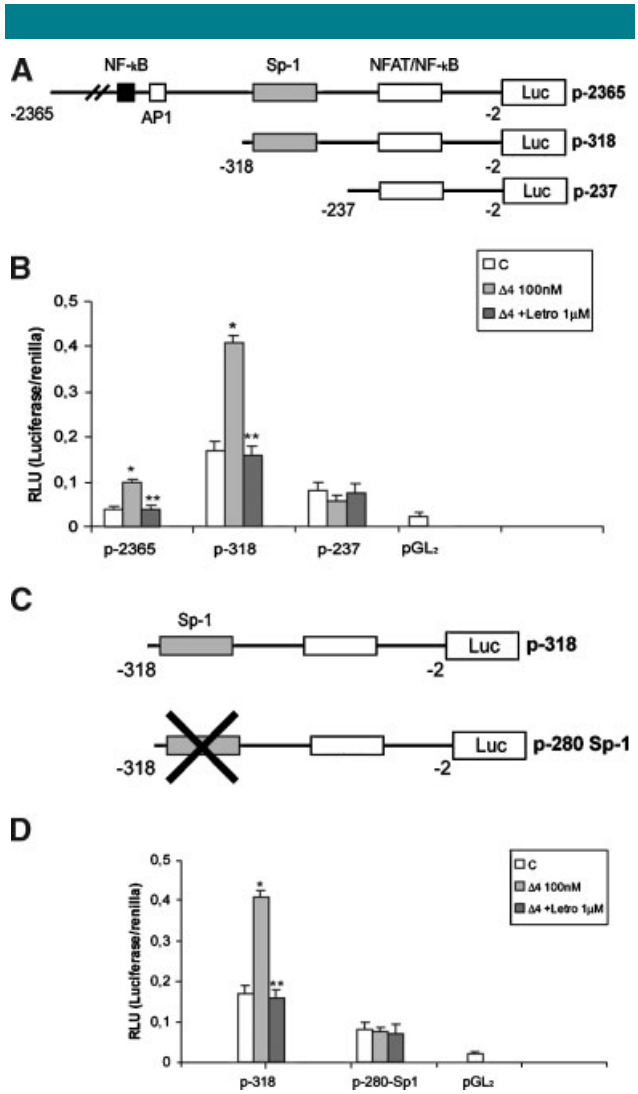

Fig. 2. Effects of estradiol "in situ" production on expression of human FasLpromoter/luciferase reporter gene construts in TM4 cells. A: Schematic map of the FasL promoter fragments used in this study. All of the promoter constructs contain the same 3′ boundary (−2). The 5′ boundaries of the promoter fragments varied from −237 to −2365. Each fragment was subcloned into the pGL_2 vector. B: Transcriptional activity of TM4 cells with promoter constructs is shown. TM4 cells were treated in the absence (C) or in the presence of Δ4 (100 nM), and Δ4 + letrozole (1 μM) for 24 h. The values represent the means ± SE of three different experiments. In each experiment, the activities of the transfected plasmids were assayed in triplicate transfections. pGL_2: basal activity measured in cells transfected with pGL_2 basal vector. *$P < 0.01$ compared to control; **$P < 0.01$ compared to Δ4 treated samples. C: Schematic representation of the p-318 and p-280 Sp-1 constructs. The deletion of Sp-1 sequence is present in p-280 Sp-1 construct containing the region from −318 to −2 of FasL promoter gene. Each fragment was subcloned into the pGL_2 vector. D: Transcriptional activity of TM4 cells with p-280 Sp-1 construct is shown. TM4 cells were treated in the absence (C) or in the presence of Δ4 (100 nM), and Δ4 + letrozole (1 μM) for 24 h. The values represent the mean ± SE of three different experiments. In each experiment, the activities of the transfected plasmids were assayed in triplicate transfections. *$P < 0.01$ compared to control; **$P < 0.01$ compared to Δ4-treated samples.

analysis, we demonstrated in TM4 protein extracts the presence of both ER(s) (Fig. 3A, lane 2), As positive control, the breast cancer cell line MCF-7 (ERα positive) and human prostate cancer cell line LNCaP (ERβ positive) were used (Fig. 3A, lane 1).
In the presence of the two different ER antagonists ICI 182,780 (10 μM) and tamoxifen (10 μM) (Tam) the up-regulation of E2 on FasL expression was abrogated demonstrating that this effect was specifically dependent by ER (Fig. 3B,C).
To specify which isoforms of ER were mainly involved in FasL transactivation, we cotransfected HeLa cells (ER negative) with p-318 FasL promoter and the wild type human ERα or ERβ expression vector. The treatment with E2 (100 nM) for 24 h showed an increased transcriptional activation of FasL promoter only in cells cotransfected with ERα (Fig. 3D).
Finally, to demonstrate further the direct involvement of ERα in FasL transactivation we used 100 nM of the selective agonists of ERα [1,3,5-Tris(4-Hydroxyphenyl)-4-propyl-1H-pyrazole (PPT)] and ERβ [diarylpropionitrile (DPN)] in TM4 cells transiently transfected with p-318 FasL promoter. The treatment with PPT showed an increase of FasL promoter activity while no change was observed in the presence of DPN (Fig. 3E).

Effects of 17-β estradiol treatment on Sp1 DNA binding activity in TM4 cells

On the basis of the evidences that the up-regulatory effects of E2 on FasL require the crucial presence of Sp-1-RE, EMSA was performed using synthetic oligodeoxyribonucleotides corresponding to the putative Sp-1 binding site. In the presence of TM4 nuclear extracts (10 μg) we observed the formation of a specific complex (Fig. 4A, lane 1), which was abrogated by a 100-fold molar excess of unlabeled probe (Fig. 4A, lane 2). This inhibition was not observed when a mutated Sp-1 oligonucleotide was used as competitor (Fig. 4A, lane 3). E2-treatment induced a strong increase in Sp-1 DNA binding activity (Fig. 4A, lane 4) compared with basal levels. In the presence of ICI 182,780 the Sp-1 DNA binding activity was drastically reduced (Fig. 4A, lane 5). The addition of mithramycin (100 nM), that binds to GC boxes and prevents sequential Sp-1 binding, decreased the binding of E2 treated TM4 nuclear extracts on Sp-1 DNA sequence (Fig. 4A, lane 6). In a cell free system we observed in the presence of Sp-1 reconbinant protein a single band that causes the same shift respect to the complex revealed in TM4 nuclear extracts (Fig. 4A, lane 7) which was abrogated by 100-fold molar excess of unlabeled probe (Fig. 4A, lane 8). Transcribed and translated in vitro ERα protein did not bind directly to Sp-1 probe (Fig. 4A, lane 9). When the nuclear extracts from TM4 cells treated with E2 were incubated with either anti-Sp-1 or anti-ERα antibody, the original band DNA-protein complex was immunodepleted (Fig. 4B, lanes 3 and 4), whereas anti-ERβ antibody gave no effects (lane 5).
Taken together these results suggest that ERα is recruited by Sp-1 in our DNA binding complex.

17-β Estradiol enhances recruitment of Sp-1/ERα to the promoter region of FasL gene in TM4 cells

Interaction of ERα and Sp-1 with the FasL gene promoter was also investigated using a ChIP assay. After sonication and immunoprecipitation by anti ERα or anti Sp-1 antibodies, PCR was used to determine binding of ERα/Sp-1 protein to the −318 to −2 DNA region of the FasL gene promoter. Our results indicated that treatment with E2 induced an increased recruitment of Sp-1/ERα complex to the FasL promoter. The latter event was reduced in the presence of E2 + ICI. The enhanced recruitment of Sp-1/ERα was correlated with greater association of polymerase II to the FasL regulatory region

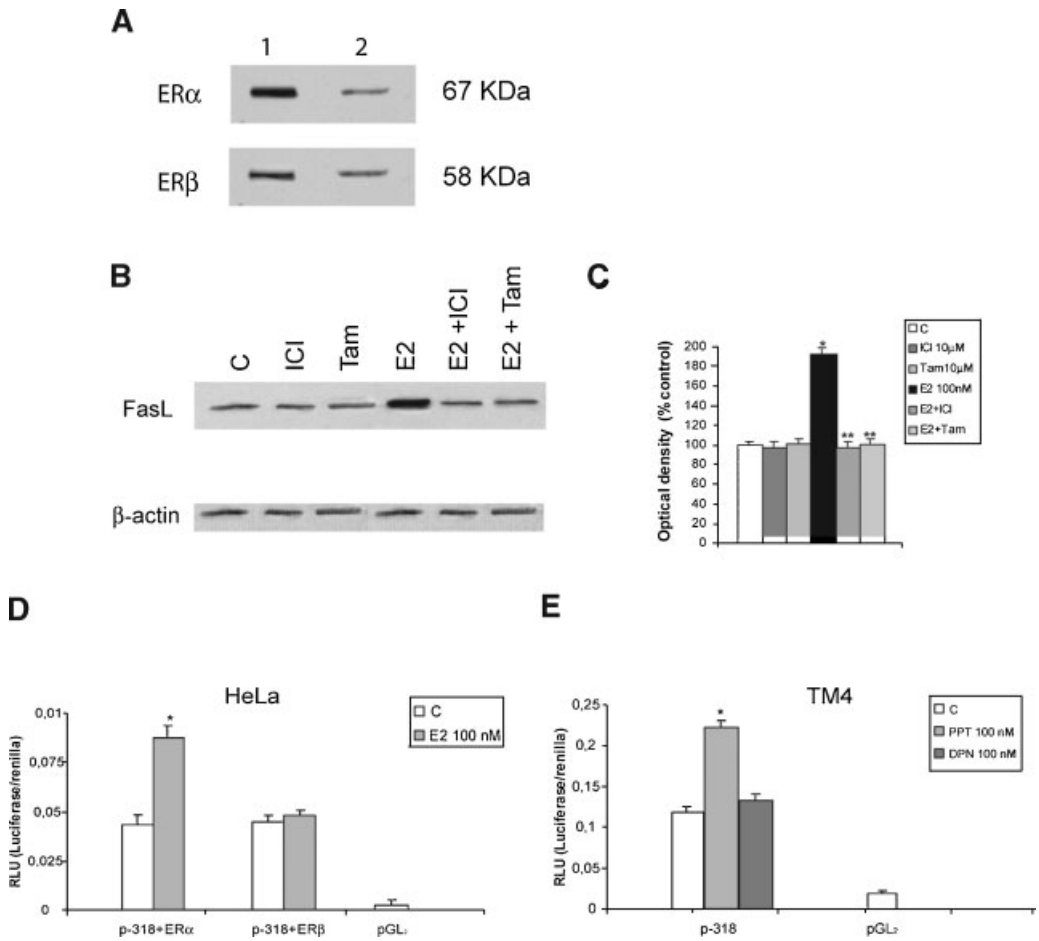

Fig. 3. 17β-Estradiol enhances FasL transcriptional activity through ERα. A: Lysates from TM4 cells were used to evaluate by Western blot analysis the expression of ERα and ERβ (lane 2). The human breast cancer cell line MCF-7 and human prostate cancer cell line LNCaP were used as positive control for ERα and ERβ respectively (lane 1). B,C: Immunoblot of FasL from TM4 cells treated in the absence (C) or in the presence of E2 (100 nM) for 24 h. The pure anti-estrogen ICI 182,780 (10 μM) and tamoxifen (Tam 10 μM) were used. The histograms represent the means ± SE of three separate experiments in which band intensities were evaluated in term of optical density arbitrary units and expressed as percentage of the control assumed as 100%. *$P < 0.01$ compared to control; **$P < 0.01$ compared to E2 treated samples. D: HeLa cells were transiently cotransfected with p-318 FasL promoter construct (−318/−2) and ERα or ERβ plasmids. The cells were untreated (C) or treated with E2 (100 nM) for 24 h. The values represent the means ± SE of three different experiments. In each experiment, the activities of the transfected plasmids were assayed in triplicate transfections. *$P < 0.01$ compared to control. E: TM4 cells transfected with p-318 FasL promoter construct were untreated (C) or treated with PPT (100 nM) and DPN (100 nM) for 24 h. *$P < 0.01$ compared to control.

(Fig. 5A). No PCR product was observed using DNA immunoprecipitated with normal mouse serum IgG.

Discussion

In testis, Fas/FasL interaction has been thought to play an important role in the establishment of immunoprivilege. Several reports have demonstrated that Sertoli cells through FasL may trigger apoptotic cell death of sensitive lymphoid cells, which express on their cell surface Fas receptor. This has provided new insights into the concepts of tolerance and immunoprivilege (Bellgrau et al., 1995; Sanberg et al., 1996; Ferguson and Griffith, 1997). For instance, testis grafts from mice expressing FasL survived when transplanted into allogeneic animals. On the contrary, grafts derived from "gld" mice, which lack functional FasL, were rejected (Bellgrau et al., 1995).

In the present report, for the first time, we have provided evidences that, in TM4 cell line, an aromatizable androgen Δ4 induces a strong increase in FasL mRNA, protein content and promoter activity. These effects are reversed by addition of letrozole, an aromatase inhibitor, addressing how E2 "in situ" production by aromatase activity plays a crucial role in modulating the immunoprivileged status of these somatic cells. A further support to the specificity of the above described results raises from the evidence that no noticeable effect was produced by mibolerone, a non-aromatizable steroid.

It is well known that postnatal development and function of testicular Sertoli cells is regulated primarily by FSH, a glycoprotein hormone secreted by the pituitary gland (Dorrington and Armstrong, 1975). In the prepubertal testis, FSH is required for Sertoli cells proliferation to achieve the adult number of these cells (Griswold, 1998). This proliferative stage of Sertoli cells development is also characterized by the presence of FSH-dependent cytochrome P450 aromatase activity (Carreau et al., 2003; Sharpe et al., 2003). In our recent work (Catalano et al., 2003) we have documented in TM4 cell line a strong dose-dependent stimulation of aromatase activity

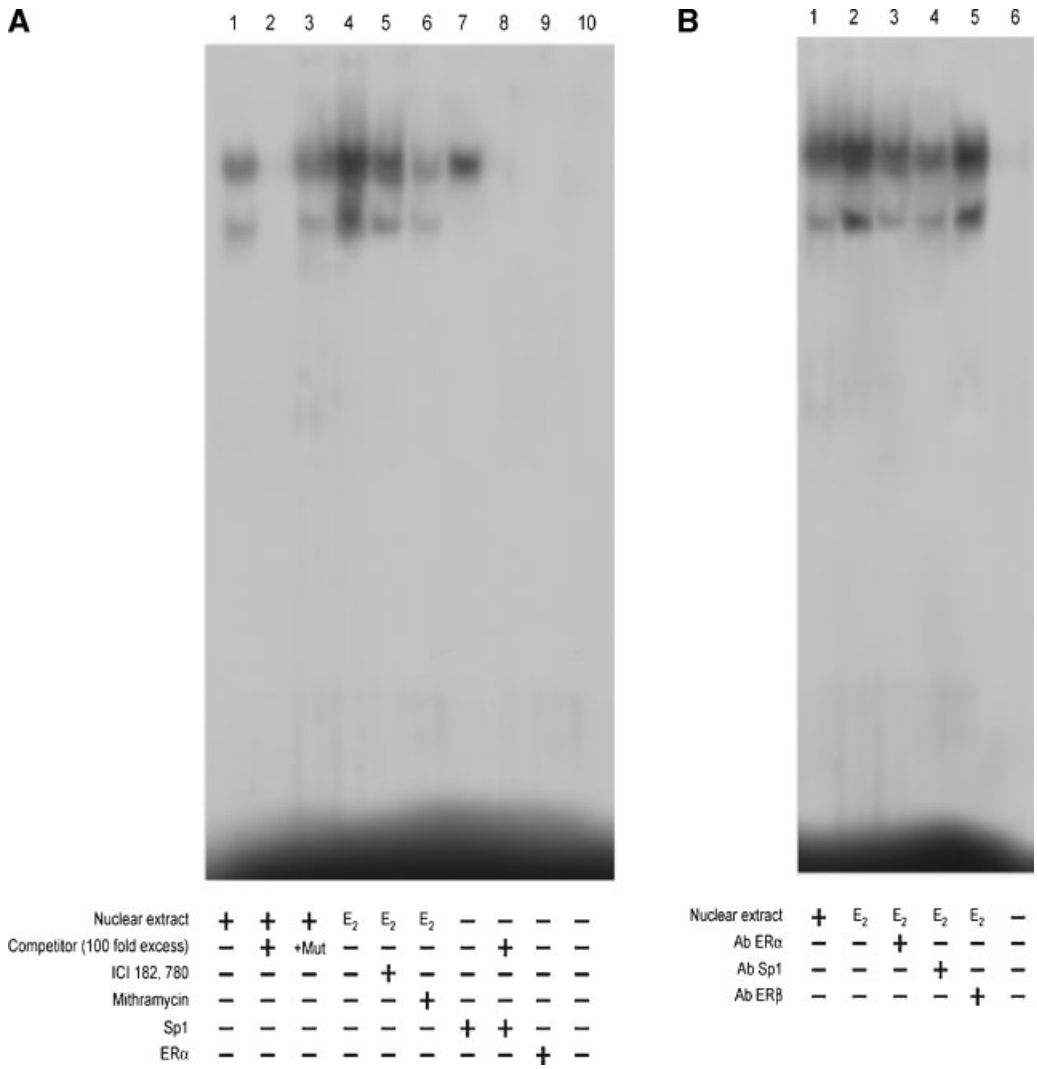

Fig. 4. Electrophoretic mobility shift assay of the Sp-1 binding site in the FasL promoter region. A: Nuclear extracts from TM4 cells were incubated with a double-stranded Sp1-specific consensus sequence probe labeled with [γ-^{32}P] ATP and subjected to electrophoresis in a 6% polyacrylamide gel (lane 1). Competition experiments were perfomed adding as competitor a 100-fold molar excess of unlabeled probe (lanes 2 and 8) or a 100-fold molar excess of unlabeled oligonucleotide containing a mutated Sp-1 (lane 3). Nuclear extracts were obtained from TM4 cells treated with 100 nM of E2 (lane 4), E2 + ICI 182,780 (10 μM) (lane 5), E2 + mithramycin (100 nM) (lane 6) for 24 h. As control we used human Sp-1 recombinant protein and transcribed and translated in vitro ERα protein (lane 7 and 9). Lane 10 contains probe alone. B: Anti-ERα, anti Sp-1 and anti-ERβ antibodies (lanes 3–5) were incubated with E2-treated TM4 nuclear extracts. Lane 6 contains probe alone.

induced by $(Bu)_2$cAMP similar to that described previously in immature Sertoli cells (Andò et al., 2001). In the present study it is worth to emphasize that FSH induced an increased FasL expression through the enhancement of aromatase activity.

To elucidate the molecular mechanism involved in Δ4 enhanced FasL expression, we transiently transfected TM4 cells with different constructs containing deleted segments of the human FasL promoter.

A maximal constitutive reporter gene activity was observed with p-318 construct, containing the region between −318 and −2 bp from the transcriptional start site of the human FasL promoter. This is in agreement with previous results demonstrating that FasL gene promoter region from 318 to −237 bp plays a major role in promoting basal transcription in TM4 cells (McClure et al., 1999). Moreover, the induced activation by Δ4 was not observed in cells transfected with p-237 construct (−237 to −2) suggesting that the region between −318 and −237 bp contains elements that mediate the potentiating effects of estrogen on FasL expression.

A broadening number of transactivating factors has been identified as regulators of FasL gene expression (Kavurma and Khachigian, 2003), as nuclear factor in activated T cells (NF-AT) (Latinis et al., 1997), nuclear factor-kappa B (NF-KB) (Matsui et al., 1998), activator protein-1 (AP-1) (Kasihatla et al., 1998), interferon regulatory factor-1 (IFN-1) (Kirschhoff et al., 2002), early growth response factor (Egr) (Mittelstadt and Ashwell, 1998) and specificity protein-1 (Sp-1) (Kavurma et al., 2001). Sp-1 is involved in the transcriptional regulation of many genes and has also been identified to be important in the regulation of FasL gene expression and apoptosis. Indeed, this transcription factor is able to activate FasL promoter via a distinct recognition element, and inducible FasL promoter activation is abrogated by expression of the dominant-negative mutant form of Sp-1 (Kavurma et al., 2001). In addition, it has been recently

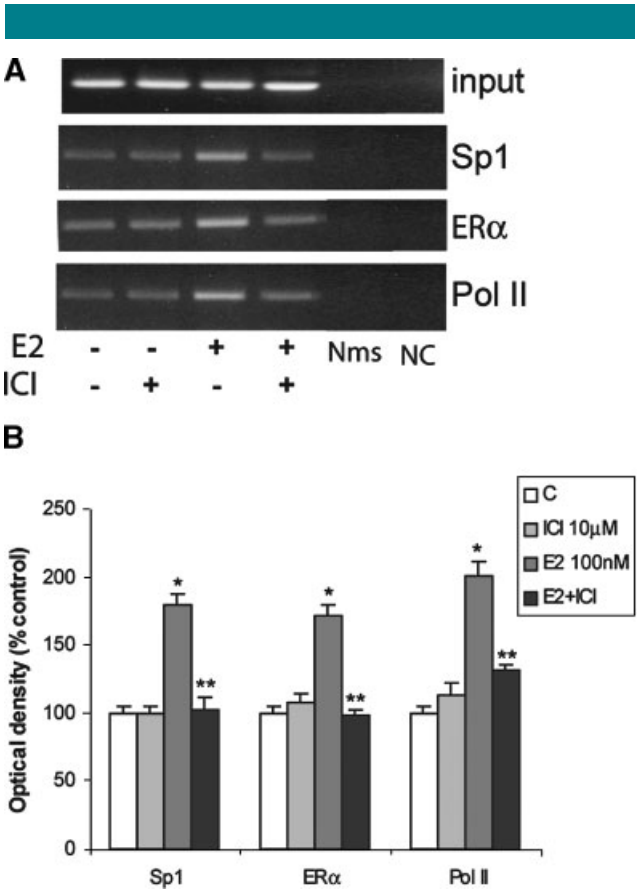

Fig. 5. 17β-Estradiol increases Sp-1/ERα recruitement to FasL promoter. A: Soluble precleared chromatin was obtained from TM4 cells treated for 1 h with 100 nM E2, 10 μM ICI and E2 + ICI or left untreated (C) and immunoprecipitated (IP) with an anti-Sp-1, anti ERα, anti polymerase II antibodies and with a normal mouse serum (Nms) as negative control. The FasL promoter sequences containing Sp-1 were detected by PCR with specific primers, as described in "Materials and Methods". To control input DNA, FasL promoter was amplified from 30 μl of initial preparations of soluble chromatin (before immunoprecipitations). PCR products obtained at 25 cycles are shown. Sample without the addition of DNA was used as negative control (NC). This experiment was repeated three times with similar results. B: The histograms represent the means ± SE of three separate experiments in which band intensities were evaluated in term of optical density arbitrary units and expressed as percentage of the control assumed as 100%. *$P < 0.01$ compared to control; **$P < 0.01$ compared to E2-treated samples.

demonstrated that nuclear extracts of TM4 Sertoli cells contain high levels of Sp-1 and Sp-3 that specifically bind to the GGGCGG consensus sequence present in the FasL gene, and overexpression of Sp-1 but not Sp-3 is able to increase the basal transcription of the FasL promoter (McClure et al., 1999). The latter observation fits with our functional studies demonstrating that Sp-1 is a crucial effector of estradiol signal in enhancing FasL gene expression. For instance, it is well known that ERs can transactivate gene promoters without directly binding to DNA but instead through interaction with other DNA-bound factors in promoter regions lacking TATA box. This has been most extensively investigated in relationship to protein complexes involving Sp-1 and ERα at GC boxes, which are classic binding sites for members of the Sp-1 family of transcription factors. Sp-1 protein plays an important role in the regulation of mammalian and viral genes, and recent results have shown that E2 responsiveness of c-fos, cathepsin D, retinoic acid receptor α1 and insulin-like grow factor-binding protein 4 gene expression in breast cancer cells is linked to specific GC rich promoter sequences that bind ER/Sp-1 complex in which only Sp-1 protein binds DNA (Krishnan et al., 1994; Cowley et al., 1997; Porter et al., 1997; Sun et al., 1998; Qin et al., 1998; Saville et al., 2000).

In our work, the interaction between ERα and Sp-1 is clearly evidenced by gel mobility shift analysis and chromatin immunoprecipitation assay. Besides, the functional assays performed in ER-negative HeLa cells showed that ERα and not ERβ mediates the estrogen-induced increase in FasL gene expression. The specificity of ERα to induce transcription of FasL in TM4 was demonstrated using selective agonists for the ER subtypes. For instance we evidenced that only PPT was able to enhance FasL promoter activity.

Our results stemming from functional analysis, EMSA and ChiP assays led us to recruit FasL among those genes whose expression is upregulated by E2 through a direct interaction of ERα with Sp-1 protein.

In conclusion, the present study demonstrates that aromatizable steroids, normally present in the testicular milieu, through their conversion into E2 by aromatase activity, are able to increase FasL expression in TM4 Sertoli cells. The aromatase enzyme assures that estrogens through a short autocrine loop maintain Sertoli cells proliferation before their terminal differentiation. Thus, we propose that at the latter crucial maturative stage, FasL may achieve an intracellular content sufficient to protect Sertoli cells from any injury induced by Fas expressing immunocells, then potentiating the immunoprivileged condition of the testis.

Acknowledgments

We thank Dr C.V. Paya for providing us with the pGL2 promoter FasL (p-2365, p-318, p-237) and Dr Domenico Sturino for English revision of the manuscript.

Literature Cited

Andrews NC, Faller DV. 1991. A rapid micropreparation technique for extraction of DNA-binding proteins from limiting numbers of mammalian cells. Nucleic Acids Res 19:2499.

Andò S, Sirianni R, Forastieri P, Casaburi I, Lanzino M, Rago V, Giordano F, Giordano C, Carpino A, Pezzi V. 2001. Aromatase expression in prepubertal Sertoli cells: Effect of thyroid hormone. Mol Cell Endocrinol 178:11–21.

Armstrong DT, Dorrington JH. 1977. Estrogen biosynthesis in ovaries and testes. Adv Sex Horm Res 32:17–258.

Bart J, Green HJ, van der Graaf WT, Hollema H, Hendrikse NH, Vaanburg W, Sleijfer DT, de Vries EG. 2002. An oncological view on the blood-testis barrier. Lancet Oncol 3:357–363.

Bellgrau D, Gold D, Selawry H, Moore J, Franzusoff A, Duke RC. 1995. A role for CD95 ligand in preventing graft rejection. Nature 377:630–632.

Bradford MM. 1976. A rapid and sensitive method for quantitation of microgram quantities of protein utilizing the principle of protein-dye binding. Anal Biochem 72:248–254.

Carreau S, Lambard S, Delalande C, Denis-Galeraud I, Bilinska B, Bourguiba S. 2003. Aromatase expression and role of estrogens in male gonad: A review. Reprod Biol Endocrinol 1:35.

Catalano S, Pezzi V, Chimento A, Giordano C, Carpino A, Young M, McPhaul MJ, Andò S. 2003. Triiodothyronine decreases the activity of the proximal promoter (PII) of the Aromatase gene in the mouse Sertoli cell line TM4. Mol Endocrinol 17:923–934.

Cowley SM, Hoare S, Mosselman S, Parker MG. 1997. Estrogen receptor alpha and beta form heterodimers on DNA. J Biol Chem 272:19858–19862.

D'Abrizio P, Baldini E, Russo PF, Biordi L, Graziano FM, Rucci N, Properzi G, Francavilla S, Ulisse S. 2004. Ontogenesis and cell specific localizzation of Fas ligand expression in the rat testis. Int J Androl 27:304–310.

De Cesaris P, Filippini A, Cervelli C, Riccioli A, Muci S, Storace G, Stefanini M, Riparo E. 1992. Immunosuppressive molecules produced by Sertoli cells cultured in vitro: Biological effects on lymphocytes. Biochem Biophys Res Commun 186:1639–1646.

Dorrington JH, Armstrong DT. 1975. Follicle-stimulating hormone stimulates estradiol-17 β synthesis in cultured Sertoli cells. Cell Biol 72:2677–2681.

Ferguson TA, Griffith TS. 1997. A vision of cell death: Insight into immune privilege. Immunol Rey 156:167–184.

Ferguson TA, Green DR, Griffith TS. 2002. Cell death and immune privilege. Int Rev Immunol 21:153–172.

Filippini A, Riccioli A, Padula F, Lauretti P, D'Alessio A, De Cesaris P, Gandini L, Lenzi A, Riparo E. 2001. Control and impairment of immune privilege in the testis and semen. Human Reprod Update 7:444–449.

Francavilla S, D'Abrizio P, Rucci N, Silvano G, Properzi G, Straface E, Cordeschi G, Necozione S, Gnessi L, Arizzi M, Ulisse S. 2000. Fas and Fas ligand expression in fetal and adult human testis with normal or deranged spermatogenesis. J Clin Endocrinol Metab 85:2692–2700.

French LE, Hahne M, Viard I, Radlgruber G, Zanone R, Becker K, Muller C, Tschopp J. 1996. Fas and Fas ligand in embryos and adult mice: Ligand expression in several immune-privileged tissues and coexpression in adult tissues characterized by apoptotic cell turnover. J Cell Biol 133:335–343.

Griffith TS, Brunner T, Fletcher SM, Green DR, Ferguson TA. 1995. Fas ligand-induced apoptosis as a mechanism of immune privilege. Nature 270:1189–1192.
Griswold MD. 1998. The central role of Sertoli cells in spermatogenesis. Semin Cell Dev Biol 9:411–416.
Griswold MD, Morales C, Sylvester SR. 1988. Molecular biology of the Sertoli cell. Oxf Rev Reprod Biol 10:124–161.
Guller S. 1997. Role of Fas ligand in conferring immune privilege to non-lymphoid cells. Ann NY Acad Sci 828:268–272.
Kasihatla S, Brunner T, Genestier L, Echeverri F, Mahboubi A, Green DR. 1998. DNA damaging agents induce expression of Fas lignd and subsequent apoptosis in T lynphocytes via the actiation of NF-kB and AP-1. Mol Cell 1:543–551.
Kavurma MM, Khachigian LM. 2003. Signaling and transcriptional control of FasL gene expression. Cell Death Differ 10:36–44.
Kavurma MM, Santiago FS, Bonfoco E, Khachigian LM. 2001. Sp-1 phosphorylation regulates apoptosis via extracellular FasL-Fas engagement. J Biol Chem 276:4964–4971.
Kirschhoff S, Sebens T, Baumann S, Krueger A, Zawatzky R, Li-Webber M, Meini E, Neipel F, Fieckenstein B, Krammer PH. 2002. Viral IFN-regulatory factors inhibit activation-induced cell death via two positive regulatory IFN-regulatory factor 1-dependent domains in the CD95 ligand promoter. J Immunol 168:1226–1234.
Krishnan V, Wang X, Safe S. 1994. Estrogen receptor-Sp1 complexes mediate estrogen-induced cathepsin D gene expression in MCF-7 human breast cancer cells. J Biol Chem 269:15912–15917.
Latinis KM, Norian LA, Eliason SL, Koretzky GA. 1997. Two NFAT transcription factor binding sites partecipate in the regulation of CD95 (Fas) ligand expression in activated human T cells. J Biol Chem 272:31427–31434.
Lee J, Richburg JH, Younkin SC, Boekelheide K. 1997. The Fas system is a key regulator of germ cell apoptosis in testis. Endocrinology 138:2081–2088.
Levallet J, Bilinska B, Mittre H, Genissel C, Fresnel J, Carreau S. 1998. Expression and immunolocalization of functional cytochrome P450 aromatase in mature rat tesicular cells. Biol Reprod 58:919–926.
Lynch DH, Ramsdell F, Alderson MR. 1995. Fas and FasL in the homeostatic regulation of immune responses. Immunol Today 16:569–574.
Mather J. 1980. Establishment and characterization of two distinct mouse testicular epithelial cell lines. Biol Reprod 23:243–252.
Matsui K, Fine A, Zhu B, Marshak-Rothstein A, Ju ST. 1998. Identification of two NF-kappa B sites in mouse CD95 ligand (Fas ligand) promoter: Funcional anlaysis in T cell hybridoma. J Immunol 161:3469–3473.
McClure RF, Heppelmann CJ, Paya CV. 1999. Constitutive Fas ligand gene transcription in Sertoli cells is regulated by Sp1. J Biol Chem 274:7756–7762.
Mittelstadt PR, Ashwell JD. 1998. Cyclosporin A-sensitive transcription factor Egr-3 regulates Fas ligand expression. Mol Cell Biol 18:3744–3751.
Mor G, Sapi E, Abrahams VM, Rutherford T, Song J, Hao XY, Muzaffar S, Kohen F. 2003. Interaction of the estrogen receptors with the Fas ligand promoter in human monocytes. J Immunol 170:114–122.
Nagata S, Goldstein P. 1995. The Fas death factor. Science 267:1449–1456.
Porter W, Saville B, Holvik D, Safe S. 1997. Funcional synergy between the transcription factor Sp-1 and the estrogen receptor. Mol Endocrinol 11:1569–1580.
Qin C, Singh P, Safe S. 1998. Transcriptional activation of insulin-like growth factor binding protein 4 by 17β-estradiol in MCF-7 cells: Role of estrogen receptor-Sp1 complexes. Endocrinology 140:2501–2508.
Saas P, Walker P, Hahne M, Quiquerez AL, Schnuriger V, Perrin G, French L, Meir EGV, deTribolet N, Tschopp J, Dietrich PY. 1997. Fas ligand expression by astrocytoma in vivo: Maintaining immune privilege in the brain? J Clin Invest 99:1173–1178.
Sanberg PR, Borlongan CV, Saporta S, Cameron DF. 1996. Testis-derived Sertoli cells survive and provide localized immunoprotection for xenografts in rat brain. Nat Biotechnol 114:1692–1695.
Sapi E, Brown WD, Aschkenazi S, Lim C, Munoz A, Kacinski BM, Rutherford T, Mor G. 2002. Regulation of Fas ligand expression by estrogen in normal ovary. J Soc Gynerol Investig 9:243–250.
Saville B, Wormke M, Wang F, Nguyen T, Enmark E, Kuiper G, Gustafsson JA, Safe S. 2000. Ligand-, cell-, and estrogen receptor subtype (α/β)- dependent activation at GC-rich (Sp-1) promoter elements. J Biol Chem 275:5379–5387.
Selam B, Kayisli UA, Mulayim N, Arici A. 2001. Regulation of Fas ligand expression by estradiol and progesterone in human endometrium. Biol Reprod 65:979–985.
Shang Y, Hu X, DiRenzo J, Lazar MA, Brown H. 2000. Cofactor dynamics and sufficiency in estrogen receptor-regulated transcription. Cell 103:843–852.
Sharpe RM, McKinnell C, Kivlin C, Fisher JS. 2003. Proliferation and functional maturation of Sertoli cells, and their relevance to disorders of testis function in adulthood. Reproduction 125:769–784.
Simpson ER, Mahendroo MS, Means GD, Kilgore MW, Hinshelwood MM, Graham-Lorence S, Amameh B, Ito Y, Fisher CR, Mandelson CR, Bulun SE. 1994. Aromatase cytocrome P450, the enzyme responsible for estrogen biosynthesis. Endocr Rev 15:342–355.
Suda T, Takahashi T, Goldstein P, Nagata S. 1993. Molecular cloning and expression of the Fas ligand, a novel member of the tumor necrosis factor family. Cell 75: 1169–1178.
Sun G, Porter W, Safe S. 1998. Estrogen-induced retinoic acid receptor α1 gene expression: Role of estrogen receptor-Sp1 complex. Mol Endocrinol 12:882–890.
Tora L, Mullick A, Metger D, Ponglikitmongkol M, Park I, Chambon P. 1989. The cloned human oestrogen receptor contains a mutation which alters its hormone binding properties. EMBO J 88:1981–1986.
Uckman D, Steele A, Cherry Wang BY, Chamizo W, Koutsonikolis A, Gilbert-Barness E, Good RA. 1997. Trophoblasts express Fas ligand: A proposed mechanism for immune privilege in placenta and maternal invasion. Mol Hum Reprod 3:655–662.
Van der Molen HJ, Brinkmann AO, De Jong FH, Rommeerts FF. 1981. Testicular oestrogens. J Endocrinol 89:33P–46P.
Watanabe-Fukunaga R, Brannan CI, Itoh N, Yonehara S, Copeland NG, Jenkins NA, Nagata S. 1992. The cDNA structure, expression, and chromosomal assignment of the mouse Fas antigen. J Immunol 148:1274–1279.

FEBS Letters 580 (2006) 2371–2380

Evidence that low doses of Taxol enhance the functional transactivatory properties of p53 on p21 waf promoter in MCF-7 breast cancer cells

M. Luisa Panno[a,*], Francesca Giordano[a], Fabrizia Mastroianni[b], Catia Morelli[b], Elvira Brunelli[c], M. Grazia Palma[b], Michele Pellegrino[b], Saveria Aquila[b], Antonella Miglietta[d], Loredana Mauro[a], Daniela Bonofiglio[b], Sebastiano Andò[a,b,*]

[a] *Department of Cellular Biology, University of Calabria, Ponte Pietro Bucci, Cubo 4C, 87030, Arcavacata di Rende, Cosenza, Italy*
[b] *Faculty of Pharmacy, University of Calabria, 87030, Arcavacata di Rende, Cosenza, Italy*
[c] *Department of Ecology, University of Calabria, Arcavacata di Rende, Cosenza, Italy*
[d] *Department of Experimental Medicine and Oncology, University of Torino, Turin, Italy*

Received 10 January 2006; revised 10 March 2006; accepted 14 March 2006

Available online 29 March 2006

Edited by Varda Rotter

Abstract In the present study, we evidence how in breast cancer cells low doses of Taxol for 18 h determined the upregulation of p53 and p21 waf expression concomitantly with a decrease of the anti-apoptotic Bcl-2. P53 and its gene product, the mdm2 protein, in treated cells exhibits a prevalent nuclear compartmentalization, thus potentiating p53 transactivatory properties. Indeed, the most important finding of this study consists with the evidence that Taxol at lower concentrations is able to produce the activation of p21 promoter via p53. Prolonged exposure of MCF-7 cells to Taxol (48 h) resulted in an increased co-association between p21 and PCNA compared to control and this well fits with the simultaneous block of cell cycle into the G2/M phase.

Keywords: Taxol; p21 waf; p53; Breast cancer cells

1. Introduction

Taxol is a chemotherapic drug specifically effective against prostate, ovarian, breast and lung cancer. Its primary mechanism of action is related to the ability to stabilize the microtubules and to disrupt their dynamic equilibrium [1–6].

Treatment of cells with Taxol interferes with the normal reorganization of the microtubule network, and inhibits the formation of normal spindle at metaphase required for mitosis and cell proliferation. These effects lead to an arrest of the cells in the G2/M phase of the cell cycle and eventually to apoptotic cell death [7–9].

The biological responses to Taxol may vary depending on cell type and drug concentration.

An aspect extremely intriguing rises from the evidence that low doses of Taxol in human lung cancer, though still unable to alter all microtubule network, upregulate p53 and its nuclear compartmentalization [10]. Indeed, the polymerization of microtubules with the extension of their minus end, induced by Taxol, may facilitate the translocation of p53, using dynein as carrier, from the cytosol into the nucleus [10,11].

In this compartment, p53 stimulates the expression of proteins involved in a wide network of signals that act through two major apoptotic pathways: the extrinsic death receptor signalling which triggers caspases activation and Bid cleavage, and the intrinsic mitochondrial pathway, which shifts the balance in the Bcl-2 family towards the pro-apoptotic members, enhancing mitochondrial permeabilization with consequent release of cytochrome *c* and direct caspases activation [12]. These events have been previously reported in human neuroblastoma, ovarian and breast carcinoma cells that underwent Taxol treatment [13–15].

Taxol-initiated apoptosis has been also associated with increase of p21 waf/Cip protein, a key regulator of cell cycle and DNA synthesis, which expression is regulated by p53-dependent and/or independent mechanisms [16–19].

P21 binds to various cyclin–CDK complexes and inhibits their activity, thus resulting in a block in cell cycle [20]. An alternative mechanism through which p21 inhibits cell cycle progression lays on its capability to recruit PCNA, then enabling this factor to interact with the DNA polymerase δ and ε activities [21,22].

In the present study, we have explored if low doses of Taxol "per se" are able to enhance the transactivatory properties of p53 producing the upregulation of p53-classically dependent gene, such as p21 waf, involved in the regulation of cell apoptosis and in the progression of cell cycle.

2. Materials and methods

2.1. Materials

DMEM/Ham's F-12, L-glutamine, penicillin/streptomycin, calf serum (CS), bovine serum albumin, aprotinin, leupeptin, phenylmethylsulfonyl fluoride (PMSF), sodium orthovanadate and Taxol were purchased from Sigma (Milan, Italy). FuGENE 6 was from Roche

*Corresponding authors. Fax: +39 0984 492911 (M.L. Panno), +39 0984 496203 (S. Andò).
E-mail addresses: mamissina@yahoo.it (M.L. Panno), sebastiano.ando@unical.it (S. Andò).

0014-5793/$32.00
doi:10.1016/j.febslet.2006.03.055

Applied Science (Milan, Italy). Dual luciferase kit and TK Renilla luciferase plasmid were provided by Promega (Madison, WI). [γ^{32}P]-ATP and ECL system come from Amersham Biosciences.

The plasmid WWP-Luc containing human p21 waf promoter (2.4 kb) was kindly given by Dr. Wafik El-Deiry (Howard Hughes Medical Institute, Philadelphia); pCMV-wt p53 plasmid, pCMV-p53 plasmid mutant and pCMV empty vector were generously provided by Dr. G. Daniel (Department of Health and Human Service, Natl. Inst. Env. Health Sci., Res. Triangle Park, NC). Thin layer chromatography (TLC) aluminium sheets were from MERK (Milan, Italy).

2.2. Cell lines and culture conditions

Human breast cancer MCF-7 cell line was cultured in DMEM/Ham's F12 (1:1) medium supplemented with 5% CS, 1% L-glutamine and 1% penicillin/streptomycin. The cells were cultured in phenol-red-free DMEM (PRF-SFM-DMEM) containing 0.5% bovine serum albumin, 1% L-glutamine and 1% penicillin/streptomycin, 24 h before each experiment. Next, the 70% confluent cells, synchronized in PRF-SFM-DMEM (day 0) [23] were treated with different doses of Taxol (2, 6, 12, 50, 100 nM) for 18 and 48 h.

2.3. Cell viability

The viability of the cells was assessed by morphological analysis using trypan blue exclusion assay. Cells in the exponential growth phase were plated and grown overnight; then, the medium was changed and shifted for 24 h with PRF-SFM-DMEM. At the end of this incubation the cells were exposed for 18 and 48 h to different concentrations of Taxol, as reported in Fig. 1. Cells were trypsinized and incubated in a 0.5% trypan blue solution for 10 min at room temperature and viable numbers were determined microscopically by counting trypan blue negative cells in a counting chamber (Burker, Brand, Germany).

2.4. Transfections and luciferase assay

MCF-7 cells were seeded (1×10^5 cells/well) in DMEM/F12 supplemented with 5% CS in 24-well plates. Cells were co-transfected with the plasmid WWP-Luc containing human p21 waf promoter and pCMV-empty vector or pCMV-p53 mutant plasmid or pCMV-wt p53 plasmid, in SFM using FuGENE6 according to the manufacture's instructions with a mixture containing 0.1 μg/well of each specific plasmid and 25 ng/well of TK Renilla luciferase plasmid. 24 h after the transfection the medium was changed and the cells were treated in PRF-SFM-DMEM in the presence of 2, 6 and 12 nM of Taxol for 18 h. The firefly and Renilla luciferase activities were measured by using a dual luciferase kit. The firefly luciferase data for each sample were normalized on the basis of the transfection efficiency measured by Renilla luciferase activity.

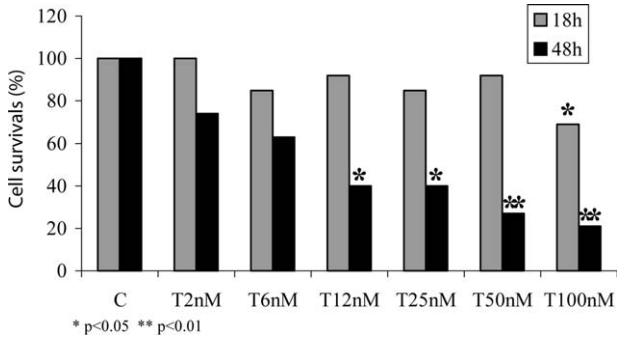

Fig. 1. Cell viability of MCF-7 cells after Taxol treatment. MCF-7 cells were plated in six-well plates at a density of 2×10^5 cells/well and grown 24 h to be completely attached to the surface of the plates. The day after, the medium was switched to serum-free medium for 24 h. Next, the cells were added of different doses of Taxol ranging from 2 nM until 100 nM and incubated for 18 and 48 h. Values are the average of four triplicate independent experiments, and are expressed as percentage of the controls, determined by standardizing untreated cells to 100%. $^{*}P < 0.05$ $^{**}P < 0.01$ as compared to untreated cells. The S.D. was lower than 0.25%.

2.5. Immunoprecipitation and Western blotting

MCF-7 cells were grown in 100 mm dishes to 70–80% confluence, shifted to SFM for 24 h and lysed. Cytoplasmic protein lysates were obtained with a buffer containing 50 mM HEPES, pH 7.5, 150 mM NaCl, 1.5 mM $MgCl_2$, 10 mM EGTA, pH 7.5, 10% glycerol, 1% Triton X-100 and protease inhibitors (2 μM Na_3VO_4, 1% PMSF, 20 μg/ml aprotinin). Following the collection of cytoplasmic proteins, the nuclei were lysed with the buffer containing 20 mM KOH–HEPES, pH 8, 0.1 mM EDTA, 5 mM $MgCl_2$, 0.5 M NaCl, 20% glycerol, 1% Np-40 and inhibitors (as above) [24].

The association of PCNA (Proliferating Cell Nuclear antigen) and p21 waf/Cip and/or phospho p21 (Thr 145) proteins was assessed by immunoprecipitation (IP) and Western blotting (WB) in 500 μg protein lysates using appropriate antibodies (as specified in the figure legends), while the association of dynein and p53 proteins was determined by immunoprecipitating the nuclear fractions with anti-dynein antibody and then blotting for anti-p53 antibody and anti-β-tubulin. In IPs, protein lysates were incubated in HNTG buffer (20 mM HEPES, pH 7.5, 150 mM NaCl, 0.1% Triton X-100, 10% glycerol and 0.2 mM Na_3VO_4) at 4 °C for 4 h with the primary antibodies, and then agarose beads conjugated with Protein A/G Agarose (Sigma) were added for another 1 h. The immunoprecipitated proteins were washed three times with the HNTG buffer and separated by SDS–PAGE (polyacrylamide gel electrophoresis).

The expression of different proteins was tested by WB in 50 μg of protein lysates or in 500 μg of immunoprecipitated cell proteins using an anti-p21 WAF, anti-phospho-p21 waf (Thr 145), anti-PCNA, anti-p53, anti-mdm2, anti β-actin, anti-p85, anti-Lamin B, anti-GAP-DH, anti-β-tubulin and anti-dynein pAbs from Santa Cruz Biotechnology (Heidelberg, Germany), anti-phospho-Akt (Ser 473), anti phospho p-Bcl-2 (Ser 70), anti-pBcl-2 and anti-caspase-9 pAbs from Cell Signaling Technology (Beverly, MA, USA).

Proteins were transferred to a nitrocellulose membrane, probed with primary antibody and then stripped and reprobed with the appropriate antibodies. The antigen–antibody complex was detected by incubation of the membranes for 1 h at room temperature with a peroxidase-coupled anti-IgG antibody and revealed using the ECL system. Blots were then exposed to film and bands of interest were quantified by densitometer (Mod 620 BioRad). The results obtained were expressed in term of arbitrary densitometric units.

2.6. Immunofluorescent microscopy

50% confluent cultures, grown on coverslips, were shifted to SFM for 24 h and then treated either for 18 or 48 h with 2, 6 or 50 nM of Taxol. Cells were then fixed in 4% paraformaldehyde, permeabilized with 0.2% Triton X-100, washed three times with PBS, and incubated for 1 h with a mixture of primary Abs recognizing p53 and p21. The anti-p53 monoclonal Ab (mAb) (Santa Cruz) at 2 mg/ml was used for p53 staining; anti p21 polyclonal Ab (pAb) (Santa Cruz) at 2 mg/ml was used to detect p21. Following the incubation with primary Abs, the slides were washed three times with PBS, and incubated with a mixture of two secondary Abs, each 1 mg/ml concentrated. A rhodamine-conjugated donkey anti-mouse IgG (Calbiochem) was used as a secondary Ab for p53 and a fluorescein-conjugated donkey anti-rabbit IgG (Calbiochem) was used for p21. The cellular localization of p53 and p21 was studied with confocal microscope with 1000× magnification. The optical sections were taken at the central plane.

2.7. FACS analysis

Serum-starved cells for 24 h were given Taxol for 18 and 48 h at the doses reported in the figures. After this incubation cells were trypsinized, washed with PBS and fixed for 1 h in ice-cold 70% ethanol. The samples were then washed once with PBS and resuspended in 1 ml of staining solution (10 mg/ml RNasi A, 10 mg/ml propidium iodide in PBS). The samples were then incubated at room temperature in the dark for at least 30 min. FACS analysis was performed using CellFeet software (Becton Dickinson, NJ). At least 2×10^4 cells/sample were measured.

2.8. PI-3 kinase activity

PI-3K activity associated with p85, was assessed by standard protocol provided by the manufacturer of the p85 antibody (Upstate Biotechnology). Briefly, p85 was IP from 500 μg of protein lysate with an anti-p85 p-Ab, the negative control was performed using a cell lysate where p110 catalyzing subunit of PI3K, was previously removed by pre-

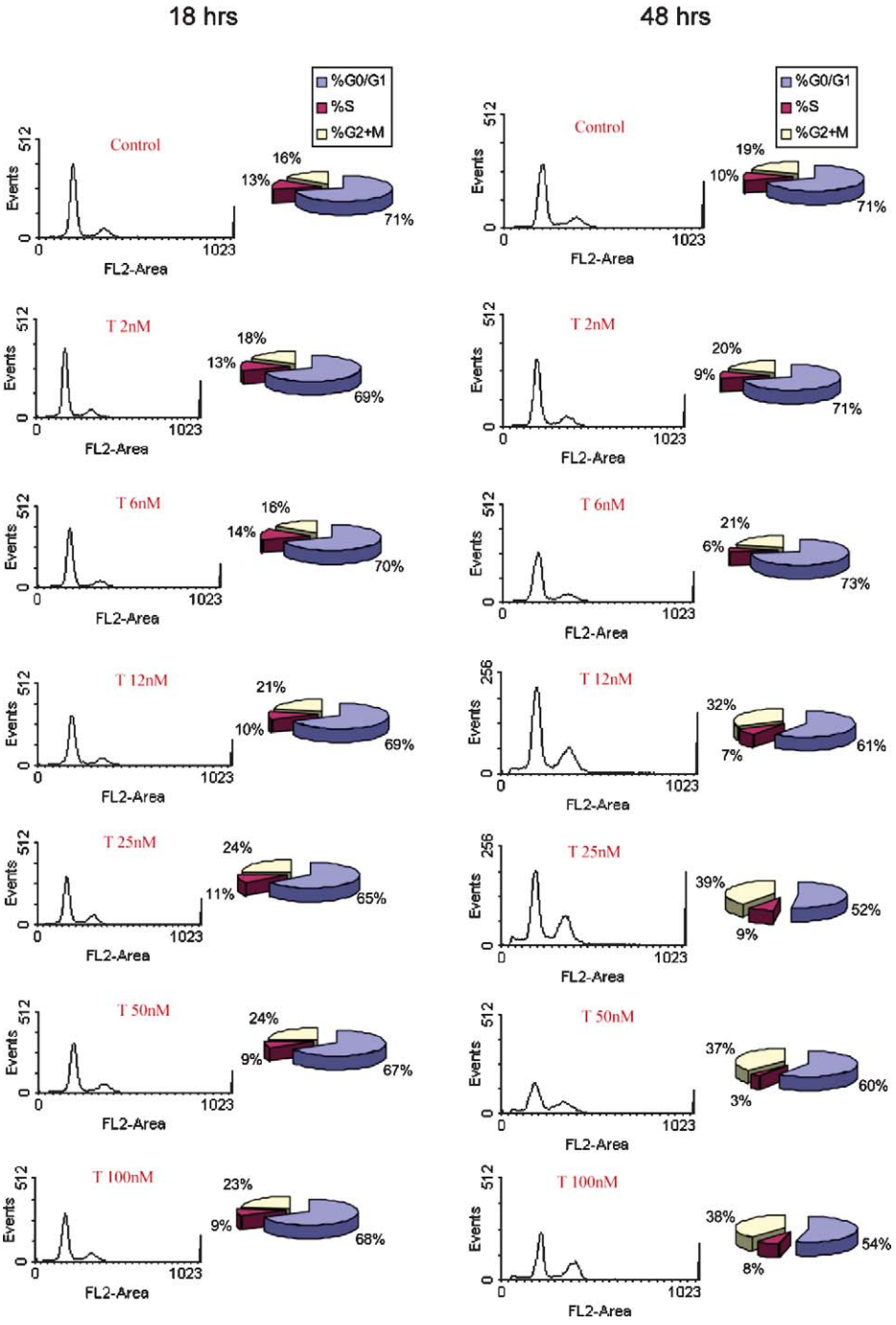

Fig. 2. Effect of different doses of Taxol on cell cycle progression of MCF-7 breast cancer cells. Serum-starved MCF-7 cells for 24 h were incubated for 18 and 48 h with the different concentrations of Taxol as shown in figure. Then the cells were collected and stained with propidium iodide (see Section 2) to be analyzed by FACS. DNA histograms were measured using Cell Fit software and the percentage of G0/G1, S and G2/M cells were calculated. Data are representative of four independent experiments.

incubation with the respective antibody (1 h at room temperature) and subsequently immunoprecipitated with Protein A/G-agarose. As a positive control, MCF-7 were treated with 100 nM insulin for 24 h before lysis and immunoprecipitated with anti-p85 from 500 μg of cell lysates. The immunoprecipitates were washed once with cold PBS, twice with 0.5 M LiCl, 0.1 M Tris (pH 7.4) and finally with 10 mM Tris, 100 mM NaCl, 1 mM EDTA. The presence of PI3K activity in immunoprecipitates was determined by incubating the beads with reaction buffer containing 10 mM HEPES (pH 7.4), 10 mM $MgCl_2$, 50 μM ATP, 20 μCi [γ^{32}-P] ATP, and 10 μg of L-α-phosphatidylinositol-4,5-bis phosphate (PI-4,5-P_2) for 20 min at 37 °C. The reactions were stopped by adding 100 μl of 1 M HCl. Phospholipids were extracted with 200 μl of $CHCl_3$/methanol. For extraction of lipids, 200 μl of chloroform:methanol (1:1, v/v) were added to the samples and vortexed for 20 s. Phase separation was facilitated by centrifugation at 5000 rpm for 2 min in a tabletop centrifuge. The upper phase was removed, and the lower chloroform phase was washed once more with clear upper phase. The washed chloroform phase was dried under a stream of nitrogen gas and redissolved in 30 μl of chloroform. The labelled products of the kinase reaction, the PI phosphates, then were spotted onto *trans*-1,2-diaminocyclohexane–*N*,*N*,*N*′,*N*′-tetraacetic acid-treated silica gel 60 TLC plates. Radioactive spots were visualized by autoradiography.

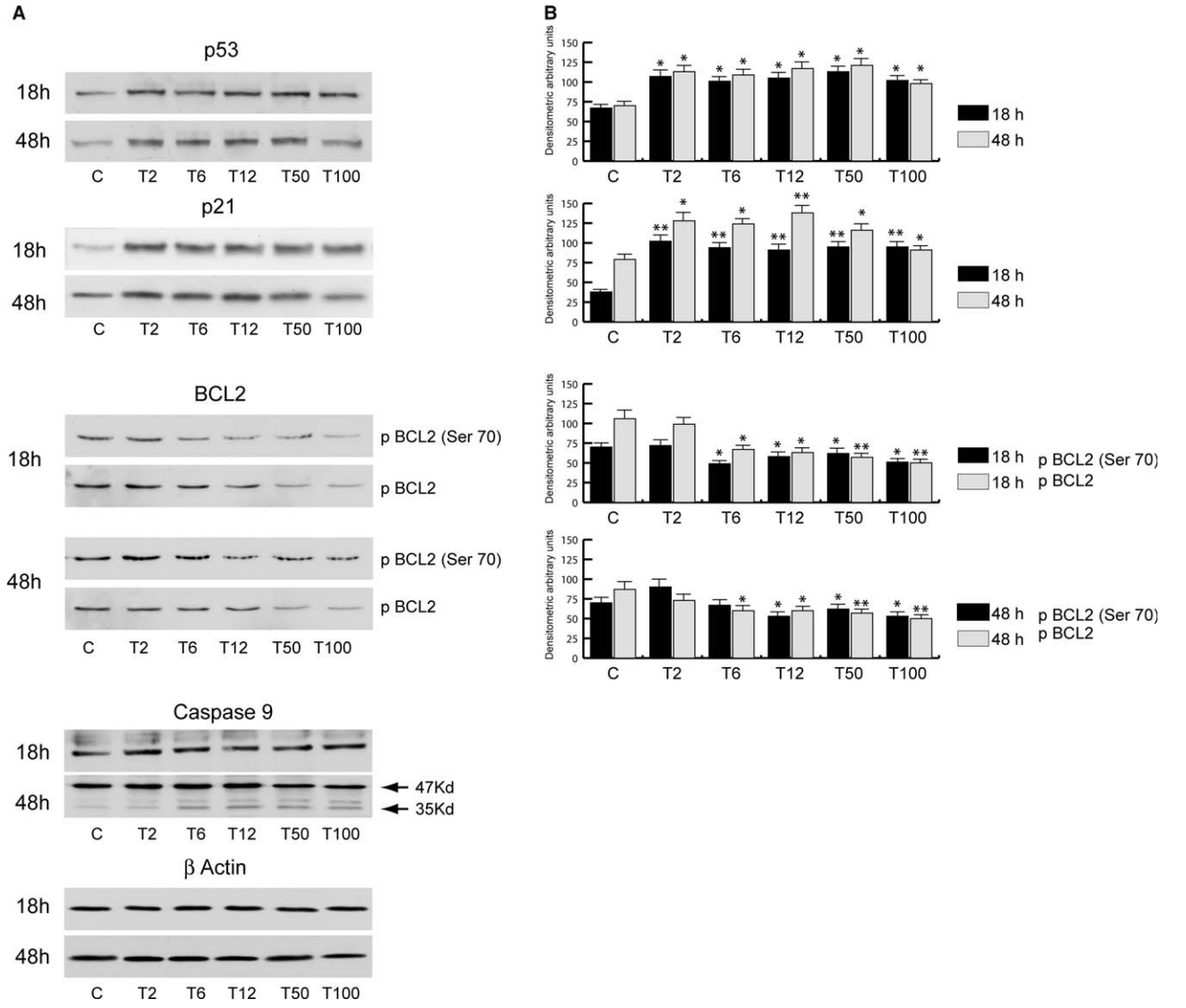

Fig. 3. Low doses of Taxol affect p53 expression and its target proteins p21 WAF and Bcl-2. (A) MCF-7 cells underwent Taxol treatment (from 2 to 100 nM) for 18 and 48 h were harvested and lysed to detect p53 protein expression in 50 μg of total cell lysates. The same filter was stripped and reprobed with anti-p21 waf, anti-Bcl-2, anti caspase-9 and anti-β-actin antibodies. C: control; T: Taxol at different nM concentrations. β-Actin serves as a loading control. Representative results are shown. (B) The histograms represent the mean ± S.D. of three separate experiments in which bands intensity for p53, p21 and Bcl-2 were evaluated in term of arbitrary densitometric units. $^{*}P < 0.05$; $^{**}P < 0.01$ vs C.

2.9. DNA ladder formation

The ladder assay is based on the oligonucleosomal DNA fragmentation of nuclear DNA that can be visualized by ethidium bromide staining following electrophoresis. MCF-7 cells were plated in 100-mm dishes (1×10^6 cells/dish); serum-starved cells were treated with Taxol (2, 6, 50 and 100 nM) for 48 h.

At the end of the incubation period cells were trypsinized and combined with floating cells in the same culture. DNA was isolated by lysing the cells in 400 μl of 0.2% Triton-X, 20 mM EDTA, and 10 mM Tris, pH 8.0, for 20 min on ice. The DNA fragments were harvested by centrifugation for 20 min at 12000 rpm. After the addition of 400 μl of phenol–chloroform the supernatant was centrifuged at 12000 rpm for 5 min and then was precipitated with sodium acetate (400 μl) and ethanol (800 μl) for 24 h at −20 °C.

Afterwards the supernatant was centrifuged at 12000 rpm for 20 min, dried and incubated for 1 h at room temperature with a buffer containing 500 μg/ml RNase A. The DNA fragments were resolved by electrophoresis at 75 V on 1% agarose gel impregnated with ethidium bromide, detected by UV transillumination, and photographed.

2.10. Statistical analysis

Each data point represents the mean ± S.D. of at least three experiments. The data were analyzed by analysis of variance using the STATPAC computer program.

3. Results

3.1. Taxol decreases basal growth rate of MCF-7 cells in a dose/time-related manner

High doses of Taxol (100 nM) since 18 h of treatment inhibited MCF-7 cells proliferation. The same inhibitor effects were produced by lower doses of Taxol starting from 12 nM after 48 h of incubation (Fig. 1). These results well correlates with FACS analysis demonstrating a block of MCF-7 cell cycle into the G2/M phase after 48 h of drug treatment at the doses ranging from 12 to 100 nM (Fig. 2).

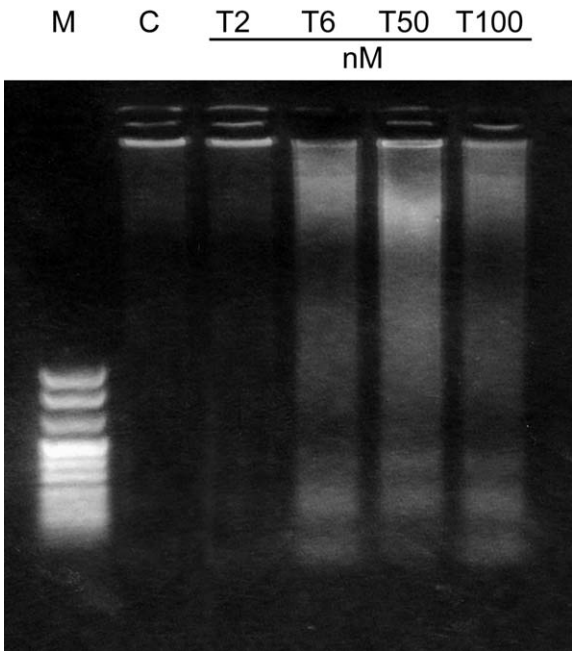

Fig. 4. Treatment of MCF-7 cells with Taxol induces DNA fragmentation. DNA gel electrophoresis of Taxol-treated (T) (lanes 2–5) and control (C) (lane 1) MCF-7 cells. DNA from MCF7 cell treated for 48 h with 2, 6, 50 and 100 nM of Taxol was extracted as detailed in Section 2, then separated in 1.5% agarose gel electrophoresis. DNA from a 48 h control (untreated) culture was prepared in the same way. M, Marker.

3.2. Cell survival pathway is affected by taxol

To investigate if Taxol "per se" might produce early changes in cell apoptotic and/or survival signals, first of all we focused our attention on the effects of the drug on p53 and p21 waf expression.

It is worth to mention that low doses of Taxol incubated for 18 and 48 h are able to enhance both p53 and p21 waf protein expressions, while the anti-apoptotic Bcl-2, in its total content and consequently in its phosphorylative status (phospho-Bcl Ser70) resulted downregulated (Fig. 3 A and B). However, it is note worthy to observe how the relative phospho-Bcl-2 levels tend to be enhanced by Taxol treatment since the decrease of Bcl-2 protein content occurs much faster than its phosphorylation. Indeed, the ratio of densitometric values of the bands between phospho-Bcl-2 /Bcl-2 protein varied from 0.6 in control sample, to 1.2 in treated sample. Drug treatment triggers cell apoptotic events only after 48 h, eliciting the cleavage of caspase-9, which is detectable from Taxol 6 nM and persists at the higher doses (Fig. 3A). This was also confirmed by agarose DNA electrophoresis that demonstrates the formation of the characteristic ladder of DNA at 6, 50 and 100 nM of Taxol (48 h), while it is absent at lower concentration of the drug as well as in the control sample (Fig. 4).

On the basis of the reported findings, even in the presence of low doses of Taxol, p53 may potentiate its transactivatory properties on the regulatory region of target gene through its faster translocation into the nucleus. To prove this we studied p53 nuclear/cytosolic compartmentalization in MCF-7 cells in the presence of low and high doses of the drug incubated for both 18 and 48 h.

3.3. Taxol induced P53 and P21 intracellular relocation

WB analysis performed, respectively, in the nuclear and cytosolic cell lysates showed that p53 and its gene product, the mdm2 protein, after 18 h of drug treatment, exhibit a prevalent nuclear compartmentalization, while p21 waf protein

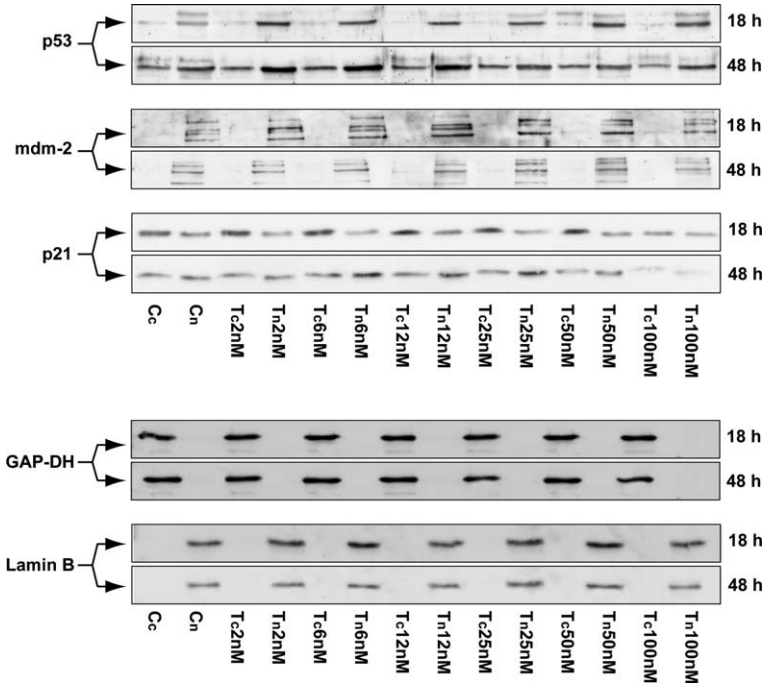

Fig. 5. Different subcellular compartmentalization of p53, mdm2 and p21 waf in cells treated with Taxol. MCF-7 cells treated with Taxol, at the concentrations reported in the figure, were harvested and cytosolic (c) and nuclear (n) protein lysates were subject to WB with an anti-p53, anti-mdm2, anti-p21 antibodies. C, control; T, Taxol-treated cells. The expressions of a nuclear protein, Lamin B, and a cytoplasmatic enzyme, GAP-DH, were assessed by stripping and reprobing the filters to verify the purity of fractions.

appears mostly localized in the cytosol (Fig. 5). Drug treatment of MCF-7 cells for 48 h increases p53 levels in both nuclear and cytosolic compartments until 25 nM of cell exposure to Taxol. At the same time, p21 waf protein tends to diffuse from the cytosol into the nucleus (Fig. 5). P53 uses dynein to translocate into the nucleus since it co-immunoprecipitates with the microtubule-motor protein and with β-tubulin (Fig. 6). In the end, we observed that the amount of protein bound to dynein in the nuclear compartment is increased upon Taxol treatment at 48 h.

The subcellular localization of both p53 and p21 proteins was also investigated by confocal microscopy using immunofluorescent staining of p53 (rhodamine-conjugated antibody, red staining) and p21 (fluorescein-conjugated antibody, green staining) proteins.

At 18 h of drug treatment, p53 tended to accumulate much more into the nucleus (a very strong nuclear staining was ob-

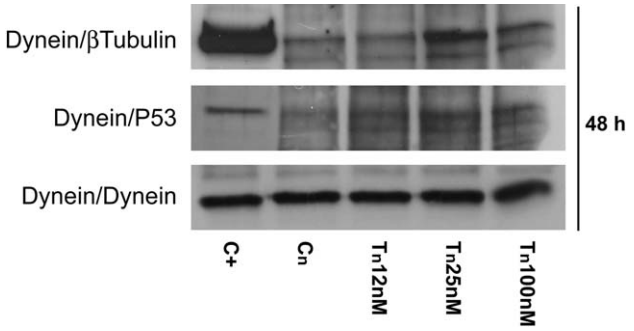

Fig. 6. P53 co-immunoprecipitates with dynein. MCF-7 cells treated with Taxol (12, 25, 100 nM) for 48 h were harvested and nuclear (n) protein lysates were subject to IP experiment by using an anti-dynein antibody/protein A/G complex followed by WB with anti-β-tubulin antibody; anti-p53 antibody; anti-dynein antibody. C+, 50 μg of soluble cell protein; Cn, nuclear control.

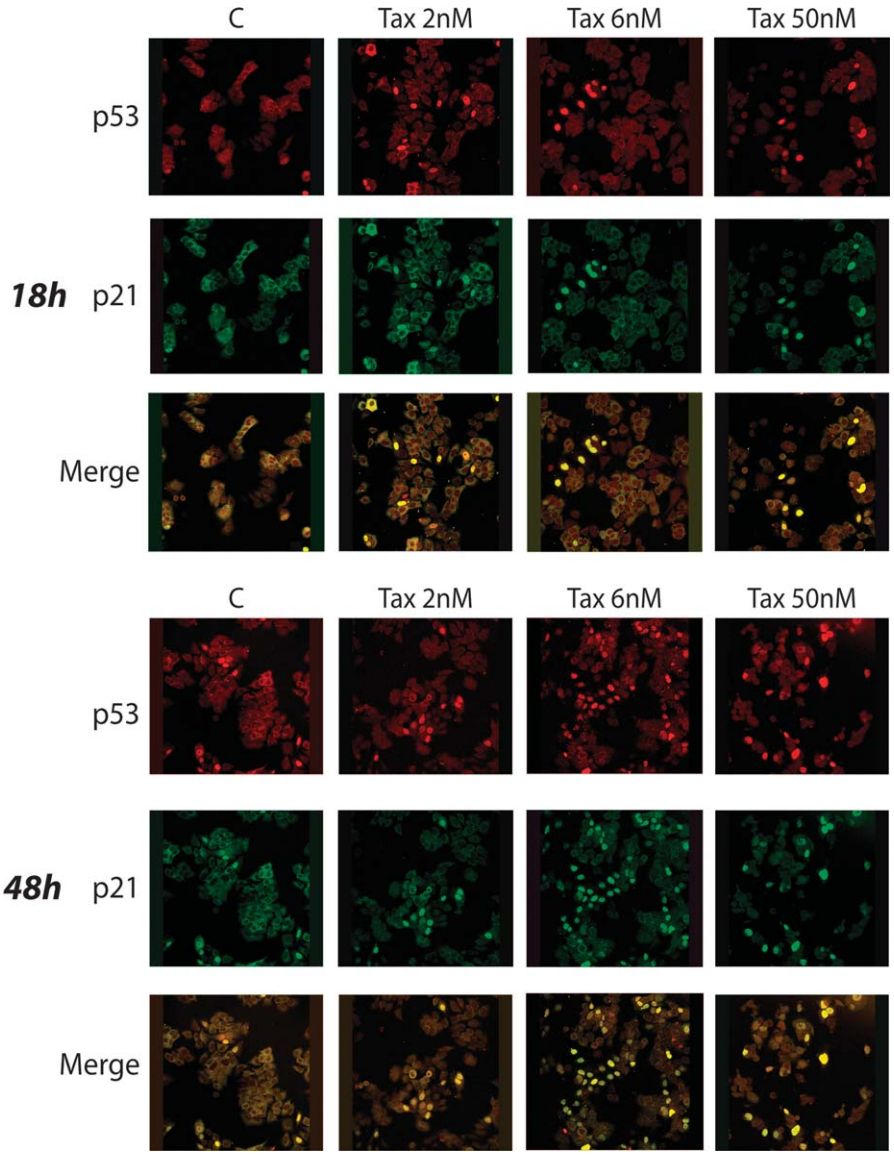

Fig. 7. Immunolocalization of p53 and p21 WAF in MCF-7 cells treated with Taxol. MCF-7 cells were treated with Taxol, at the indicated doses, for 18 and 48 h and subsequently fixed and stained with a rhodamine-conjugated donkey anti-mouse IgG as secondary Ab for p53 (red), or with a fluorescein-conjugated donkey anti-rabbit IgG for p21 (green). Staining was analysed by confocal laser-scanning microscopy. Co-localization of p53 and p21 waf is visible as yellow staining generated where the color images merge. Images are optical sections at intervals of 0.3 μm along the *z*-axis from the bottom of the cell to the top of the nucleus.

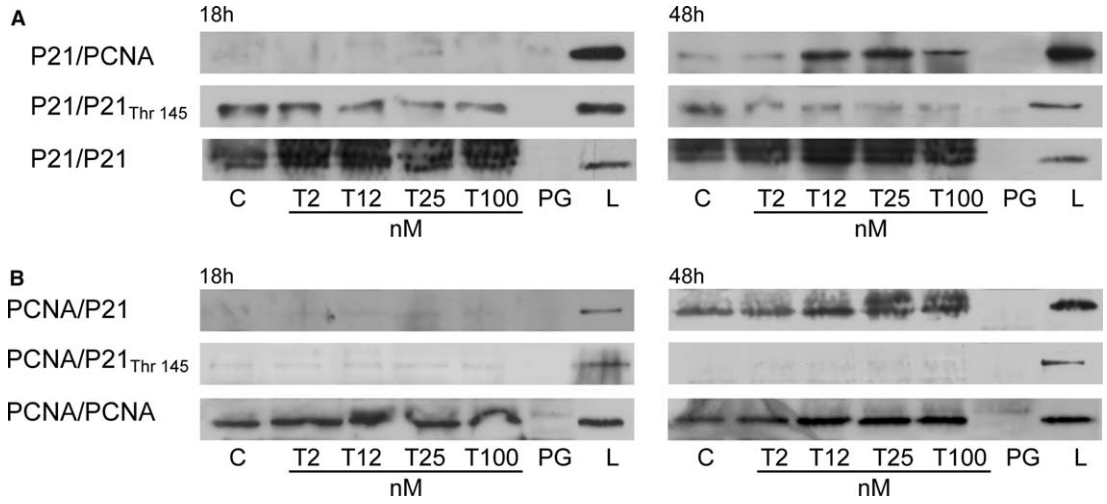

Fig. 8. Expression of p21-PCNA complex in MCF-7 cells treated with different doses of Taxol. MCF-7 cells treated with Taxol at the indicated concentrations (nM) for both 18 and 48 h were lysed and immunoprecipitated in (A) with: an anti-p21 waf antibody/protein A/G complex followed by WB with specific anti-PCNA antibody (upper panel), with anti-p21 (Thr 145) antibody (middle panel) and with anti-p21 antibody (lower panel); in B with: an anti PCNA antibody/protein A/G complex followed by WB with specific anti-p21 antibody (upper panel), with anti-p21 (Thr 145) antibody (middle panel) and with anti-PCNA antibody (lower panel). C, control; L, 50 μg of soluble cell protein not subjected to IP; PG, 0.5 mg of soluble cell protein immunoprecipitated only with protein A/G-agarose beads; T, Taxol treated cells. Results are representative of three independent experiments.

served in about 10% of cells treated with 2 and 6 nM Taxol, and in 30% of cells treated with 50 nM Taxol) respect to control sample, where, instead, a quite uniform localization in both nuclear and cytoplasmatic compartments is showed (Fig. 7). At the same time, in untreated cells, p21 resulted to be prevalently retained in the cytosol and following Taxol treatment it tends to translocate in the nucleus.

For instance, at 48 h of incubation, while 5% of control cells showed a strong nuclear co-localization of p53 and p21, in cells treated with 2 and 6 nM of Taxol the percentage increased to 15% and 50%, respectively. Nevertheless, it is worth to mention that the detectable cell compartmentalization of p53 and p21 waf proteins, in the presence of high concentrations of Taxol (50 nM), are in all likelihood not reliable since morphological changes turning cell polygonal shape into rounding ones occur and produces loss of adhesion (Fig. 7).

The cytosolic retention of p21 waf at 18 h, probably makes it unable to interact with nuclear proteins like PCNA and to inhibit cell cycle.

To determine if the level of co-association between p21 and PCNA in MCF-7 treated cells may correlate with the inhibition of cell cycle progression we performed, at both 18 and 48 h, two sets of IP experiments by using whole-cell lysates incubated:

(i) with anti-p21 waf antibody followed by immunoblotting with an anti-PCNA antibody (Fig. 8A); and
(ii) with anti-PCNA antibody followed by immunoblotting with an anti-p21 antibody (Fig. 8B).

As shown in Fig. 8A, PCNA protein was present in immunoprecipitates from MCF-7 cells treated for 48 h with 12, 25 and 100 nM of Taxol. The highest levels of co-IP of p21/PCNA were concomitant with the alteration of cell cycle.

The same filters obtained at 18 and 48 h of drug treatment were reprobed with an anti-phospho-p21 waf (Thr 145) antibody, that represents the phosphorylated form of the protein unable to inhibit cell cycle. In accordance, the results demonstrated that in untreated and treated MCF-7 cells the phospho-p21 waf (Thr 145) is present at 18 h and it slightly decreases under Taxol (Fig. 8A). On the other hand, Taxol treatment prolonged up to 48 h significantly reduced the level of phosphorylated p21 waf protein compared with that obtained at 18 h. To asses that p21 is immunoprecipitated in all experimental conditions we reprobed the same blots with an anti-p21 antibody.

In the reverse IP experiment (IP with anti-PCNA antibody and blot with anti-p21 antibody) (Fig. 8B) the results confirm that PCNA and p21 waf associated only following 48 h drug treatment, while phospho-p21 (Thr 145) is not present in the IPs both at 18 and 48 h. The same filters were then blotted for anti-PCNA antibody to verify PCNA protein in immunoprecipitates.

3.4. Evidence that low doses of taxol are able to potentiate transactivatory properties of P53

53 nuclear compartmentalization, induced by low doses of Taxol, leads us to assume that the treatment with the drug per se may potentiate the functional transactivating properties of this protein.

PTo support this assumption we treated MCF-7 transfected with a p21 promoter conjugated with a luciferase reporter gene. Our results show, for the first time, how low doses of Taxol are able to induce the activation of p21 promoter (Fig. 9). This activation was drastically potentiated by the ectopic overexpression of wild-type p53 and abrogated in the presence of p53 mutant construct.

3.5. Effect of low doses of taxol on PI3K/Akt signal

When we evaluated the effect of the drug on the PI3K/Akt pathway, which is crucial in maintaining cell survival signal, we observed that Taxol (25 and 100 nM) for 18 h induced an early activation of PI3K and consequently this leads to an increase of phospho-Akt levels (Fig. 10A and B). Such

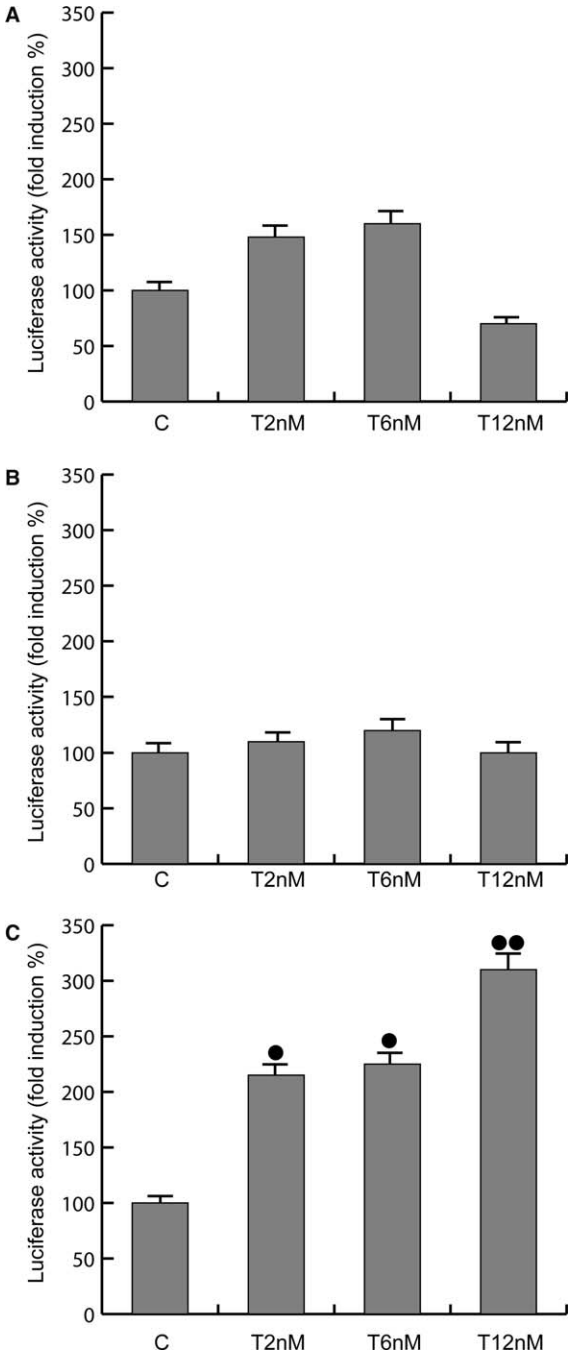

Fig. 9. Taxol induces p21 WAF promoter activity via p53. MCF-7 cells were co-transfected with the p21 waf promoter-luciferase construct and pCMV empty vector (A), pCMV-p53 mutant (B) and pCMV-p53 wild-type (C). After 8 h of transfection cells were treated with low doses of Taxol (T): 2, 6 and 12 nM for 18 h. MCF-7 cells were lysed and luciferase activities were measured using the dual luciferase reporter assay system as described under Section 2. Each column/bar represents the relative p21 waf promoter (luciferase) activity and is the mean ± S.D. of three independent experiments in triplicate. Levels of significance vs control (C): $^{\bullet}P < 0.05$; $^{\bullet\bullet}P < 0.01$.

effect is not longer noticeable at 48 h of drug exposure when G2/M cell population, analyzed in flow cytometry, appears to increase significantly together with a concomitant down regulation of the anti-apoptotic signal: Bcl-2 protein, as previously documented.

4. Discussion

Taxol has been shown to be effective as an anticancer agent in a variety of tumoral cell types [8,25–27].

As a result of cell exposure to Taxol, events characteristic to cell cycle arrest and apoptosis might take place. These effects seem to be linked to the different concentration of the drug as well as to the tissues and/or cell line used.

In the present study we demonstrate how low doses of Taxol have some apparent conflictory effects: an enhanced p53 expression involved in the regulation of programmed cell death on one hand, and the activation of PI3 kinase involved in cell survival on the other. The apparent contradictory effects have been previously reported by other authors in the same breast cancer cell type where the rapid enhancement of PI3K/Akt together with an increased of survivin expression, occurs only to counteract the increased p53 expression [28]. Indeed, it is well known how p53 might inhibit PI3K/Akt pathway by double mechanisms: first through the PTEN activation, a specific inhibitor of PI3K activity, as well as through an enhanced Akt degradation via proteosoma [29,30]. However, the functional effect of the enhanced PI3K/Akt signal, induced by low doses of Taxol, seems to be vanished by the decrease of the anti-apoptotic Bcl-2, which in such a way, fails to have any protective role in controlling mitochondrial permeability and then to inhibit the release of cytochrome *c*. Indeed, in the same circumstance, low doses of Taxol (6 nM) incubated for 48 h in MCF-7 cells are able to induce the cleavage of caspase-9 and the formation of DNA ladder. These apoptotic events precede the block of cell cycle, which occurs as from 12 nM of Taxol.

The reduced levels of Bcl-2, linked to the enhanced p53 expression under Taxol treatment, counteract the activation of PI3K/Akt pathway. P53 protein, in turn, through its binding to the negative response *cis*-elements of the Bcl-2 gene promoter may transcriptionally downregulate the expression of the anti-apoptotic protein [31].

Here, we observed that in the presence of low doses of Taxol, p53 co-immunoprecipitates with dynein, a microtubule-motor protein that requires ATP to move along microtubules with their cargoes.

Our data, together with previous results, suggest that in such circumstances p53 may use dynein to translocate into the nucleus, an event which is potentiated by Taxol treatment [10,11]. Besides, an other protein that comes down in a p53/dynein complex is the β-tubulin prevalently present in treated cells. Thus, the effect of the polymerizing agent on microtubule assemblement, consistent with their end elongation, might functionally contribute to p53 nuclear translocation where the p53-transactivatory properties would appear enhanced. The deep drop of Bcl-2 expression and the enhancement of p21 waf protein may stem from this.

Indeed, the most important finding of the present study is consistent with the evidence that Taxol, at lower concentrations, is able to transactivate p21 promoter resulting in the enhancing of p21 protein expression. This response is linked to p53 wild-type expression in MCF-7 cells, since the presence of a p53 mutant abrogates the transactivation of p21 promoter under Taxol treatment. In the same vein, the nuclear localization of p53 induced by low doses of Taxol after 18 h is followed by the enhancement of its gene product: the mdm2 protein, which shows the same sub-cellular distribution reported for p53.

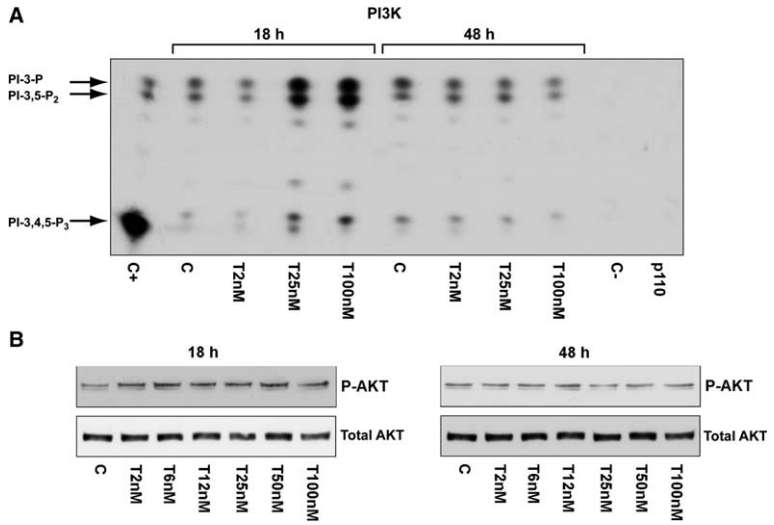

Fig. 10. Transitory Taxol activation of PI3 kinase pathway. (A) MCF-7 cells treated with Taxol (at the indicated doses) for 18 and 48 h were lysed and immunoprecipitated with an anti-p-85 antibody. The immunocomplexes were assayed for their ability to phosphorylate PI to PIP using [γ^{32}P]-ATP at 37 °C for 20 min. The PIP was resolved by TLC and autoradiographed. As a positive control (C+) MCF-7 cells were treated with 100 nM of insulin for 24 h. The negative control (p110) was performed using MCF-7 lysate, where p110, the catalyzing subunit of PI3K, was previously removed by preincubation with the respective antibody (1 h at room temperature) and subsequently immunoprecipitated with protein A/G-agarose. PI-3,4,5-P3: phosphatidylinositol 3,4,5-triphosphate; PI-3,5-P2: phosphatidylinositol 3,5-diphosphate; PI-3-P: phosphatidylinositol 3-phosphate. An additional negative control (C−) is represented by MCF-7 cells previously treated with worthmanin for 30 min. Untreated cells: (C), Taxol-treated cells: (T). The autoradiographs presented are representative of experiments that were performed at least three times with repetitive results. (B) WB of phospho-Akt (Ser 473) levels from MCF-7 cells treated with the indicated doses of Taxol (T) at 18 and 48 h of incubation. Total Akt levels are showed as a loading control. Results are representative of three independent experiments.

It is worth to observe that in this scenario MCF-7 cell cycle is not substantially modified, given that p21 waf result mostly stored in the cytosol and this could prevent its binding with nuclear factors such as PCNA [32–34]. Indeed, at the same time, the enhanced activation of phospho-Akt, as here reported, may serve to recruit p21 protein into the cytosol, where it is unable to act as an inhibitor of CDKs and thereby to inhibit cell cycle progression [16,33,34]. Results from this study showed that prolonged treatment of MCF-7 cells with Taxol up to 12 nM induced an evident co-association between p21 protein and PCNA which was concomitant with the decay of the phosphorylative status of p21 waf (Thr 145) together with the arrest of cell cycle. These findings supported the evidence that when phospho-Akt is not activated due to the prolonged treatment with Taxol, p21, mainly present in the ipo-phosphorylated form, is able to co-immunoprecipitate with PCNA. The latter event well correlates with the block of cell cycle into the G2/M phase that progressively increases with the elapsing of time of the drug exposure as well as with the dose of Taxol used.

In conclusion, in the present study we have demonstrated how low doses of Taxol, without affecting cell cycle, may induce the enhanced expression of p53 protein and its prevalent nuclear translocation with well featured apoptotic events occurring in breast cancer cells. This, furthermore, supports the potential benefit of the association of low doses of Taxol with the classic chemotherapic agents. The combined treatment may potentiate the effect of low doses of chemotherapics reducing thus the harmful systemic effects mostly occurring during the treatment of breast carcinomas.

Acknowledgements: We thank Dr. Wafik El-Deiry (Howard Hughes Medical Institute, Philadelphia) for kindly providing the plasmid WWP-Luc containing human p21 waf promoter and Dr. G. Daniel (Department of Health and Human Service, Natl. Inst. Env. Health Sci., Res. Triangle Park, NC) for his generous gift of the pCMV-wt p53 plasmid, pCMV-p53 plasmid mutant and pCMV empty vector.

We thank Prof. D. Sturino for English revision of the manuscript.

Financial support: This work was supported by A.I.R.C., 2003.

References

[1] Horwitz, S.B. (1992) Mechanism of action of taxol. Trends Pharmacol. Sci. 13, 131–136.
[2] Rao, S., Krauss, N.E., Heerding, J.M., Swindell, C.S., Ringell, L., Orr, G.A. and Horwitz, S.B. (1994) 3′-(*p*-Azidobenzamido)taxol photolabels the N-terminal 31 amino acids of beta-tubulin. J. Biol. Chem. 269, 3131–3134.
[3] Rao, S., Orr, G.A., Chaudhary, A.G., Kingston, D.G.Y. and Horwitz, S.B. (1995) Characterization of the taxol binding site on the microtubule. 2-(*m*-Azidobenzoyl) taxol photolabels a peptide (amino acids 217–231) of beta-tubulin. J. Biol. Chem. 270, 20235–20238.
[4] Jordan, M.A. and Wilson, L. (1998) Microtubules and actin filaments: dynamic targets for cancer chemotherapy. Curr. Opin. Cell. Biol. 10, 123–130.
[5] Caplow, M., Shanks, J. and Ruhlen, R. (1994) How taxol modulates microtubule disassembly. J. Biol. Chem. 38, 23399–23402.
[6] Horwitz, S.B. (1994) Taxol (paclitaxel): mechanisms of action. Ann. Oncol. 6, S3–S6.
[7] Woods, C.M., Zhu, J., McQueney, P.A., Bollag, D. and Lazarides, E. (1995) Taxol-induced mitotic block triggers rapid onset of a p53-independent apoptotic pathway. Mol. Med. 5, 506–526.
[8] Rowinsky, E.K. and Donehower, R.C. (1995) Paclitaxel (taxol). N. Engl. J. Med. 15, 004–1014.
[9] Eastman, A. and Rigas, J.R. (1999) Modulation of apoptosis signaling pathways and cell cycle regulation. Semin. Oncol. 26, 41–52.
[10] Giannakakou, P., Sackett, D.L., Ward, Y., Webster, K.R., Blagosklonny, M.W. and Fojo, T. (2000) p53 is associated with

cellular microtubules and is transported to the nucleus by dynein. Nat. Cell Biol. 2, 709–717.
[11] Giannakakou, P., Nakano, M., Nicolaou, K.C., O'Brate, A., Yu, J., Blagosklonny, M.W., Greber, U.F. and Fojo, T. (2002) Enhanced microtubule-dependent trafficking and p53 nuclear accumulation by suppression of microtubule dynamics. Proc. Natl. Acad. Sci. 16, 10855–10860.
[12] Haupt, S., Berger, M., Goldberg, Z. and Haupt, Y. (2003) Apoptosis-the p53 network. J. Cell Sci. 15, 4077–4085.
[13] Andre, N., Braguer, D., Brasseur, G., Goncalves, A., Lemesle-Meunier, D., Guise, S., Jordan, M.A. and Briand, C. (2000) Paclitaxel induces release of cytochrome *c* from mitochondria isolated from human neuroblastoma cells. Cancer Res. 19, 5349–5353.
[14] Ofir, R., Seidman, R., Rabinski, T., Krup, M., Yavelsky, V., Weinstein, Y. and Wolfson, M. (2002) Taxol-induced apoptosis in human SKOV3 ovarian and MCF7 breast carcinoma cells is caspase-3 and caspase-9 independent. Cell Death Differ. 9, 636–642.
[15] Park, S.J., Wu, C.H., Gordon, J.D., Zhong, X., Emami, A. and Safa, A.R. (2004) Taxol induces caspase-10 dependent apoptosis. J. Biol. Chem. 49, 51057–51067.
[16] Heliez, C., Baricault, L., Barboule, N. and Valette, A. (2003) Paclitaxel increases p21 synthesis and accumulation of its AKT-phosphorylated form in the cytoplasm of cancer cells. Oncogene 22, 3260–3268.
[17] Harper, J.W., Adami, G.R., Wei, N., Keyomarsi, K. and Elledge, S.J. (1993) The p21 Cdk-interacting protein Cip1 is a potent inhibitor of G1 cyclin-dependent kinases. Cell 75, 805–816.
[18] Michieli, P., Chedid, M., Lin, D., Pierce, J., Mercer, E. and Givol, D. (1994) Induction of WAF1/CIP1 by a p53 independent pathway. Cancer Res. 54, 3391–3395.
[19] Zeng, Y. and El-Deiry, W. (1996) Regulation of p21WAF1/CIP1 expression by p53-independent pathways. Oncogene 12, 1557–1564.
[20] Sherr, C. and Roberts, J. (1999) CDK inhibitors: positive and negative regulators of G1-phase progression. Genes Dev. 13, 1501–1512.
[21] Kelman, Z. and O'Donnell, M. (1995) Structural and functional similarities of prokaryotic and eukaryotic DNA polymerase sliding clamps. Nucleic Acids Res. 23, 3613–3620.
[22] Gulbis, J., Kelman, Z., Hurwitz, J., O'Donnell, M. and Kuriyan, J. (1996) Structure of the C-terminal region of p2(WAF1/CIP1) complexed with human PCNA. Cell 87, 297–306.
[23] Andò, S., Panno, M.L., Salerno, M., Sisci, D., Mauro, L., Lanzino, M. and Surmacz, E. (1998) Role of IRS-1 signaling in insulin-induced modulation of estrogen receptors in breast cancer cells. Biochem. Biophys. Res. Commun. 253, 315–319.
[24] Morelli, C., Garofalo, C., Bartucci, M. and Surmacz, E. (2003) Estrogen receptor alpha regulates the degradation of insulin receptor substrates 1 and 2 in breast cancer cells. Oncogene 22, 4007–4016.
[25] McGuire, W.P., Rowinsky, E.K., Rosenshein, E.K., Grumbine, F.C., Ettinger, D.S., Armstrong, D.K. and Donehower, R.C. (1989) Taxol: a unique antineoplastic agent with significant activity in advanced ovarian epithelial neoplasms. Ann. Intern. Med. 111, 273–279.
[26] Liebmann, J.E., Cook, J.A., Lipschultz, C., Teague, D., Fisher, J. and Mitchell, J.B. (1993) Cytotoxic studies of paclitaxel (Taxol) in human tumour cell lines. Br. J. Cancer 68, 1104–1109.
[27] Eisenhauer, E.A. and Vermorker, J.B. (1998) The taxoids. Comparative clinical pharmacology and therapeutic potential. Drugs 55, 5–30.
[28] Ling, X., Bernacki, R.J., Brattain, M.G. and Li, F. (2004) Induction of survivin expression by taxol (paclitaxel) is an early event, which is independent of taxol-mediated G2/M arrest. J. Biol. Chem. 279, 15196–15203.
[29] Mayo, L.D., Dixon, J.E., Durden, D.L., Tonks, N.K. and Donner, D.B. (2002) PTEN protects p53 from Mdm2 and sensitizes cancer cells to chemotherapy. J. Biol. Chem. 277, 5484–5489.
[30] Gottlieb, T.M., Leal, J.F., Seger, R., Taya, Y. and Oren, M. (2002) Cross-talk between Akt, p53 and Mdm2: possible implications for the regulation of apoptosis. Oncogene 218, 1299–1303.
[31] Miyashita, R., Krajewski, S., Krajewska, M., Wang, H.G., Lin, H.K., Liebermann, D.A., Hoffman, B. and Reed, J.C. (1994) Tumor suppressor p53 is a regulator of bcl-2 and bax gene expression in vitro and in vivo. Oncogene 9, 1799–1805.
[32] Nicholson, K.M. and Anderson, N.G. (2002) The protein kinase B/AKT signalling pathway in human malignancy. Cell. Signal. 14, 381–395.
[33] Li, Y., Dowbenco, D. and Lasky, L.A. (2001) AKT/PKB phosphorylation of p21 Cip/WAF1 enhances protein stability of p21 Cip/WAF1 and promotes cell survival. J. Biol. Chem. 277, 11352–11361.
[34] Rossig, L., Jadidi, A.S., Urbich, C., Badorff, C., Zeihr, A.M. and Dimmeler, S. (2001) AKT-dependent phosphorylation of $p21^{Cip1}$ regulates PCNA binding and proliferation of endothelial cells. Mol. Cell. Biol. 21, 5644–5657.

JOURNAL OF CELLULAR PHYSIOLOGY 209:977–986 (2006)

Peroxisome Proliferator-Activated Receptor (PPAR)γ Is Expressed By Human Spermatozoa: Its Potential Role on the Sperm Physiology

SAVERIA AQUILA,[1,4] DANIELA BONOFIGLIO,[1] MARIAELENA GENTILE,[2,4] EMILIA MIDDEA,[1,4] SABRINA GABRIELE,[1] MARIA BELMONTE,[1] STEFANIA CATALANO,[1,4] MICHELE PELLEGRINO,[2] AND SEBASTIANO ANDÒ[3,4]*

[1]*Department of Pharmaco-Biology, University of Calabria, Arcavacata di Rende (Cosenza), Italy*
[2]*Department of Cellular Biology, University of Calabria, Arcavacata di Rende (Cosenza), Italy*
[3]*Faculty of Pharmacy, University of Calabria, Arcavacata di Rende (Cosenza), Italy*
[4]*Centro Sanitario, University of Calabria, Arcavacata di Rende (Cosenza), Italy*

The peroxisome proliferation-activated receptor gamma (PPARγ) is mainly expressed in the adipose tissue and integrates the control of energy, lipid, and glucose homeostasis. The present study, by means of RT-PCR, Western blot, and immunofluorescence techniques, demonstrates that human sperm express the PPARγ. The functionality of the receptor was evidenced by 15-deoxy-12,14-prostaglandin J_2 (PGJ2) and rosiglitazone (BRL) PPARγ-agonists that were tested on capacitation, acrosome reaction, and motility. Both treatments also increase AKT phosphorylations and influence glucose and lipid metabolism in sperm. The specificity of PGJ2 and BRL effects through PPARγ on human sperm was confirmed by an irreversible PPARγ antagonist, GW9662. Our findings provide evidence that human sperm express a functional PPARγ whose activation influences sperm physiology. In conclusion, the presence of PPARγ in male gamete broadens the field of action of this nuclear receptor, bringing us to look towards sperm as an endocrine mobile unit independent of the systemic regulation. J. Cell. Physiol. 209: 977–986, 2006. © 2006 Wiley-Liss, Inc.

The peroxisome proliferator-activated receptor gamma (PPARγ) is member of the nuclear receptor superfamily that integrates the control of energy, lipid, and glucose homeostasis (Rangwala and Lazar, 2004; Kota et al., 2005). Like all nuclear receptors, PPARγ has a modular structure that comprises: the N-terminal A/B domain, harboring a ligand-independent transcriptional activation function (AF-1), the DNA-binding domain, which contains two zinc fingers, and the C-terminal region, containing the ligand-binding domain and the ligand-dependent activation domain AF-2. The principal site of expression of PPARγ is the adipose tissue (Gurnell, 2005), but this receptor is also present, albeit at lower levels, in many other tissues and cell types such as epithelial cells (Pan et al., 2005), B- and T-cells (Kostadinova et al., 2005), macrophages (Genolet et al., 2004), endothelial cells (Nicol et al., 2005), neutrophils (Standiford et al., 2005 and references therein), and smooth muscle cells (Wang et al., 2006).

The activity of PPARγ is governed by the binding to small lipophilic ligands. Endogenous ligands include a versatile array of compounds such as polyunsaturated fatty acids and eicosanoids derived from nutrition or metabolic pathways and comprising the prostaglandin D2 metabolite 15-deoxy-12,14-prostaglandin J_2 (PGJ2) (Kobayashi et al., 2005). PPARγ is also activated by synthetic compounds termed thiazolidinediones (TZDs), class of insulin-sensitizing agents that are used to treat type II diabetes (Petersen et al., 2000). Uncertainty surrounds, despite intensive investigation and years of clinical use of TZDs, the mechanisms by which activation of PPARγ promotes insulin sensitivity. In addition to their anti-hyperglycemic effects, these compounds also dramatically reduce circulating levels of triglycerides and non-esterified free fatty acids. To date, much still remains unclear and unknown about the specific target tissues of TZDs. Adipose tissue is one likely target, and other candidate sites for TZD action include skeletal muscle, liver and pancreatic beta cells, and tissue-specific conditional knockouts of PPARγ are now being used to address all these questions (Kintscher and Law, 2005 and references therein). However, the function of PPARγ is not restricted to adipogenesis and insulin sensitization. In peripheral monocytes and macrophages, PPARγ-agonists are reported to inhibit the production of inflammatory cytokines (Skolnik et al., 2002). PPARγ ligands can also induce differentiation and apoptosis in breast (Yee et al., 2003), prostate cancer (Xu et al., 2003), and non-small cell lung cancer (Chang and Szabo, 2000).

The mechanisms controlling the interaction between energy balance and reproduction are the subject of intensive investigations and compelling evidence demonstrates a close link between energy status and reproductive function (Quandt, 1984; Moschos et al., 2002). The integrated control of those systems is

Saveria Aquila and Daniela Bonofiglio equally contributed to this work.

Contract grant sponsor: PRIN 2004 Prot. N. 0067227, AIRC–2004, MURST and Ex 60% -2005.

*Correspondence to: Sebastiano Andò, Faculty of Pharmacy, University of Calabria, Arcavacata di Rende (Cosenza) 87036, Italy. E-mail: sebastiano.ando@unical.it

Received 9 May 2006; Accepted 30 June 2006

DOI: 10.1002/jcp.20807

probably a multi-faceted phenomenon conducted by an array of signals governing energy homeostasis, metabolism, and fertility. Interestingly, it was documented that augmented insulin sensitivity may improve ovulatory function and fertility in women with polycystic ovary syndrome (Seli and Duleba, 2002). In mice, the loss of the PPARγ gene in oocytes and granulosa cells resulted in impaired fertility (Cui et al., 2002).

The energy homeostasis depends on very well tuned machinery balancing energy storage and expenditure. The transcriptional regulation, affecting the levels of expression of key proteins is the most effective mechanism on a longer time scale, however it is now quite clear that some transcriptional factors as nuclear receptors, in addition to their classic genomic action, also regulate cellular processes through their non-genomic mechanism (Cato et al., 2002). Different nuclear receptors such as progesterone receptor (Shah et al., 2005), estrogen receptor α, and estrogen receptor β (Aquila et al., 2004) were found to be present in human-ejaculated spermatozoa, regulating cellular processes through their non-genomic mechanisms. All these findings strengthen the importance of the nuclear receptors non-genomic signaling, which may represent their exclusive modality of action in spermatozoa as they are apparently transcriptional inactive cells. Sperm functionalities need to be rapidly activated to accommodate dynamic changes in the surrounding milieu. These mechanisms would enable the sperm to use tools which are already present and which get functionally activated or repressed.

The significance of PPARγ in male fertility is not yet been investigated and no published reports are available on the impact of PPARγ agonists on male fertility. In the current study, we showed the expression of PPARγ in human sperm providing a unique approach to study lipid and glucose metabolism at molecular level in the male gamete.

MATERIALS AND METHODS

Chemicals

PMN Cell Isolation Medium was from BIOSPA (Milan, Italy). Total RNA Isolation System kit, enzymes, buffers, nucleotides 100-bp ladder used for RT-PCR were purchased from Promega (Milan, Italy). Moloney Murine Leukemia Virus (M-MLV) was from Gibco BRL—Life Technologies Italia (Milan, Italy). Oligonucleotide primers were made by Invitrogen (Milan, Italy). BSA protein standard, Laemmli sample buffer, pre-stained molecular weight markers, Percoll (colloidal PVP coated silica for cell separation), Sodium bicarbonate, Sodium lactate, Sodium pyruvate, Dimethyl Sulfoxide (DMSO), Earle's balanced salt solution, 15-deoxy-12,14-prostaglandin J_2 (PGJ2), the irreversible PPARγ antagonist GW9662 (GW), and all other chemicals were purchased from Sigma Chemical (Milan, Italy). Acrylamide bisacrylamide was from Labtek Eurobio (Milan, Italy). Triton X-100, Eosin Y was from Farmitalia Carlo Erba (Milan, Italy). Gel band purification kit, ECL Plus Western blotting detection system, Hybond^{TM} ECL^{TM}, [-^{32}P]ATP, HEPES Sodium Salt were purchased from Amersham Pharmacia Biotech (Buckinghamshire, UK). Triglycerides assay kit and Cholesterol-oxidase (CHOD)–peroxidase (POD) enzymatic colorimetric kit were from Inter-Medical (Biogemina Sas, Catania, Italy). Goat polyclonal actin antibody (I–19), polyclonal rabbit anti-PPARγ antibody, polyclonal rabbit anti-phosphotyrosine antibody (PY99), rabbit anti-p-Akt1/Akt2/Akt3 S473 antibody, total anti-Akt1/Akt2 antibody, peroxidase-coupled anti-rabbit and anti-goat, anti-rabbit IgG FITC-conjugated, Protein A/G-agarose plus were from Santa Cruz Biotechnology (Heidelberg, Germany). BRL49653 (BRL) was a kind gift from GlaxoSmithKline (West Sussex, UK).

Semen samples and spermatozoa preparations

Human semen was collected, according to the WHO-recommended procedure by masturbation from men undergoing semen analysis for couple infertility in our laboratory. Sperm samples with normal parameters of semen volume, sperm count, motility, vitality, and morphology, according to the WHO Laboratory Manual (World Health Organization, 1999), were included in this study. In each experiment, three normal samples were pooled. Washed pooled sperm were subjected to the treatments and incubated for the indicated times. Then, samples were centrifuged and the upper phase was used to determinate the cholesterol levels, while the pellet containing sperm was used for RT-PCR or lysed to perform Western blots, triglycerides assay, acyl-CoA dehydrogenase assay, G6PDH activity. At the beginning, prior the centrifugation, several aliquots were used to perform sperm motility, viability, and acrosin activity. Spermatozoa preparations were performed as previously described (Aquila et al., 2002). The study was approved by the local medical–ethical committees and all participants gave their informed consent.

Processing of ejaculated sperm

After liquefaction, normal semen samples were pooled and subjected to centrifugation (800*g*) on a discontinuous Percoll density gradient (80:40% v:v) (World Health Organization, 1999). The 80% Percoll fraction was examined using an optical microscope equipped with a 100× oil objective to ensure that a pure sample of sperm was obtained. An independent observer, who observed several fields for each slide, inspected the cells. Percoll-purified sperm were washed with unsupplemented Earle's medium and were incubated in the same medium (uncapacitating medium) for 30 min at 37°C and 5% CO_2, without (control) or with treatments (experimental). Some samples were incubated in capacitating medium (Earle's balanced salt solution medium supplemented with 600 mg BSA/100 ml and 200 mg sodium bicarbonate/100 ml). When the cells were treated with an inhibitor, a pre-treatment of 15 min was performed and subsequently the sperm were incubated with the substances reported in the manuscript for 30 min.

Evaluation of sperm motility and viability

Sperm motility was assessed by means of light microscopy examining an aliquot of each sperm sample in absence (NC) or in the presence of increasing BRL or PGJ2 (1 to 20 μM) and/or 10 μM GW alone or combined with 10 μM BRL or 10 μM PGJ2. Sperm motility was expressed as percentage of total motile sperm. Viability was assessed by red-eosin exclusion test using Eosin Y to evaluate potential toxic effects of the treatments. A blinded observer scored 200 cells for stain uptake (dead cells) or exclusion (live cells). Viability was evaluated before and after pooling the samples and there were no adverse effects among the different treatments on human sperm viability.

RNA isolation, reverse transcriptase-polymerase chain reaction (RT-PCR)

Total RNA was isolated from human-ejaculated spermatozoa purified as previously described (Aquila et al., 2002). Before RT-PCR, RNA was incubated with ribonuclease-free deoxyribonuclease (Dnase) I in single-strength reaction buffer at 37°C for 15 min. This was followed by heat inactivation of Dnase I at 65°C for 10 min. Two micrograms of Dnase-treated RNA samples were reverse transcribed by 200 IU M-MLV reverse transcriptase in a reaction volume of 20 μl (0.4 μg oligo-dT, 0.5 mM deoxy-NTP and 24 IU Rnasin) for 30 min at 37°C, followed by heat denaturation for 5 min at 95°C. PCR amplification of complementary DNA (cDNA) was performed with 2 U of Taq DNA polymerase, 50 pmol primer pair in 10 mM Tris-HCL (pH 9.0) containing 0.1% Triton X-100, 50 mM KCl, 1.5 mM $MgCl_2$, and 0.25 mM each dNTP. PCR amplification of cDNA was performed with 2 U of Taq DNA polymerase, 50 pmol primer pair for PPARγ. Contamination by leucocytes and germ cells in our sperm cells preparations was assessed by amplifying CD45 and c-kit transcripts respectively. The applied PCR primers and the expected lengths of the resulting PCR products are shown in Table 1. The cycle profiles used are

TABLE 1. Oligonucleotide sequences used for RT-PCR

Gene	Sequenze (5′–3′)	Size of PCR product (bp)
PPARγ	5′–GAGTTCATGCTTGTCAAGGATGC–3′ 5′–CGATATCACTGGAGATCTCGCC–3′	233
c-kit	5′–AGTACATGGACATGAAACCTGG–3′ 5′–GATTCTGCTCAGACATCGTCG–3′	780
CD45	5′–CAATAGCTACTACTCCATCTAAGCCA–3′ 5′–ATGTCTTATCAGGAGCAGTACATG–3′	230

described in Table 2. For all PCR amplifications, negative (reverse transcription-PCR performed without M-MLV reverse transcriptase) and positive controls were included (MCF7 breast cancer cells for PPARγ (Elstner et al., 1998), human germ cells for c-Kit, and human leucocytes for CD45). The PCR-amplified products were subjected to electrophoresis in 2% agarose gels stained with ethidium bromide and visualized under UV transillumination.

Gel extraction and DNA sequence analysis

The PPARγ RT-PCR product was extracted from the agarose gel by using a gel band purification kit, the purified DNA was subcloned into PCR 2.1 vector and then sequenced by MWG AG Biotech (Ebersberg, Germany).

Western blot analysis of sperm proteins

Sperm samples, washed twice with Earle's balanced salt solution (uncapacitating medium), were incubated without or with the indicated treatments, and then centrifuged for 5 min at 5,000*g*. The pellet was resuspended in lysis buffer as previously described (Aquila et al., 2002). Equal amounts of protein (70 μg) were boiled for 5 min, separated by 10% polyacrylamide gel electrophoresis, transferred to nitrocellulose sheets, and probed with an appropriate dilution of the indicated antibody. The bound of the secondary antibody was revealed with the ECL Plus Western blotting detection system according to the manufacturer's instructions. The negative control was performed using a sperm lysate that was immunodepleted of PPARγ (Aquila et al., 2004) (i.e., pre-incubate lysate with anti-PPARγ antibody, 1 h at room temperature, and immunoprecipitate with Protein A/G-agarose).

As internal control, all membranes were subsequently stripped (glycine 0.2 M, pH 2.6 for 30 min at room temperature) of the first antibody and reprobed with anti-β actin or total Akt1/2 antibodies.

Immunofluorescence assay

Sperm cells, recovered from Percoll gradient, were rinsed three times with 0.5 mM Tris-HCl buffer, pH 7.5 and fixed with absolute methanol for 7 min at −20°C. PPARγ staining was carried out, after blocking with normal horse serum (10%), using a rabbit polyclonal anti-human PPARγ as primary antibody and an anti-rabbit IgG FITC-conjugated (1:100) as secondary antibody. Sperm cells incubated without the primary antibody or with normal rabbit serum instead of the primary antibody were utilized as the negative controls. The slides were examined under a fluorescence microscope (Olympus BX41, Milan Italy), and a minimum of 200 spermatozoa for slide were scored.

TABLE 2. Cycling conditions for the different sets of pairs

Gene	Cycle profile	No. of cycles
PPARγ	Denaturation: 95°C/1 min Annealing: 60°C/1 min Extention: 72°C/2 min	40
c-kit	Denaturation: 95°C/1 min Annealing: 52°C/1 min Extention: 72°C/2 min	40
CD45	Denaturation: 95°C/1 min Annealing: 55°C/1 min Extention: 72°C/2 min	40

Measurement of cholesterol in the sperm culture medium

Cholesterol was measured in duplicate by a CHOD–POD enzymatic colorimetric method according to manufacturer's instructions in the incubation medium from human spermatozoa. Sperm samples, washed twice with uncapacitating medium, were incubated in the same medium (control) or in capacitating medium for 30 min at 37°C and 5% CO_2. Some samples were incubated in the presence of increasing PGJ2 concentrations (1 to 20 μM). Other samples were incubated in the presence of 10 μM GW alone or combined with 10 μM PGJ2. At the end of the sperm incubation, the culture media were recovered by centrifugation, lyophilized and subsequently dissolved in 1 ml of buffer reaction. The samples were incubated for 10 min at room temperature, then the cholesterol content was measured spectrophotometrically at 505 nm. Cholesterol standard used was 200 mg/dl. The limit of sensitivity for the assay was 0.05 mg/dl. Inter- and intraassay variations were 0.04% and 0.03%, respectively. Cholesterol results are presented as mg per 10×10^6 number of spermatozoa.

Acrosin activity assay

Acrosin activity was assessed by the method of Kennedy et al. (1989). Percoll-purified sperms were washed in Earle's medium and centrifuged at 800*g* for 20 min. Sperms were resuspended (final concentration of 10×10^6 sperms/ml) in different tubes containing no treatment (control) or the indicated treatments (experimental). Then 1 ml of substrate–detergent mixture (23 mmol/L BAPNA in DMSO and 0.01% Triton X-100 in 0.055 mol/L NaCl, 0.055 mol/L HEPES at pH 8.0, respectively) for 3 h at room temperature was added. Aliquots (50 μl) were removed at 0 and 3 h, and the percentages of viable cells were determined. No significant differences were detected between the control and experimental conditions. After incubation, 0.5 mol/L benzamidine was added (0.1 ml) to each of the tubes and then centrifuged at 1,000*g* for 30 min. The supernatants were collected and the acrosin activity measured spectrophotometrically at 410 nm. In this assay, the total acrosin activity is defined as the amount of the active (non-zymogen) acrosin associated with sperm plus the amount of active acrosin that is obtained by proacrosin activable. The acrosin activity was expressed as $\mu IU/10^6$ sperms. Quantification of acrosin activity was performed as previously described (Aquila et al., 2003).

Triglycerides assay

Triglycerides were measured in duplicate by a GPO–POD enzymatic colorimetric method according to manufacturer's instructions in sperm lysates. Sperm samples, washed twice with uncapacitating medium, were incubated in the same medium (control) or in capacitating medium for 30 min at 37°C and 5% CO_2. Other samples were incubated in the presence of the indicated treatments. At the end of the sperm incubation, 10 μl of lysate was added to the 1 ml of buffer reaction and incubated for 10 min at room temperature. Then the triglycerides content was measured spectrophotometrically at 505 nm. Data are presented as $\mu g/10^6$ sperms.

Assay of acyl-CoA dehydrogenase activity

Assay of acyl-CoA dehydrogenase was performed on sperm incubated in the presence of the indicated treatments, using a modification of the method described by Lehman et al. (1990). In brief, after lysis, 70 μg of sperm protein was added to buffer containing 20 mM Mops, 0.5 mM EDTA, and 100 μM FAD^+ at pH 7.2. Reduction of FAD^+ to FADH was read at 340 nm upon addition of octanoyl-CoA (100 μM) every 20 sec for 1.5 min. Data are expressed in nmol/min/mg protein. The enzymatic activity was determined with three control media: one without octanoyl-CoA as substrate, one without the co-enzyme (FAD^+), and the third without either substrate or co-enzyme (data not shown). Every experiment was performed six times, in duplicate within each experiment.

Glucose-6-phosphate dehydrogenase (G6PDH) activity

The conversion of $NADP^+$ to NADPH, catalyzed by G6PDH, was measured by the increase of absorbance at 340 nm. Sperm

samples, washed twice with uncapacitating medium, were incubated in the same medium (control) for 30 min at 37°C and 5% CO_2. Some samples were treated with increasing concentration of BRL or with 3.3 nM insulin, or 10 μM GW alone or combined with 10 μM BRL. Other samples were treated with 10 μM BRL plus 3.3 nM insulin or 10 μM GW plus 10 μM BRL and 3.3 nM insulin. After incubation, 50 μl of sperm extracts were loaded into individual cuvettes containing buffer (100 mM triethanolamine, 100 mM $MgCl_2$, 10 mg/ml glucose-6-phosphate, 10 mg/ml $NADP^+$, pH 7.6) for spectrophotometric determination. The absorbance of samples was read at 340 nm every 20 sec for 1.5 min. Data are expressed in nmol/min/10^6 sperms. The enzymatic activity was determined with three control media: one without glucose-6-phosphate as substrate, one without the co-enzyme ($NADP^+$), and the third without either substrate or co-enzyme (data not shown). Every experiment was performed eight times, in duplicate within each experiment.

STATISTICAL ANALYSIS

The experiments for RT-PCR were repeated on at least three independent occasions, whereas Western blot analysis was performed in at least six independent experiments. The data obtained from motility, viability (six replicate experiments using duplicate determinations), CHOD–POD enzymatic colorimetric method, Triglycerides Assay, acyl-CoA dehydrogenase activity (six replicate experiments using duplicate determinations), G6PDH (eight replicate experiments using duplicate determinations) were presented as the mean ± SD. The differences in mean values were calculated using analysis of variance (ANOVA) with a significance level of $P < 0.05$.

RESULTS

Expression of PPARγ in human sperm

RT-PCR and western blot. To determine whether mRNA for PPARγ is present in human-ejaculated spermatozoa, RNA isolated from percoll-separated sperm of normal men was subjected to reverse PCR. The primer sequences were based on the human PPARγ gene sequence and the RT-PCR amplification revealed the expected PCR product size of 233 bp of the coding region of the human PPARγ cDNA (Fig. 1A). This product was sequenced and found to be corresponding to the classical human PPARγ. No detectable levels of mRNA coding either CD45, a specific marker of human leucocytes, or c-kit, a specific marker of human germ cells, were found in the same semen samples (Fig. 1A), ruling out any potential contamination. In addition, the RT-PCR products were not a result of any DNA contamination as the RNA samples were subjected to DNAse treatment before RT-PCR.

The presence of PPARγ protein in human-ejaculated sperm was investigated by Western blot using an antibody raised against the carboxyl-terminus of the human PPARγ protein (Fig. 1B). One immunoreactive band, corresponding to the molecular mass values of 70 kDa, was observed at the same mobility of the MCF-7 extract, used as positive control. The negative control (lane 2) was performed using a sperm lysate, where PPARγ was previously removed by pre-incubation with the respective antibody (1 h at room temperature) and subsequently immunoprecipitated with protein A/G-agarose.

Immunolocalization. Using a immunofluorescence technique and the same antibody used for Western blot, we obtained a positive signal for PPARγ in human spermatozoa. In the majority of population of uncapacitated sperm, immunoreactivity is predominantly compartmentalized to the subacrosomial region and the midpiece while the tail is almost completely unstained (Fig. 2A). No fluorescent signal was obtained when primary antibody was omitted (Fig. 2B) or when the normal rabbit IgG was used instead of the primary antibody (Fig. 2C), thus further confirming the specificity of the antibody binding.

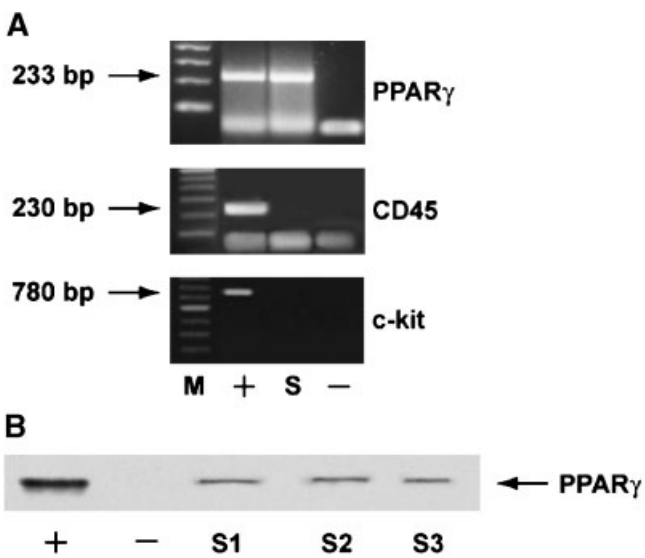

Fig. 1. PPARγ expression in human-ejaculated spermatozoa. **A**: Reverse transcription-PCR analysis of human PPARγ, CD45, and c-Kit genes in percolled human spermatozoa (S), negative control (no M-MLV reverse transcriptase added) (−), positive controls (MCF7 breast cancer cells for PPARγ, human germ cells for c-Kit and human leucocytes for CD45) (+), marker (lane M). Arrows indicated the expected size of the PCR products. **B**: Western blot of PPARγ protein in human sperm, expression in three samples of ejaculated spermatozoa from normal men (S1, S2, S3). MCF-7 extract was used as control (+). The negative control (see Materials and Methods, is represented in lane 2 (−). The experiments were repeated at least three times for RT-PCR, six times for Western blot and the autoradiographs of the figure show the results of one representative experiment.

PPARγ-agonists influence on capacitation, acrosome reaction and motility is PPARγ-mediated

We first investigated whether PPARγ-agonists are able to influence the sperm extratesticular maturation evaluating their action on both capacitation and acrosome reaction. Further, in all the experiments we used both a natural PPARγ-ligand, PGJ2 (1, 10, and 20 μM) and a synthetic ligand BRL (1, 10, and 20 μM), obtaining similar results, therefore in the text, we reported the data relative to the natural PPARγ-ligand.

Sperm membrane cholesterol efflux contributes to one signaling mechanism that controls sperm capacitation (Travis and Kopf, 2002) and it has been demonstrated that it initiates signaling events leading to tyrosine phosphorylation of sperm proteins, also representative of the capacitation status (Visconti et al., 1995). Washed sperm were treated with increasing concentration of PGJ2 (1, 10, and 20 μM) and incubated under uncapacitating conditions (*see Materials and Methods*). At the end of incubation, the samples were centrifuged, the upper phase was used to determinate the cholesterol levels, while the sperm were lysed to evaluate protein tyrosine phosphorylation. Our results showed a significant increase in both tyrosine phosphorylation (Fig. 3A) and cholesterol efflux (Fig. 3B) upon 1 to 20 μM PGJ2 treatment. Both processes were inhibited by using the specific PPARγ-antagonist GW suggesting an involvement of this receptor in the induction of capacitation.

Acrosin activity, performed in the same experimental conditions, showed an increase by PGJ2 reversed by GW

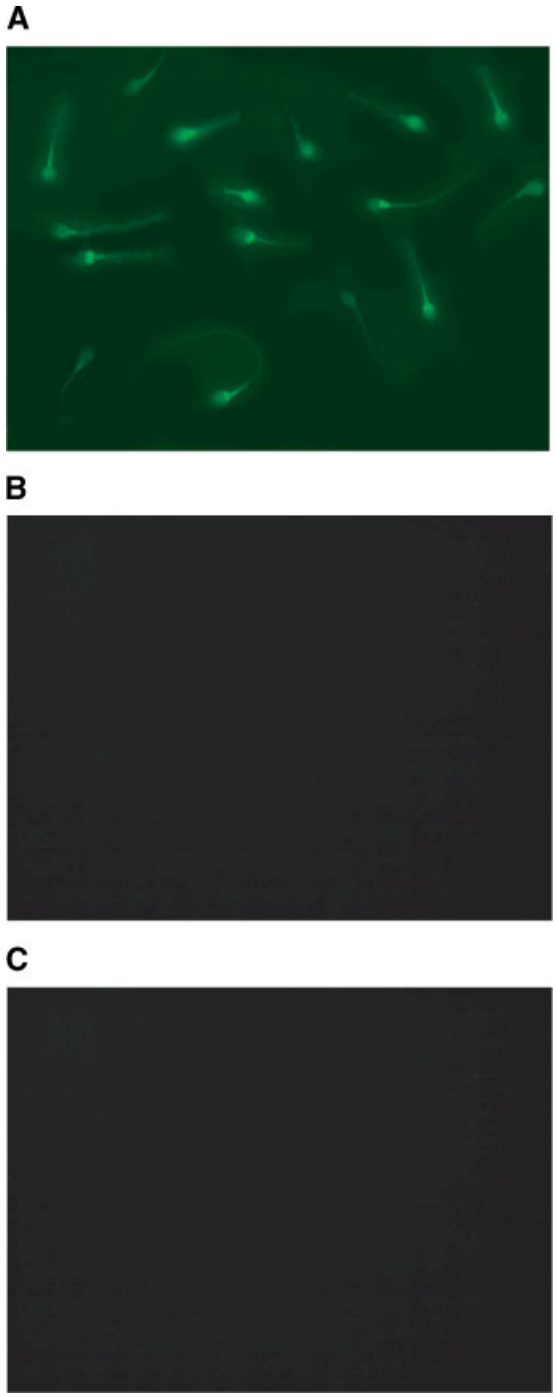

Fig. 2. Immunolocalization of PPARγ in human-ejaculated spermatozoa. **A**: PPARγ immunolocalization; (**B**) Sperm cells incubated without the primary antibody were utilized as negative control. **C**: Sperm cells incubated replacing the anti-PPARγ antibody by normal rabbit serum were utilized as negative control. The pictures shown are representative examples of experiments that were performed at least three times with reproducible results.

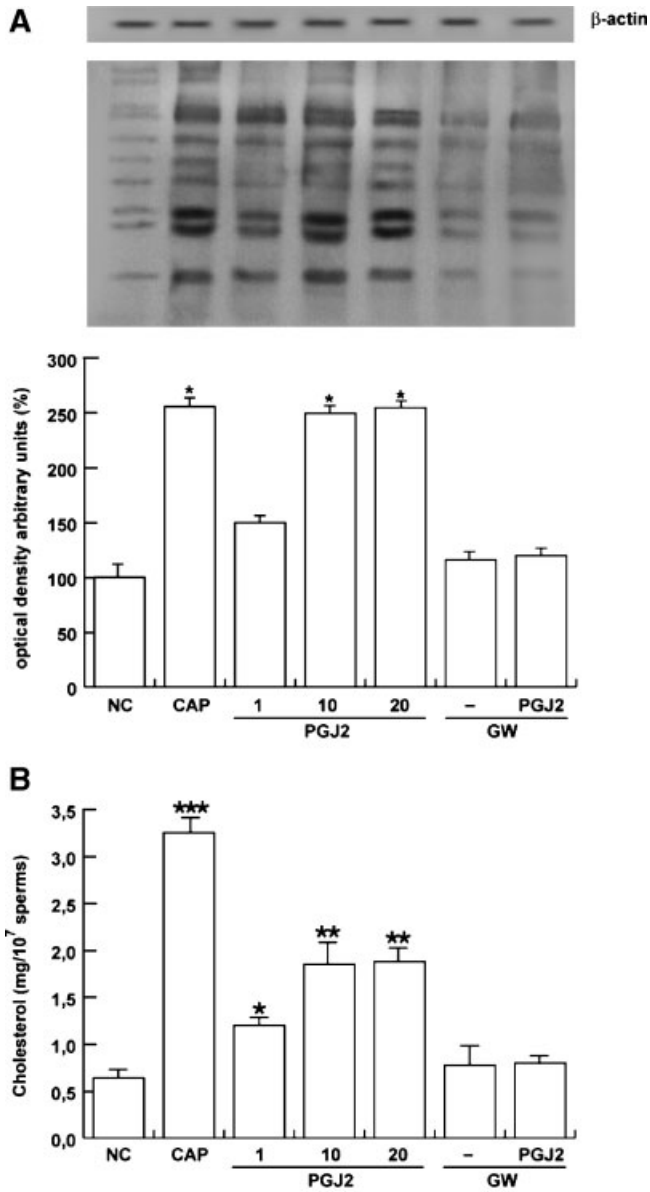

Fig. 3. PGJ2 effects on tyrosine phosphorylation of sperm proteins and cholesterol efflux are PPARγ-mediated. Washed spermatozoa were incubated in the unsupplemented Earle's medium for 30 min at 37°C and 5% CO_2, in the absence (NC) or in the presence of increasing concentration of PGJ2 (1, 10, 20 μM) or with 10 μM GW alone or combined with 10 μM PGJ2. Other samples were incubated in capacitating medium (CAP). **A**: Sperm lysates (70 μg) were used for Western blot analysis of protein tyrosine phosphorylation. On the bottom, quantitative representation after densitometry. **B**: Cholesterol in culture medium from human-ejaculated spermatozoa was measured by enzymatic colorimetric assay. Columns are mean ± SD of six independent experiments performed in duplicate. Data are expressed in mg/10^7 sperms. $^*P < 0.05$ versus control, $^{**}P < 0.01$ versus control; $^{***}P < 0.001$ versus control.

(Fig. 4A). BRL also significantly induced sperm motility (data not shown). The PGJ2-induced effects on sperm motility were antagonized by the specific GW antagonist while the antagonist alone had no significant effect (Fig. 4B).

PPARγ affects lipid metabolism in human sperm

The favorable metabolic effects of PPARγ-agonists are supposedly related to the PPARγ-driven changes in lipid metabolism. Owing to the critical role that PPARγ plays in lipid metabolism, we evaluated both the intracellular level of triglycerides and the β-oxidation of the fatty acids under PPARγ-agonists in sperm.

Stimulation with BRL induced a significant decrease in sperm triglycerides levels however GW didn't reverse the effect addressing a PPARγ-independent event (Fig. 5A). While in the samples treated with PGJ2, GW is able to block the PPARγ-agonist effect (Fig. 5B). As it concerns the β-oxidation of the fatty acids, a dose-dependent increase under PGJ2 treatment was

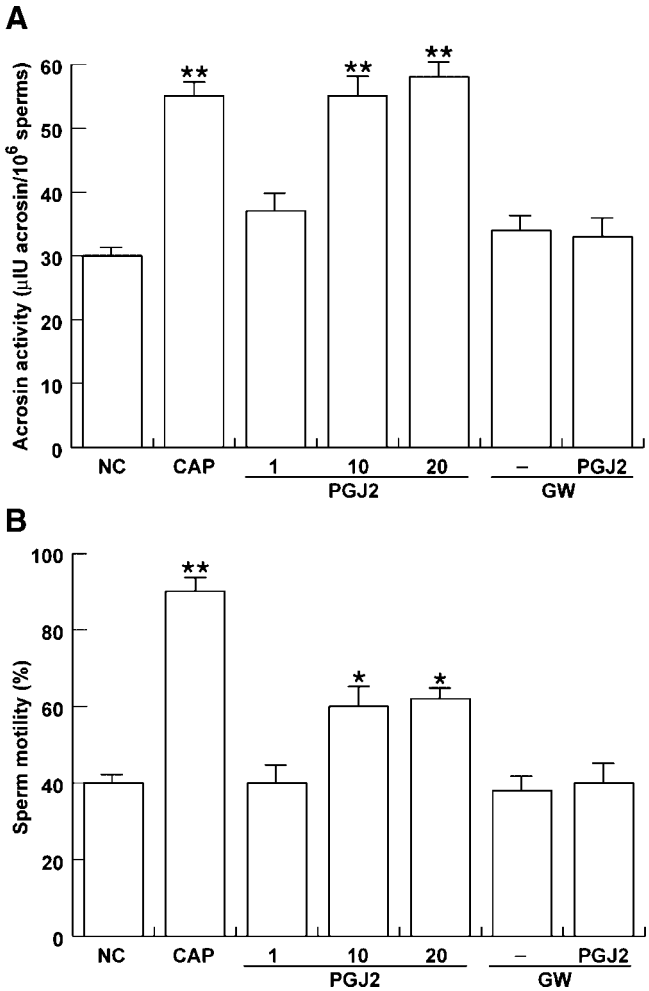

Fig. 4. PGJ2 effects on acrosin activity and sperm motility are PPARγ-mediated. Washed spermatozoa were incubated in the unsupplemented Earle's medium for 30 min at 37°C and 5% CO_2, in the absence (NC) or in the presence of increasing concentration of PGJ2 (1, 10, 20 μM) or with 10 μM GW alone or combined with 10 μM PGJ2. Other samples were incubated in capacitating medium (CAP). **A**: Acrosin activity was assessed as reported in Materials and Methods. **B**: Sperm motility was expressed as percentage of total motile sperm. Columns are mean ± SD of six independent experiments performed in duplicate. $^{*}P < 0.05$ versus control; $^{**}P < 0.01$ versus control.

observed (Fig. 5C) and GW was able to reverse PGJ2-induced effect.

PPARγ-agonist activates PI3K/Akt pathway in human sperm

PPARγ activation has been reported to regulate components of the PI3K signaling cascade in various cell types (Bonofiglio et al., 2005). We speculated that PPARγ may be involved in the control of some sperm functions, perhaps by influencing the activity of PI3K. Therefore, we examined the effects of PPARγ-agonist treatment on PI3K-mediated signaling by evaluating the phosphorylation of the major downstream signal transducer, AKT, since its phosphorylation has been correlated with its activity (Datta et al., 1999).

Increasing doses of BRL (1, 10, and 20 μM) resulted in a significant increase in the AKT phosphorylation (Fig. 6). To address whether PPARγ-agonist stimulation of AKT was specifically mediated through PPARγ, we treated sperm with 10 μM GW in the presence or absence of 10 μM BRL. BRL-stimulatory effect was reduced by

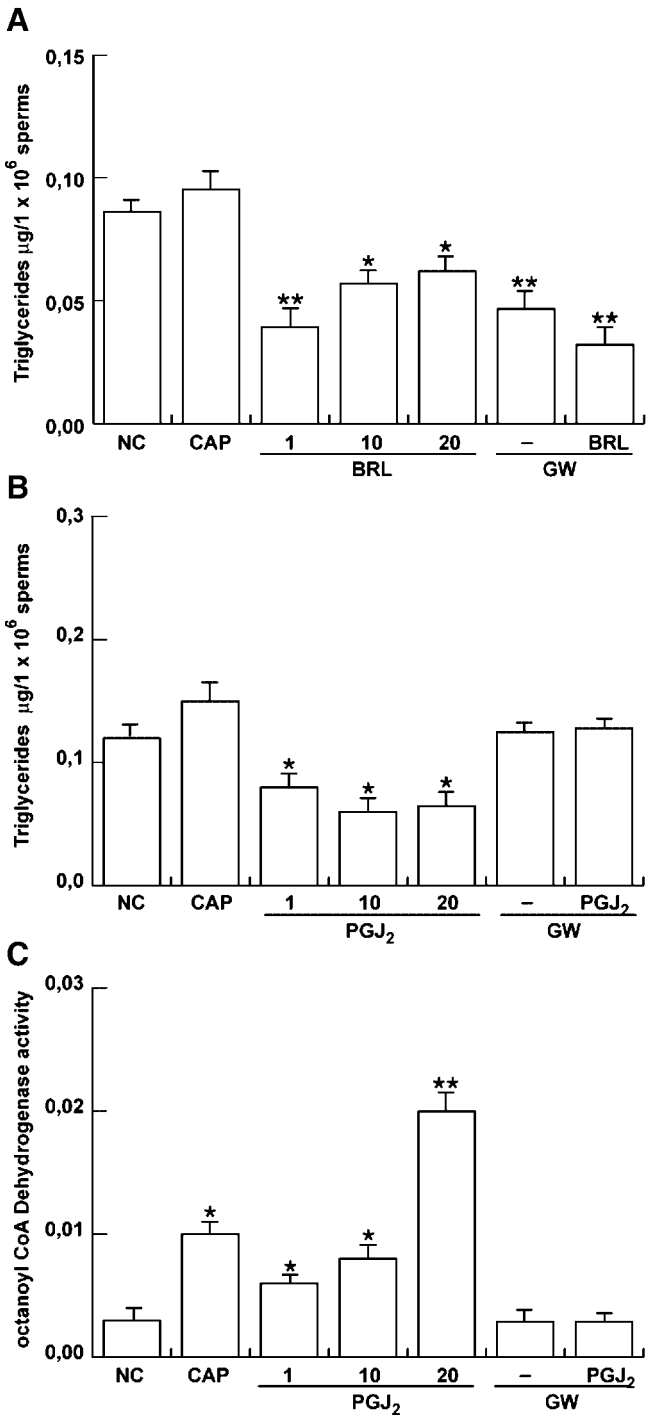

Fig. 5. PPARγ-agonists influence lipid metabolism in sperm. **A**: Sperm samples, washed twice with uncapacitating medium were incubated in the same medium (NC) or in capacitating medium (CAP) for 30 min at 37°C and 5% CO_2. Other samples were incubated in the presence of increasing BRL concentrations (1, 10, 20 μM) or in the presence of 10 μM GW alone, or combined with 10 μM BRL. **B**: Sperm samples were incubated with PGJ2 instead of BRL. Data are presented as μg/10^6 sperms. **C**: Assay of acyl-CoA dehydrogenase was performed on sperm lysates (see Materials and Methods) in the same experimental conditions above mentioned. Columns are mean ± SD of six independent experiments performed in duplicate. Data are presented as nmol/min/mg protein. Columns are mean ± SD. $^{*}P < 0.05$ versus control; $^{**}P < 0.01$ versus control.

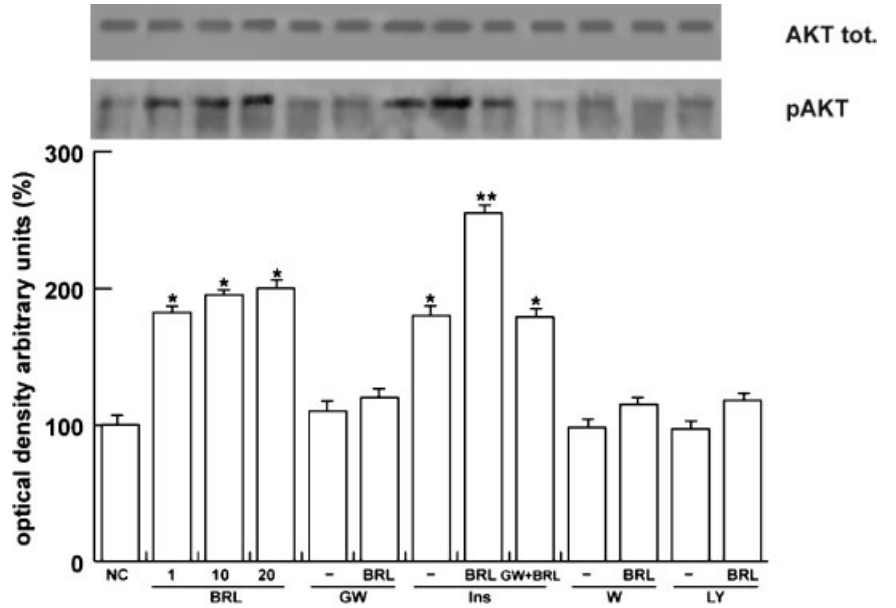

Fig. 6. BRL increases insulin-induced AKT phosphorylation in human sperm. Washed spermatozoa were incubated in the unsupplemented Earle's medium for 30 min at 37°C and 5% CO_2, in the absence (NC) or in the presence of increasing BRL (1, 10, 20 μM). Some samples were incubated in the presence of 10 μM GW alone or combined with 10 μM BRL, in the presence of 3.3 nM Ins alone or combined with 10 μM BRL or combined with 10 μBRL plus 3.3 nM insulin (Ins), in the presence of 10 μM worthmannin (W) alone or combined with 10 μM BRL, in the presence of 10 μM LY294002 (LY) alone or combined with 10 μM BRL. In the upper part, is reported total AKT. On the bottom, is reported the densitometric evaluation. The autoradiographs presented are representative examples of experiments that were performed at least four times with repetitive results. *$P < 0.01$ versus control, **$P < 0.001$ versus control.

GW. We also tested the effects of PI3K inhibitors, 10 μM wortmannin, and 10 μM LY294002, confirming that the action of PPARγ on AKT is through PI3K activation.

AKT plays multifunction roles in insulin action and its activation has been shown to be dependent on PI3K (Datta et al., 1999). In addition, we recently showed that in sperm insulin activates PI3K pathway (Aquila et al., 2005b), therefore we aimed to investigate the interrelation between insulin and PPARγ. It was also reported that BRL is an insulin-sensitizing agent since it belongs to TZDs (Petersen et al., 2000). Insulin alone induced a significant increase in AKT phosphorylation according to our previous data (Aquila et al., 2005b). In the presence of BRL, insulin displayed greater stimulatory effect. Therefore BRL increased PI3K activation induced by insulin (Fig. 6), suggesting an insulin-sensitizing action also in sperm. All these treatments were also used in combination with GW showing an involvement of PPARγ in BRL action.

PPARγ affects glucose metabolism through the pentose phosphate pathway (PPP) in human sperm

Given the beneficial effects of PPARγ ligands in therapies aimed at lowering glucose levels in type 2 diabetes, a role of PPARγ in glucose metabolism has been explored (Lenhard et al., 1997). An important metabolic response to insulin in the regulation of glucose homeostasis is related to the G6PDH activity (Stumpo and Kletzien, 1984), while the effect of PPARγ action on this enzymatic activity was never investigated. In our previous study, we demonstrated that insulin regulate in autocrine fashion sperm G6PDH activity (Aquila et al., 2005a). Thus, we speculated that in sperm, insulin and PPARγ are possibly interrelated and relevant on glucose metabolism through the PPP.

As shown in Figure 7, 10 μM BRL activates G6PDH activity and insulin in a higher extent. In the presence of BRL, insulin action was further enhanced and this effect was reversed by GW. Our results address a regulatory role of PPARγ in sperm glucose metabolism and worthy evidence an insulin-sensitizing effect by BRL.

DISCUSSION

Lipid and carbohydrate homeostasis in higher organisms is under the control of an integrated system that has the capacity to rapidly respond to metabolic changes. The PPARγ is a nuclear fatty acid receptor that has been implicated in energy homeostasis and in many pathological processes (Knouff and Auwerx, 2004). Specifically, it modulates lipid homeostasis in

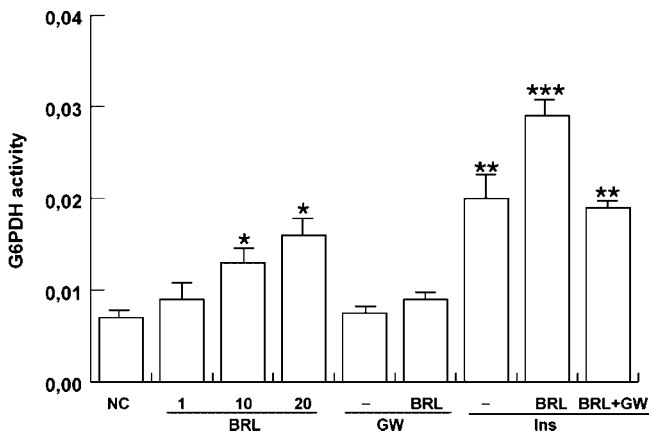

Fig. 7. BRL effect on G6PDH activity. Sperm were washed with the unsupplemented Earle's medium and were treated in the absence (NC) or in the presence of increasing BRL (1, 10, 20 μM). Some samples were incubated in the presence of 10 μM GW alone or combined with 10 μM BRL, in the presence of 3.3 nM insulin alone or plus 10 μM BRL or combined with 10 μM BRL plus 10 μM GW. Columns are mean ± SD of eight independent experiments performed in duplicate. Data are expressed as nanomoles per minute per 10^6 sperms. *$P < 0.05$ versus control; **$P < 0.01$ versus control, ***$P < 0.001$ versus control.

metabolically active sites, including the liver, adipocytes, muscle, and macrophage (Desvergne and Wahli, 1999 and references therein). Here we show that PPARγ is also expressed in human-ejaculated spermatozoa. The effects of both natural and synthetic PPARγ ligands on different sperm functions were investigated.

First, we have demonstrated the presence of PPARγ in human-ejaculated spermatozoa at different levels: mRNA expression, protein expression, and immunolocalization. As it concerns the presence of mRNA in mammalian ejaculated spermatozoa, originally it was hypothesized that these transcripts were carried over from earlier stages of spermatogenesis, however new reports revaluate significance of mRNA in these cells (Miller, 2000; Ostermeier et al., 2002) and the issue is currently under investigation. In good agreement with RT-PCR data, our immunohistochemical assays demonstrated that PPARγ protein is detectable in sperm, with specific signals being located in the subacrosomial region and in the middlepiece, to a lesser extent in the tail. PPARγ is highly expressed in adipose tissues but is expressed at much lower levels in other tissues, including major insulin target tissues, skeletal muscle, and liver (Desvergne and Wahli, 1999 and references therein). Expression of PPARγ in the male gamete, further confirmed by Western Blot, is a novel intriguing finding since it may have an important role in the regulation of sperm metabolism.

To investigate the functional role of PPARγ in sperm, we evaluated its action on different events that characterize the sperm cell as capacitation, acrosome reaction, and motility. PPARγ is activated by endogenous arachidonic acid metabolites such as PGJ2 (Desvergne and Wahli, 1999 and references therein) and it is the target for binding to a class of synthetic compounds, termed the TZD. In our experiments, we used both natural and synthetic ligands obtaining similar results on the abovementioned processes (in the figures are showed only the results referred to PGJ2 treatment). Particularly, we observed a significant increase in both cholesterol efflux and tyrosine phosphorylation of sperm proteins, this latter event tightly related to the capacitation (Visconti et al., 1995) and resulting downstream the cholesterol efflux. These effects were reduced by GW indicating a PPARγ involvement. PPARγ has been shown to be implicated in cholesterol export from macrophages and the ability of TZDs to promote cholesterol efflux is completely dependent on PPARγ, as assessed by the inability of these compounds to augment the efflux of cholesterol from *Pparg*$^{-/-}$ macrophages (Chawla et al., 2001). The molecular route by which TZDs promote cholesterol efflux involves a transcriptional cascade that is controlled by PPARγ (Zhang and Chawla, 2004 and references therein). Here we have to take into account that sperm are considered transcriptionally inactive, therefore very likely PPARγ in sperm acts through a non-genomic action. As it concerns acrosome reaction and motility, our results are in concordance with recent studies on human spermatozoa where prostaglandins are reported to enhance both processes (Aitken et al., 1986; Aitken and Kelly, 1985), although in addition, we showed that the effects of these compounds are PPARγ-mediated.

Several investigators have identified a pivotal role for PPARγ in fat cell differentiation, lipid storage, vascular function, and energy metabolism. Overall, the favorable metabolic effects of TZDs are supposedly related to the PPARγ-driven changes in lipid metabolism. It has long been recognized that capacitated sperm display an increase metabolic rate presumably to affect the changes in sperm signaling and function during capacitation process. The relationship between the signaling events associated with capacitation and changes in sperm energy metabolism is poorly understood. Under PPARγ-agonists treatment, our results evidenced a reduction in triglycerides content in sperm while at the same time, we observed an increased Fatty Acids (FA) β-oxidation. Particularly, the behavior of the two PPARγ-agonists diverges when we tested their effects on triglycerides levels: it appears that the action of PGJ2 is PPARγ-mediated while BRL effect is PPARγ-independent. It is well known that BRL treatment reduces hypertriglyceridemia however, it is not clear how TZDs lower free FA levels. Since they seem to have little or no effect on basal rates of lipolysis, it was supposed that the decrease in plasma-free FA levels is probably due to an increase in free FA clearance (oxidation and/or esterification) (Ciaraldi et al., 2002). Supporting this notion, we may hypothesize that during capacitation when energy expenditure increases, lipid reserve is mobilized and also used as energy substrate available.

The PPARγ controls many different target genes involved in both lipid metabolism and glucose homeostasis (Desvergne and Wahli, 1999). Given the beneficial effects of PPARγ ligands in therapies aimed at lowering glucose levels in type 2 diabetes, a role of PPARγ in glucose metabolism has been explored. Sperm energy metabolism is very complex because there are many metabolic pathways where hexoses can be diverted. In this sense, these cells not only have the glycolysis and Krebs cycle catabolic pathways but also the glycogen synthesis and pentose phosphate cycle, a very complex system that allows for a fine regulation of energy levels depending on their functional status. It emerged from our recent studies that insulin, one of the main regulators of energy homeostasis in somatic cells, may be also crucial in the management of sperm glucose metabolism since in autocrine fashion, it regulates G6PDH and glycogen synthase activities (Aquila et al., 2005a, b). It is generally accepted that TZDs exert their insulin sensitizing action through PPARγ, however, how exactly this occurs, it remains to be clarified. We previously showed that insulin activated G6PDH in sperm and in this study that the activation is additive or synergistic to that of BRL. In these circumstances, G6PDH activity would theoretically increase glucose utilization as a consequence of improved insulin signaling in sperm as well as a cause of insulin sensitization.

The enhanced activity of this enzyme produces an increase of NADPH that is essential for fatty acid synthesis from acetyl CoA. These fatty acids have two possible fates: β-oxidation to produce ATP or reesterification back into triacylglycerol. Inter-relationships of the classes of substrates of free FA and glucose utilized for energy as first proposed by Randle (1964), has been long established and also hypothesized in the spermatozoa (Andò and Aquila, 2005). In this study, we observed in ejaculated sperm that FA β-oxidation tested utilizing the octanoil-CoA as substrate, appears to be stimulated by PPARγ agonists. It may be assumed that PPARγ works to stimulate such enzymatic activity providing additional metabolic fuel to sustain capacitation process. Therefore, the autonomous capability of sperm to release insulin suggests that they through an autocrine short loop may provide the recruitment of energy substrate according to sperm metabolic needs

and that PPARγ may serve as a molecular means for maintaining energy balance, regulating sperm energy dissipation during capacitation.

The regulation of lipid and carbohydrate metabolism might have important implications in male reproduction for developing models of PPARγ function as a therapeutic target. In particular, TZDs are widely used in patients with diabetes, who also have high risk of infertility (Baccetti et al., 2002). The mechanisms controlling the interaction between energy balance and reproduction are the subject of intensive investigations. For example, negative energy balance caused by inadequate nutrient supply or excessive consumption is able to affect the fertility of female mammals. Interestingly, insulin-sensitizing agents such as BRL were also shown to ameliorate the ovulatory function of polycystic ovarian syndrome patients (Froment et al., 2005).

The physiological significance of the present observations are still incomplete. Prostaglandins are involved in the male reproductive tract, and high concentrations of prostaglandins are reported to exist in seminal fluid (Templeton et al., 1978) and cervical mucus (Charbonnel et al., 1982). In addition, human spermatozoa have been shown to synthesize prostaglandins (Roy and Ratnam, 1992). Prostaglandins treatment is reported to enhance sperm fertilizing ability (Aitken et al., 1986; Aitken and Kelly, 1985; Shimizu et al., 1998). On the basis of our data, PPARγ activation may induce both capacitation and acrosome reaction; however, it is also possible that prostaglandin, together with administration of BRL, could increase PPARγ activation in different pathological conditions thus leading to sperm function alterations.

Taken together, these results indicate that the role of PPARγ is more complex than was originally believed. Our findings also showed that sperm is a new target tissue for the lipid- and glucose-lowering effects of the TZDs in humans. Thus, the modulation of levels of PPARγ and/or its ligands may afford novel therapeutic opportunities for the treatment of the male fertility disorders imputable to metabolic diseases. Further work will be required to more fully elucidate the role that PPARγ plays in this area. Whatever the outcome, however, it is clear that future studies of reproductive regulation must take into account of this receptor.

ACKNOWLEDGMENTS

Our special thank to D. Sturino (Faculty of Pharmacy, University of Calabria—Italy) for the English review of the manuscript and to Dr. Vincenzo Cunsulo (Biogemina SAS, Catania—Italy).

LITERATURE CITED

Aitken RJ, Kelly RW. 1985. Analysis of the direct effects of prostaglandins on human sperm function. J Reprod Fertil 73:139–146.

Aitken RJ, Irvine S, Kelly RW. 1986. Significance of intracellular calcium and cyclic adenosine 3′,5′-monophosphate in the mechanisms by which prostaglandins influence human sperm function. J Reprod Fertil 77:451–462.

Andò S, Aquila S, 2005. Arguments raised by the recent discovery that insulin and leptin are expressed in and secreted by human ejaculated spermatozoa. Mol Cell Endocrinol 245:1–6.

Aquila S, Sisci D, Gentile ME, Middea E, Siciliano L, Andò S. 2002. Human ejaculated spermatozoa contain active P450 aromatase. J Clin Endocrinol Metab 87:3385–3390.

Aquila S, Sisci D, Gentile M, Carpino A, Middea E, Catalano S, Rago V, Ando S. 2003. Towards a physiological role for cytochrome P450 aromatase in ejaculated human sperm. Hum Reprod 18:1650–1659.

Aquila S, Sisci D, Gentile ME, Middea E, Catalano S, Carpino A, Rago V, Andò S. 2004. Estrogen Receptor (ER) α and ER β are both expressed in human ejaculated spermatozoa: Evidence of their direct interaction with phosphatidylinositol-3-OH kinase/Akt pathway. J Clin Endocrinol Metab 89:1443–1451.

Aquila S, Gentile M, Middea E, Catalano S, Ando S. 2005a. Autocrine regulation of insulin secretion in human ejaculated spermatozoa. Endocrinology 146:552–557.

Aquila S, Gentile M, Middea E, Catalano S, Morelli C, Pezzi V, Ando S. 2005b. Leptin secretion by human ejaculated spermatozoa. J Clin Endocrinol Metab 90:4753–4761.

Baccetti B, La Marca A, Piomboni P, Capitani S, Bruni E, Petraglia F, De Leo V. 2002. Insulin-dependent diabetes in men is associated with hypothalamo-pituitary derangement and with impairment in semen quality. Hum Reprod 17:2673–2677.

Bonofiglio D, Gabriele S, Aquila S, Catalano S, Gentile M, Middea E, Giordano F, Ando S. 2005. Estrogen receptor alpha binds to peroxisome proliferator-activated receptor response element and negatively interferes with peroxisome proliferator-activated receptor gamma signaling in breast cancer cells. Clin Cancer Res 11:6139–6147.

Cato ACB, Nestl A, Mink S. 2002. Rapid actions of steroid receptors in cellular signaling pathways. Sci STKE 138:RE9.

Chang TH, Szabo E. 2000. Induction of differentiation and apoptosis by ligands of peroxisome proliferator-activated receptor gamma in non-small cell lung cancer. Cancer Res 60:1129–1138.

Charbonnel B, Kremer M, Gerozissis K, Dray F. 1982. Human cervical mucus contains large amounts of prostaglandins. Fertil Steril 38:109–111.

Chawla A, Boisvert WA, Lee CH, Laffitte BA, Barak Y, Joseph SB, Liao D, Nagy L, Edwards PA, Curtiss LK, Evans RM, Tontonoz P. 2001. A PPAR gamma-LXR-ABCA1 pathway in macrophages is involved in cholesterol efflux and atherogenesis. Mol Cell 7:161–171.

Ciaraldi TP, Cha BS, Park KS, Carter L, Mudaliar SR, Henry RR. 2002. Free fatty acid metabolism in human skeletal muscle is regulated by PPARgamma and RXR agonists. Ann NY Acad Sci 967:66–70.

Cui Y, Miyoshi K, Claudio E, Siebenlist UK, Gonzalez FJ, Flaws J, Wagner K-U, Hennighausen L. 2002. Loss of the peroxisome proliferation-activated receptor gamma (PPARgamma) does not affect mammary development and propensity for tumor formation but leads to reduced fertility. J Biol Chem 277:17830–17835.

Datta SR, Brunet A, Greenberg ME. 1999. Cellular survival: A play in three Akts. Genes Dev 13:2905–2927.

Desvergne B, Wahli W. 1999. Peroxisome proliferator-activated receptors: Nuclear control of metabolism. Endocr Rev 20:649–688.

Elstner E, Muller C, Koshizuka K, Williamson EA, Park D, Asou H, Shintaku P, Said JW, Heber D, Koeffler HP., 1998. Ligands for peroxisome proliferator-activated receptor γ and retinoic acid receptor inhibit growth and induce apoptosis of human breast cancer cells in vitro and in BNX mice. Proc Natl Acad Sci USA 95:8806–8811.

Froment P, Gizard F, Staels B, Dupont J, Monget P. 2005. A role of PPARgamma in reproduction? Med Sci 2:507–511.

Genolet R, Wahli W, Michalik L. 2004. PPARs as drug targets to modulate inflammatory responses? Curr Drug Targets Inflamm Allergy 3:361–375.

Gurnell M. 2005. Peroxisome proliferator-activated receptor gamma and the regulation of adipocyte function: Lessons from human genetic studies. Best Pract Res Clin Endocrinol Metab 19:501–523.

Kennedy WP, Kaminsky JM, Van Der Ven HH, Jeyendran RS, Reid DS, Blackwell J, Biefeld P, Zaneveld LJD. 1989. A simple, clinical assay to evaluate the acrosin activity of human spermatozoa. J Androl 10:221–231.

Kintscher U, Law RE. 2005. PPARgamma-mediated insulin sensitization: The importance of fat versus muscle. Am J Physiol Endocrinol Metab 288:E287–291.

Knouff C, Auwerx J. 2004. Peroxisome proliferator-activated receptor-gamma calls for activation in moderation: Lessons from genetics and pharmacology. Endocr Rev 25:899–918.

Kobayashi Y, Ueki S, Mahemuti G, Chiba T, Oyamada H, Saito N, Kanda A, Kayaba H, Chihara J. 2005. Physiological levels of 15-deoxy-Delta12,14-prostaglandin J2 prime eotaxin-induced chemotaxis on human eosinophils through peroxisome proliferator-activated receptor-gamma ligation. J Immunol 175:5744–5750.

Kostadinova R, Wahli W, Michalik L. 2005. PPARs in diseases: Control mechanisms of inflammation. Curr Med Chem 12:2995–3009.

Kota BP, Huang TH, Roufogalis BD. 2005. An overview on biological mechanisms of PPARs. Pharmacol Res 51:85–94.

Lehman TC, Hale DE, Bhala A, Thorpe C. 1990. An acyl-coenzyme A dehydrogenase assay utilizing the ferricenium ion. Anal Biochem 186:280–284.

Lenhard JM, Kliewer SA, Paulik MA, Plunket KD, Lehmann JM, Weiel JE. 1997. Effects of troglitazone and metformin on glucose and lipid metabolism: Alterations of two distinct molecular pathways. Biochem Pharmacol 54:801–808.

Miller D. 2000. Analysis and significance of messenger RNA in human ejaculated spermatozoa. Mol Reprod Dev 56:259–226.

Moschos S, Chan JL, Mantzoros CS. 2002. Leptin and reproduction: A review. . Fertil Steril 77:433–444.

Nicol CJ, Adachi M, Akiyama TE, Gonzalez FJ. 2005. PPARgamma in endothelial cells influences high fat diet-induced hypertension. Am J Hypertens 18:549–556.

Ostermeier GC, Dix DJ, Miller D, Khatri P, Krawetz SA. 2002. Spermatozoal RNA profiles of normal fertile men. Lancet 360:772–777.

Pan GD, Wu H, Liu JW, Cheng NS, Xiong XZ, Li SF, Zhang GF, Yan LN., 2005. Effect of peroxisome proliferator-activated receptor-gamma ligand on inflammation of human gall bladder epithelial cells. World J Gastroenterol 11:6061–6065.

Petersen KF, Krssak M, Inzucchi S, Cline GW, Dufour S, Shulman GI. 2000. Mechanism of troglitazone action in type 2 diabetes. Diabetes 49:827–831.

Quandt SA. 1984. Nutritional thriftiness and human reproduction: Beyond the critical body composition hypothesis. Soc Sci Med 19:177–182.

Randle P. 1964. The interrelationships of hormones, fatty acid and glucose in the provision of energy. Postgrad Med J 40:457–463.

Rangwala SM, Lazar MA. 2004. Peroxisome proliferator-activated receptor gamma in diabetes and metabolism. Trends Pharmacol Sci 25:331–336.

Roy AC, Ratnam SS. 1992. Biosynthesis of prostaglandins by human spermatozoa in vitro and their role in acrosome reaction and fertilization. Mol Reprod Dev 33:303–306.

Seli E, Duleba AJ. 2002. Optimizing ovulation induction in women with polycystic ovary syndrome. Curr Opin Obstet Gynecol 14:245–254.

Shah C, Modi D, Sachdeva G, Gadkar S, D'Souza S, Puri C. 2005. N-terminal region of progesterone receptor B isoform in human spermatozoa. Int J Androl 28:360–371.

Shimizu Y, Yorimitsu A, Maruyama Y, Kubota T, Aso T, Bronson RA. 1998. Prostaglandins induce calcium influx in human spermatozoa. Mol Hum Reprod 4:555–561.

Skolnik PR, Rabbi MF, Mathys JM, Greenberg AS. 2002. Stimulation of peroxisome proliferator-activated receptors alpha and gamma blocks HIV-1 replication and TNFalpha production in acutely infected primary blood cells, chronically infected U1 cells, and alveolar macrophages from HIV-infected subjects. J Acquir Immune Defic Syndr 31:1–10. Erratum in: J Acquir Immune Defic Syndr 2003.33:657.

Standiford TJ, Keshamouni VG, Reddy RC. 2005. Peroxisome proliferator-activated receptor-{gamma} as a regulator of lung inflammation and repair. Proc Am Thorac Soc 2:226–231.

Stumpo DJ, Kletzien RF. 1984. Regulation of glucose-6-phosphate dehydrogenase mRNA by insulin and the glucocorticoids in primary cultures of rat hepatocytes. Eur J Biochem 144:497–502.

Templeton AA, Cooper I, Kelly RW. 1978. Prostaglandin concentrations in the semen of fertile men. J Reprod Fertil 52:147–150.

Travis AJ, Kopf GS. 2002. The role of cholesterol efflux in regulating the fertilization potential of mammalian spermatozoa. J Clin Invest 110:731–736.

Visconti PE, Baley JL, Moore GD, Pan D, Olds-Clarke P, Kopf GS. 1995. Capacitation in mouse spermatozoa I. Correlation between the capacitation state and protein phosphorylation. Development 121:1129–1137.

Wang K, Zhou Z, Zhang M, Fan L, Forudi F, Zhou X, Qu W, Lincoff AM, Schmidt AM, Topol EJ, Penn MS. 2006. Peroxisome proliferator-activated receptor gamma down-regulates receptor for advanced glycation end products and inhibits smooth muscle cell proliferation in a diabetic and non-diabetic rat carotid artery injury model. J Pharmacol Exp Ther 317:37–43.

World Health Organization. 1999. WHO laboratory manual for the examination of human semen and sperm-cervical mucus interactions. 4th ed. Cambridge, UK: Cambridge University Press.

Xu Y, Iyengar S, Roberts RL, Shappell SB, Peehl DMJ. 2003. Primary culture model of peroxisome proliferator-activated receptor gamma activity in prostate cancer cells. Cell Physiol 196:131–143.

Yee LD, Guo Y, Bradbury J, Suster S, Clinton SK, Seewaldt VL. 2003. The antiproliferative effects of PPARgamma ligands in normal human mammary epithelial cells. Breast Cancer Res Treat 78:179–192.

Zhang L, Chawla A. 2004. Role of PPARgamma in macrophage biology and atherosclerosis. Trends Endocrinol Metab 15:500–505.